

Fall 12-13-2023

**THE IMPACT OF SEA-LEVEL RISE ON COASTAL WETLANDS
USING IN-SITU MESOCOSM EXPERIMENTS, LANDSCAPE
MODELING, AND TRADITIONAL ECOLOGICAL KNOWLEDGE
MAPPING**

Kelly San Antonio

Follow this and additional works at: https://aquila.usm.edu/masters_theses

Recommended Citation

San Antonio, Kelly, "THE IMPACT OF SEA-LEVEL RISE ON COASTAL WETLANDS USING IN-SITU MESOCOSM EXPERIMENTS, LANDSCAPE MODELING, AND TRADITIONAL ECOLOGICAL KNOWLEDGE MAPPING" (2023). *Master's Theses*. 1006.

https://aquila.usm.edu/masters_theses/1006

This Masters Thesis is brought to you for free and open access by The Aquila Digital Community. It has been accepted for inclusion in Master's Theses by an authorized administrator of The Aquila Digital Community. For more information, please contact aquilastaff@usm.edu.

THE IMPACT OF SEA-LEVEL RISE ON COASTAL WETLANDS USING IN-SITU
MESOCOSM EXPERIMENTS, LANDSCAPE MODELING, AND TRADITIONAL
ECOLOGICAL KNOWLEDGE MAPPING

by

Kelly Marie San Antonio

A Thesis
Submitted to the Graduate School,
the College of Arts and Sciences
and the School of Ocean Science and Engineering
at The University of Southern Mississippi
in Partial Fulfillment of the Requirements
for the Degree of Master of Science

Committee:

Dr. Wei Wu, Committee Chair
Dr. Kelly Darnell
Dr. Matt Bethel

December 2023

COPYRIGHT BY

Kelly Marie San Antonio

2023

Published by the Graduate School



ABSTRACT

Sea-level rise is an escalating threat to coastal wetlands as increased inundation and saltwater intrusion can lead to lowered productivity, decreased biomass, and plant death – and ultimately land loss. In chapter one, I detailed the interactive effects of inundation and nitrogen on two commonly found saltmarsh species, *Spartina alterniflora* and *Spartina patens*. I examined productivity and metrics to these stressors using a controlled mesocosm experiment in the western channel of the Pascagoula River, Mississippi. I found varying strategies of growth between species and differing responses between the short- and long-term. Overall *Spartina alterniflora* performed better with increased inundation than *Spartina patens*. Both species responded positively to nitrogen additions in the above- and belowground biomass, with the latter shown only in the long-term. In chapter two, I evaluated the impact of sea-level rise on coastal wetlands that are important for an underrepresented community in Louisiana. I worked with the Pointe-au-Chien Indian Tribe (PACIT) and Louisiana Sea Grant to understand saltmarsh resiliency to increased inundation. I applied a mechanistic landscape model to predict coastal wetland change impacted by sea-level rise in comparison to vulnerability assessments from traditional ecological knowledge (TEK). By integrating the biophysical model predictions with land-based, generational assessments, I highlighted vulnerable areas to sea-level rise while including the tribe's sustainability goals, producing a spatial tool that can be used by PACIT and land managers to prioritize saltmarsh restoration. The findings in this thesis will improve our understanding of coastal resiliency and ecosystem health under future sea-level rise and climate change.

ACKNOWLEDGMENTS

This work would not have been possible without the many people involved in my field work, laboratory processing, and technical support. I'd like to thank everyone in my lab. Makenzie Holifield (for her support in the field and laboratory processing), Devin Jen, Kodi Feldpausch, Evan Grimes, Dr. Hailong Huang, and our interns and volunteers (for field work), as well as Dr. Wu for her support and wisdom. A big thank you to my committee members Dr. Matt Bethel and Dr. Kelly Darnell, for their input, advice, and aid in this thesis. Thank you to Don Dardar from the Pointe-au-Chien Indian Tribe for his insight and assistance in our field work in the Terrebonne Bay. Other USM people I'd like to thank include Dr. Patrick Biber, Dr. Kevin Dillon, and Dr. Christopher Hayes for their aid in laboratory processing and the team from the USM Geospatial Center for georeferencing our marsh organ experiments. Lastly, I'd like to thank my funding sources, the US Army Corps of Engineers, US Environmental Protection Agency, Louisiana Sea Grant, and the University of Southern Mississippi Coastal Science Department.

DEDICATION

To my family for their unending support and encouragement during my entire graduate school experience, my friends for reminding me there is more to life than work, and my devoted boyfriend Alfonso for being my rock when seas were calm and when they were stormy.

TABLE OF CONTENTS

ABSTRACT ii

ACKNOWLEDGMENTS iii

DEDICATION iv

LIST OF TABLES viii

LIST OF ILLUSTRATIONS xi

LIST OF EQUATIONS xv

LIST OF ABBREVIATIONS xvi

CHAPTER I - THE IMPACT OF INUNDATION AND NITROGEN ON COMMON
SALTMARSH SPECIES USING MARSH ORGAN EXPERIMENTS IN MISSISSIPPI 1

1.1 Introduction 1

 1.1.2 Objectives and Hypotheses 3

1.2 Methods 4

 1.2.2 Study Species 4

 1.2.3 Study Site 5

 1.2.4 Marsh Organ Design 7

 1.2.5 Monitoring and Biomass Processing 12

 1.2.6 Statistical Analyses 14

1.3 Results 18

 1.3.1 Inundation duration 18

1.3.2 Response of biomass and morphology to inundation, nutrient, pre-condition, and channel	20
1.3.2.1 Above- and below-ground biomass	21
1.3.2.1.1 Aboveground biomass	21
1.3.2.1.2 Belowground biomass.....	22
1.3.2.2 The impact of inundation on morphological traits.....	24
1.3.2.3 The impact of channel on morphological traits	26
1.3.2.4 The impact of pre-condition on morphological traits	28
1.3.2.5 The impact of senescence or seasonality on morphological traits	29
1.3.2.6 The impact of channel on morphological traits	31
1.4 Discussion	31
1.5 Conclusion	36
 CHAPTER II - ASSESSING RESILIENCE OF A COASTAL WETLAND TO SEA- LEVEL RISE CLOSE TO A LOUISIANA NATIVE TRIBE – INTEGRATING BIOPHYSICAL PREDICTION AND TRADITIONAL ECOLOGICAL KNOWLEDGE	
.....	38
2.1 Introduction.....	38
2.1.2 Objectives and Hypotheses	40
2.2 Methods.....	40
2.2.2 Study Area	41

2.2.3 Field Work	43
2.2.4 Laboratory Processing	45
2.2.6 Model Calibration and Assessment	49
2.2.7 Model Scenarios and TEK Combination	51
2.3 Results.....	52
2.3.1 Calibration.....	52
2.3.2 Predictions under varying SLR scenarios and 10 mm/yr.....	53
2.3.3 Vulnerability from SK/SLR model.....	57
2.3.4 Combining TEK and SK vulnerability predictions.....	58
2.3.5 Sustainability and vulnerability	62
2.4 Discussion	64
2.5 Conclusion	69
CHAPTER III - LINKING THE IMPACTS OF SEA-LEVEL RISE TO <i>SPARTINA</i> 'S MECHANISMS OF ADAPTION AND TO THE COASTAL RESILIENCY OF <i>SPARTINA ALTERNIFLORA</i> -DOMINATED WETLANDS.....	71
APPENDIX A – Supplemental Data for the Thesis.....	75
REFERENCES	93

LIST OF TABLES

Table 1.1 Summary of morphological measurements on *Spartina alterniflora* (Sa.) and *Spartina patens* (Sp.). 10

Table 1.2 Summary of signs of 50% and 95% credible intervals (CIs) based on the posteriors of Bayesian models for biomass of *Spartina alterniflora* and *Spartina patens*. 23

Table 1.3 Summary of the quantiles of the derived inundation percentages when biomass reached the minimum (Min) or maximum (Max) in Year 1 and 2 (Sa. denotes *Spartina alterniflora*, Sp. denotes *Spartina patens*). 24

Table 1.4 Summary of signs of 50% and 95% credible intervals (CIs) of linear and quadratic inundation impact based on the posteriors of multi-level Bayesian models for metrics of *Spartina alterniflora* and *Spartina patens*. 25

Table 1.5 Summary of the quantiles of the derived inundation percentages when the metrics reached the minimum (Min) or maximum (Max) in Year 1 and 2 (Sa. denotes *Spartina alterniflora*, Sp. denotes *Spartina patens*). 26

Table 1.6 Summary of signs of 50% and 95% credible intervals (Cis) of nitrogen impact based on the posteriors of multi-level Bayesian models for metrics of *Spartina alterniflora* and *Spartina patens*. 27

Table 1.7 Summary of signs of 50% and 95% credible intervals (CIs) of pre-condition impact based on the posteriors of multi-level Bayesian models for metrics of *Spartina alterniflora* and *Spartina patens*. 29

Table 1.8 Summary of signs of 50% and 95% credible intervals (CIs) of senescence/seasonality impact based on the posteriors of multi-level Bayesian models for metrics of *Spartina alterniflora* and *Spartina patens*. 30

Table 1.9 Summary of signs of 50% and 95% credible intervals (CIs) of channel impact based on the posteriors of multi-level Bayesian models for metrics of <i>Spartina alterniflora</i>	31
Table 2.1 Color codes for the sustainability and vulnerability combinations in Fig. 2.3 (from Bethel et al., 2022).....	49
Table 2.2 Proportions of predicted wetland loss by year under various sea-level rise scenarios.....	53
Table 2.3 Current and predicted wetland loss area (ha) and proportion of loss by the year 2100, based on 10 mm/yr SLR (Figs. 2.5-8).....	55
Table 2.4 Classes, corresponding area, and proportion of area from Fig. 2.11.	59
Table 2.5 Classes, corresponding area, and proportion of area from Fig. 2.12.	60
Table 2.6 Proportion of vulnerable areas (ha) by class for the TEK assessment, SLR predictions, and combined TEK + SLR assessment.	61
Table 2.7 Classes, corresponding area, and proportion of area from Fig. 2.14.	64
Table A.1 <i>S. alterniflora</i> Year 1 metrics model comparisons using DIC and PPL.....	75
Table A.2 <i>S. alterniflora</i> Year 2 metrics model comparisons using DIC and PPL.....	76
Table A.3 <i>S. patens</i> Year 1 metrics model comparisons using DIC and PPL.	77
Table A.4 <i>S. patens</i> Year 2 metrics model comparisons using DIC and PPL.	78
Table A.5 <i>S. alterniflora</i> Year 1 biomass model comparisons using DIC and PPL.	79
Table A.6 <i>S. alterniflora</i> Year 2 biomass model comparisons using DIC and PPL.	79
Table A.7 <i>S. patens</i> Year 2 biomass model comparisons using DIC and PPL.....	80
Table A.8 <i>S. patens</i> Year 2 biomass model comparisons using DIC and PPL.....	80
Table A.9 Scaler vs. nutrient array metrics model comparisons using DIC.....	80

Table A.10 Site data at the Terrebonne Bay, Louisiana collected in December of 2022 unless otherwise specified (The site numbers correspond to Fig. 2.3). 90

Table A.11 Water quality data at each study site at the Terrebonne Bay, Louisiana collected in December of 2022 (The site numbers correspond to Fig 2.3 and the bottle numbers represent the locations when approaching the site with 1 closest to the site and 3 furthest away from the site). 91

LIST OF ILLUSTRATIONS

Figure 1.1 Map of the field site for the two marsh organs in relation to the Mississippi coast. 6

Figure 1.2 Side view diagram of the marsh organ structures set up in the Pascagoula River Delta. 7

Figure 1.3 The two marsh organs set up in the Pascagoula River. 9

Figure 1.4 Washed belowground biomass samples separated into live and dead containers, with dead biomass (top right) vs. live biomass (bottom right). 14

Figure 1.5 Directed Acyclic Graph (DAG) of the multi-level Bayesian Model developed to evaluate impacts of various factors (i.e., inundation, nutrient, etc.) on morphological vegetative productivity (Y). 16

Figure 1.6 Percentage of inundation time of each row in the *S. alterniflora* marsh organ For Year 1. 18

Figure 1.7 Percentage of inundation time of each row in the *S. alterniflora* marsh organ for Year 2. 19

Figure 1.8 Percentage of inundation time of each row in the *S. patens* marsh organ for Year 1. 19

Figure 1.9 Percentage of inundation time of each row in the *S. patens* marsh organ for Year 2. 20

Figure 1.10 Posteriors of nutrient impact on Year 1 *S. alterniflora* leaf count over five nitrogen additions, grouped by rows (Row 1 is the most inundated, Row 6 is the least inundated). 28

Figure 2.1 Field work showing below-ground biomass extraction with the PVC soil corer and handsaw to cut below-ground biomass samples into 5 cm sections (left) and soil cores ready for sectioning (right)..... 44

Figure 2.2 Map of southern Louisiana’s Terrebonne Bay with five sample sites (red circles) in proximity to the CRMS sites (yellow triangles) (left), and sample site location #5 with the locations for TSS water samples (red circles with black dot) and the biomass samples (red triangles) (right). 46

Figure 2.3 Classification of PACIT’s priority areas based on a combination of sustainability and vulnerability assessments from the tribe’s citizens, related to differences in perceived risk to coastal hazards (from Bethel et al, 2022). 48

Figure 2.4 Predicted wetland area (ha) under various sea-level rise scenarios (mm/yr), at years 2050, 2075, and 2100. 54

Figures 2.5-8 NWI wetland map (top left) and wetland predictions by the year 2050 (top right), 2075 (bottom left) and 2100 (bottom right), produced from the SLR mechanistic model using 10mm/year SLR. 55

Figure 2.9 Coastal wetland vulnerability classified as high (red, loss by 2050), medium (orange, loss by 2100), and low (yellow, little to no predicted loss). 57

Figure 2.10 Reclassified TEK vulnerability assessment, based on high (3) to low (1) vulnerability. 58

Figure 2.11 Saltmarsh vulnerability map based on TEK and SK data, constructed by combining the TEK vulnerability map (Fig 2.10) and the SLR saltmarsh loss prediction map (Fig 2.9)..... 59

Figure 2.12 Reclassified TEK SLR map from Fig. 2.11. High vulnerability areas are red (3), medium vulnerability is orange (2), and low vulnerability is yellow (1).....	60
Figure 2.13 Reclassified TEK sustainability assessment, based on high (3) to low (1) sustainability priority.	62
Figure 2.14 Final sustainability and vulnerability map created using the TEK SLR vulnerability map from Fig. 2.12 combined with the TEK sustainability assessment from 2.13.....	63
Figure A.1 Posteriors for <i>Spartina alterniflora</i> aboveground biomass Year 1 (left) and Year 2 (right).....	81
Figure A.2 Posteriors for <i>Spartina patens</i> aboveground biomass Year 1 (left) and Year 2 (right).	81
Figure A.3 Posteriors for <i>Spartina alterniflora</i> belowground biomass Year 1 (left) and Year 2 (right).....	82
Figure A.4 Posteriors for <i>Spartina patens</i> belowground biomass Year 1 (left) and Year 2 (right).	82
Figure A.5 Posteriors for <i>Spartina alterniflora</i> leaf count Year 1 (left) and Year 2 (right).	83
Figure A.6 Posteriors for <i>Spartina patens</i> leaf count Year 1 (left) and Year 2 (right).....	83
Figure A.7 Posteriors for <i>Spartina alterniflora</i> height Year 1 (left) and Year 2 (right)....	84
Figure A.8 Posteriors for <i>Spartina patens</i> height Year 1 (left) and Year 2 (right).	84
Figure A.9 Posteriors for <i>Spartina alterniflora</i> leaf length Year 1 (left) and Year 2 (right).	85

Figure A.10 Posteriors for <i>Spartina patens</i> leaf length Year 1 (left) and Year 2 (right). .	85
Figure A.11 Posteriors for <i>Spartina alterniflora</i> stem width Year 1 (left) and Year 2 (right).	86
Figure A.12 Posteriors for <i>Spartina patens</i> stem width Year 1 (left) and Year 2 (right)..	86
Figure A.13 Posteriors for <i>Spartina alterniflora</i> leaf width Year 1 (left) and Year 2 (right).	87
Figure A.14 Posteriors for <i>Spartina patens</i> stem count Year 1 (left) and Year 2 (right)..	87
Figure A.15 This map represents southern Louisiana’s land loss and land gain from 1932 to 2000, marked by red and light green, and predicted land loss and land gain from 2000 to 2050, as marked by yellow and darker green (Source: USGS, https://www.researchgate.net/figure/Historical-and-projected-land-loss-from-coastal-Louisiana-Map-reproduced-from-Barras-et_fig1_226220800).....	88
Figure A.16 This map shows the indigenous tribes in Southern Louisiana currently losing land due to sea-level rise (Source: Yeoman https://www.sapiens.org/culture/louisiana-native-americans-climate-change/).	89
Figure A.17 The conceptual diagram illustrating the processes and drivers in the model to predict salt marsh platform change in this study (Wu et al. 2017a, 2022).	89

LIST OF EQUATIONS

Equation 1.1 Bayesian posterior for multi-level models	17
Equation 1.2 Bayesian posterior for biomass models	17
Equation 2.1 SLR model equation	47

LIST OF ABBREVIATIONS

<i>PACIT</i>	Pointe-au-Chien Indian Tribe
<i>SK</i>	Science knowledge
<i>SLR</i>	Sea-level rise
<i>TEK</i>	Traditional ecological knowledge

CHAPTER I - THE IMPACT OF INUNDATION AND NITROGEN ON COMMON SALTMARSH SPECIES USING MARSH ORGAN EXPERIMENTS IN MISSISSIPPI

1.1 Introduction

Coastal wetlands provide a myriad of resources and services for humans and wildlife (Wu et al., 2020; Costanza et al., 1997; Engle, 2011). In these ecosystems, plants are engineers – they shape landscapes through vertical accretion of organic and inorganic materials to form wetland platforms, prevent erosion through their root systems, affect community structure, and provide habitat for various species (Morris et al., 2002; Snedden et al., 2015; Wu et al., 2020).

With these factors detailing how coastal wetland plants affect their ecosystems, any alterations or threats to plant growth may affect the system stability, particularly regarding how coastal wetlands tolerate sea level rise (Langley et al., 2013). This highlights the importance to understand how changes in inundation affect plant growth, and subsequently, how biological processes combat or adapt to these changes and to modify their physical environment (Morris et al., 2002; Kirwan et al., 2010). Previous studies show that a small amount of increased flooding may promote biomass growth and productivity but a continued increase of inundation results in decreased biomass and productivity in dominant salt marsh species (Morris et al., 2002; Langley et al., 2013; Kirwan and Guntenspergen, 2012 and 2015; McKee and Mendelsohn, 1989). Other studies show the above- and belowground biomass of *Spartina alterniflora* and *Spartina patens* was highest when inundation was at its minimum, also noting that the negative productivity response to inundation was more pronounced in the *S. patens* (Snedden et al., 2015). The similar response of vegetation to inundation can also be found in

vegetation located in less salty environments. A marsh organ experiment showed that optimum inundation levels existed for above- and belowground biomass of *Sagittaria lancifolia*, and that the biomass decreased quickly beyond the optimum inundation levels (Grimes, 2021).

The negative impact on plant productivity from excessive inundation further limits sediment trapping by aboveground biomass and reduces organic matter accumulation by belowground biomass, and therefore decreases vertical accretion, accelerates submergence, and becomes a self-accelerating cycle (Snedden et al., 2015; Mendelsohn and McKee, 1988; McKee and Mendelsohn, 1989; Leonard and Croft, 2006; Nyman et al., 1993, 2006; Kirwan and Guntenspergen, 2012 and 2015). Along with the vulnerability coastal wetlands face due to sea level rise, freshwater diversions from upper rivers can also result in prolonged inundation and higher water levels, as well as impacting salinity dynamics and nutrient cycles of wetland systems (Grimes, 2021; Snedden et al., 2007a, Snedden et al., 2007b; Wang et al., 2018).

In addition to inundation, nitrogen plays an important role in salt marsh ecosystems. These ecosystems serve as large nitrogen sinks (Bulsecu et al., 2019; Herbert, 1999; Delaune et al., 1989), acting as a stimulant for microbial organic decomposition and affecting plant growth and morphological attributes (Bulsecu et al., 2019; Langley et al., 2013; Grimes, 2021). Studies suggest that exposure to additional nitrogen can be beneficial to marsh systems as the increased nitrogen promotes plant productivity, especially *S. alterniflora* and *S. patens*, temporarily alleviates flooding stressors, and broadens its vertical range (Langley et al., 2013, Mendelsohn, 1979). In terms of the physical stability of the ecosystem, research suggests that nitrogen additions

may lead to a decline in belowground plant productivity and a weaker root system, resulting in potential destabilization of marsh platforms especially in areas that suffer from limited sediment availability (Else-Quirk et al., 2019; Wu et al., 2017; Darby and Turner, 2008).

Despite its importance, it is yet unclear how salt marsh vegetation responds to the interactive factors of inundation and nitrogen availability on the Mississippi Gulf Coast. Depending on morphological characteristics measured for resource allocation, different species show different phenotypic responses and potential plasticity to inundation and nitrogen. This understanding will facilitate better predications of coastal resilience at the landscape scale (Grimes, 2021; Wu et al., 2022).

1.1.2 Objectives and Hypotheses

I aim to:

- 1) Study the temporal patterns of a variety of morphological traits of two common salt marsh species (*Spartina alterniflora* and *Spartina patens*) impacted by inundation and nitrogen.
- 2) Evaluate short- (one year) and long-term (two years) impact of inundation and nitrogen on above- and belowground biomass of the two species.

My hypotheses tested include:

- 1) Two commonly found coastal wetland plants (*Spartina alterniflora* and *Spartina patens*) react negatively to increased inundation and positively to elevated nitrogen in productivity.
- 2) The effect of nitrogen on above- and belowground biomass will become more pronounced over time, showing larger effect over the long-term vs the short-term.

- 3) Nitrogen will alleviate some of the negative effect of inundation on both species, especially for *Spartina patens* (a high marsh plant) than *Spartina alterniflora* (a low marsh plant).

1.2 Methods

To test these hypotheses, I used an in-situ mesocosm experiment method, called a marsh organ, to understand mechanistically how different levels of inundation and elevated nutrients (nitrogen) affect vegetation growth of *Spartina alterniflora* and *Spartina patens*. Marsh organs describe inundation-productivity relationships while also allowing an insight of interactions between nutrient competition and other abiotic stressors (Grimes, 2021; Kirwan et al., 2012; Langley et al., 2013; Morris, 2007; Snedden et al., 2015). Two marsh organs were placed in the western Pascagoula River, a tidally influenced brackish marsh for facilitation of varying inundation (Grimes, 2021). Every two to three weeks during the growing season in 2021 and 2022, particularly, from the end of July when the marsh organ was set up to early November in 2021 and from April to early November in 2022, I measured vegetative metrics including leaf count, leaf length, and leaf width, as well as giving half of the randomly selected replicates at each inundation level a nitrogen additive to simulate additional nutrients. We harvested the replicates at the end of the season for year 1 and year 2 to examine short- and long-term effects of inundation and nitrogen on the above- and belowground biomass.

1.2.2 Study Species

The *Spartina* genus is comprised of intertidal C4 grass saltmarsh plants, commonly found along the Atlantic, Pacific, and Gulf coasts. This genus of saltmarsh grows in the summer, reproduces in the fall, and dies back during the winter months,

providing habitat for a variety of species through its biomass and sedimentation. While *S. alterniflora* and *S. patens* are in the same genus, and often the same region, they occupy different niches. *S. alterniflora* is a low marsh species and is found throughout the marsh platform, growing tall along shorelines where it is frequently flooded, typically at every tide and only exposed during low tide (Bertness, 1991). *S. patens* grows in the upper, more expansive salt marsh and less frequently flooded habitat, as this species has a limited ability to uptake oxygen in anoxic soils (Bertness, 1991). This *Spartina* zonation is determined by abiotic and biotic factors – *S. patens* prefers drier, less inundated, and more oxygenated soil in the high marsh and while *S. alterniflora* can persist in either low or high marsh, it is restricted to the low marsh due to competitive displacement from *S. patens* (Bertness, 1991; McKee and Patrick, 1988). When looking at studies investigating inundation-productivity relationships, some suggest that *S. alterniflora* may exhibit a quadratic or parabolic shape, indicating an optimal intermediate amount of inundation (Grimes, 2021; Kirwan et al., 2012; Morris, 2002; Wu et al. 2020). Alternately, another study showed that both *S. alterniflora* and *patens* reacted negatively as inundation increased in the Gulf of Mexico (Snedden et al., 2015; Grimes, 2021; Wu et al. 2020).

1.2.3 Study Site

The marsh organs were situated in the western channel of the lower Pascagoula River (Fig. 1.1). The Pascagoula River is the largest undammed river in the continental United States by volume and contains roughly 35% of the coastal wetlands of the Mississippi Gulf Coast (Grimes, 2021; Wu et al., 2020; Dynesius & Nilsson, 1994). This western channel, which is minimally anthropogenically impacted compared to the eastern channel, flows southward into the Mississippi Sound, with the watershed receiving

abundant rain annually which brings a large source of freshwater into the Gulf (Grimes, 2021; Mossa and Coley, 2004; Lamonds and Boswell, 1985). Due to this influx of fresh water mixing with the saltwater from the Gulf of Mexico, the marsh organ field site has fluctuating brackish water, with salinity ranging from 0 – 15 ppt (mean of 4.09 ppt and standard deviation of 5.3 ppt), measured with a refractometer during 2022. The study site at (30.393 °N and 88.608 °W) is located north of HWY 90 and not far from a USGS water gauge which was used to help design the marsh organs and determine percent inundation time during the experiment (Fig 1.1)

(https://waterdata.usgs.gov/nwis/uv?site_no=02480285&legacy=1). The saltmarsh in this area is largely comprised of *Spartina*, *Schoenoplectus*, and *Sagittaria* species (Grimes, 2021).



Figure 1.1 Map of the field site for the two marsh organs in relation to the Mississippi coast.

The red star is the marsh organ site and the orange circle is the USGS water gauge beneath HWY 90.

1.2.4 Marsh Organ Design

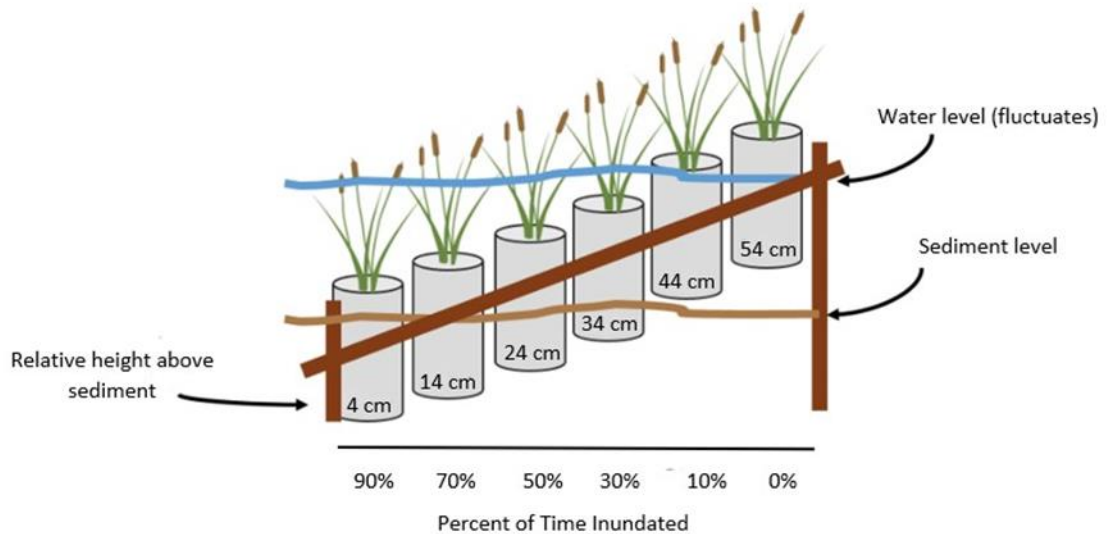


Figure 1.2 Side view diagram of the marsh organ structures set up in the Pascagoula River Delta.

The incremental pipe heights allow for varied inundation time and depth dependent on row level.

The marsh organ is constructed of PVC pipes organized by six rows that differ in height and therefore inundation depth and duration, with eight replicates in each row (Fig. 1.1). The inundation durations were designed to be 90%, 70%, 50%, 30%, 10%, and 0% from bottom to top, determined using nearby USGS tidal data and a HOBO water level logger at the site (Fig. 1.2). However, considering storm surges, precipitation, and seasonal and tidal water changes, the final inundation may vary from the design. The first marsh organ contained 48 pipes of *Spartina alterniflora* (Fig. 1.3a) and the other had 48 pipes of *Spartina patens* (Fig. 1.3b).

The two marsh organs were constructed in the summer of 2021, placed roughly thirty feet apart, facing southward, and situated perpendicular to the marsh-waterline

edge. The PVC pipes had a 15 cm (6 in) diameter and a standardized length of 61 cm (24 in) (Grimes, 2021). The pipes were screwed together, pushed into the sediment a certain amount depending on row, and then attached to the wooden frame implemented for added stability. Pipes were then packed with local sediment to ensure plant growth at the top of the pipe and to prevent sinking. A nylon mesh was placed at the bottom of the higher pipes not pushed into the sediment that still allowed natural lateral water flow but prevented sediment or plant loss.

For the first marsh organ, *S. alterniflora* was transplanted into each PVC pipe that originated from a mixture of east and west channels sites in the Pascagoula River. However, for the second marsh organ, *S. patens* was collected only from the eastern channel as no large patches of this species were found in the western channel. During transplanting, we aimed to plant five individuals of *S. alterniflora* and ten individuals of *S. patens* into each PVC pipe. These densities were based off previous literature (Currin 2019), which suggests 3-4 stems per PVC pipe, plus the extra we added to account for potential die-off. The pre-conditions of the vegetative morphology (leaf count, height, etc.) were recorded as they likely affected the vegetation growth. More local sediment was packed into the pipes after plant transplantation to account for the potential of gradual compaction and reduce risk of the plants floating out of the pipes when inundated (Grimes, 2021).



a



b

Figure 1.3 The two marsh organs set up in the Pascagoula River.

Fig. 1.3a (top) shows the marsh organ with *Spartina alterniflora* and Fig. 1.3b (bottom) shows the marsh organ with *Spartina patens*. A string grid was placed over the *Spartina patens* marsh organ to keep plants upright and in their individual pots.

Table 1.1 Summary of morphological measurements on *Spartina alterniflora* (Sa.) and *Spartina patens* (Sp.).

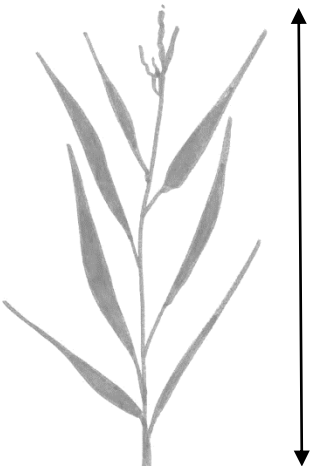
Species	Metric	Figure
Sa. & Sp.	Height from base of stem to highest part of the plant	
Sa. & Sp.	Leaf count	

Table 1.1 (continued).

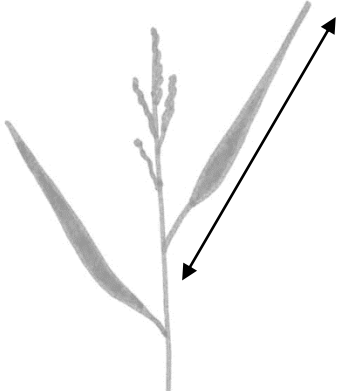
<p>Sa. & Sp.</p>	<p>Length of the second leaf from the top</p>	
<p>Sa. & Sp.</p>	<p>Width of the petiole of the second leaf from the top</p>	
<p>Sa.</p>	<p>Width of the second leaf from the top</p>	

Table 1.1 (continued).

Sp.	Stem count	
-----	------------	---

1.2.5 Monitoring and Biomass Processing

Starting in July 2021, we randomly selected two individuals from each PVC pipe replicate to measure leaf count, individual height from the base of stem to the highest part of the plant, length of the second leaf from the top, and width of the petiole of the second leaf from the top (Table 1.1). Additionally, for *Spartina alterniflora* we measured the width of the second leaf of two random individuals in each PVC pipe and for *Spartina patens* we measured total stem count in each pipe to observe plant density (Table 1.1). These measurements were done every 2 – 3 weeks during the growing season from July to November 2021 for year one and April to November 2022 for year two. Altogether, we conducted the measurements six times in 2021 (09/03, 09/24, 10/08, 10/23, 11/05, and 11/18) and twelve times in 2022 (04/08, 04/22, 05/09, 05/27, 06/17, 07/08, 07/21, 08/05, 08/29, 09/14, 10/14, and 11/02). At each visit starting on 09/10/22, we applied 25 grams per m² of NH₄⁺-N with a syringe into the soil of half of the replicates, randomly selected to simulate the scenario of added reactive nitrogen in the environment (Langley et al., 2013). Consequently, at the end of the growing season of year one in November 2021 (short-term impact), we harvested half of replicates and harvested the other half at the

end of the growing season of Year 2 in November 2022 (long-term impact), as above- and belowground biomass samples can elucidate the integrated effect of inundation and nitrogen. In each harvest, we randomly selected half of the replicates with nitrogen additions and half without in each row. Aboveground biomass was bagged and ready for immediate processing and belowground biomass was allocated into bags based on depth: 0 - 5, 6 - 10, 11 - 15, 16 - 20, 21 - 25, and 26 - 30 cm, which were then stored in laboratory refrigerators 4 °C for subsequent processing.

Aboveground biomass samples were processed within two weeks of harvest, with live and dead parts of the biomass separated into pre-weighed, oven safe aluminum trays that were then oven-dried at 75°C until a constant weight was reached, around 3 - 5 days (Wu et al., 2020). The demarcation between live and dead aboveground biomass was based on color. Live biomass had green stems and leaves while dead biomass ranged from yellow to brown stems and leaves. Pre-dried and post-dried weights were collected as measurements from these samples.

I then washed sediment and mud away from the belowground biomass using a 1 mm mesh sieve and removed extraneous objects such as sticks and snails. Once washed, I separated live and dead biomass based on the buoyancy by submerging it in water first, combined with color and turgidity (Fig. 1.4). Floating biomass with light colors and turgidity was classified as live biomass, while dark matter that sunk to the bottom of the container, and felt and looked flaccid, was classified as dead biomass. The live and dead biomass were separated into the pre-weighed aluminum trays, then weighed again, and dried in an oven for several days to remove moisture until a constant weight was reached. After removal from the oven, the sample trays were weighed to collect the dry weight.



Figure 1.4 *Washed belowground biomass samples separated into live and dead containers, with dead biomass (top right) vs. live biomass (bottom right).*

1.2.6 Statistical Analyses

Using the collected morphological attributes and biomass data, I applied multi-level Bayesian models or Bayesian models to evaluate the impact of inundation and nutrients on vegetation structure over time and vegetation productivity (Fig. 1.5; Equation 1.1). Bayesian statistics is a form of statistical inference involving the Bayes theorem. Hierarchical Bayesian models decompose high-complexity problems into a fully consistent framework (Wu et al., 2012 and 2018; Clark, 2005). Using Hierarchical Bayesian models allows data assimilation while accounting for various uncertainties and provides inference based on posterior distributions (Wu et al., 2012 and 2018). We developed models for each metric measured during sampling visits, including leaf counts, individual height, second leaf width, second leaf length, petiole width, stem width, and above- and belowground biomass. I accounted for senescence (days since installation of marsh organs in Year 1), and seasonality (temperature since onset of growing season in Year 2), pre-condition, and channel when evaluating the impact of inundation and

nutrient (Fig. 5). As biomass was measured at the end of growing seasons, their models differed from morphological characteristics in that they do not have time as a covariate.

I created and ran these models in R using the “rjags”, “MCMCvis”, and “coda” packages (https://cran.r-project.org/web/packages/available_packages_by_name.html). I compared the models using deviance information criterion (DIC) and predictive posterior loss (PPL) – selecting the best model based on the lowest DIC or PPL (Hooten and Hobbs, 2015; Wu et al., 2018). DIC was used as the main model selection criterion, but I also considered PPL during the parameter selection in addition to DIC when the models differed in their hierarchies. See tables A.1-9 in the appendix for more information on the model comparisons. Once selected, I computed the posterior distributions using Markov Chain Monte Carlo Simulation (MCMC), with summarized medians and quantiles of 95% and 50% credible intervals (CIs) for the parameters of the covariates based on the posterior outputs (Robert and Casella, 2004; Wu et al., 2018). These 95% or 50% CIs indicate a 95% or 50% probability that the covariate coefficient lies within the intervals. If the CI does not overlap zero, there exists evidence for the covariate to have strong or moderate positive or negative effect on the dependent variable (Wu et al, 2018). In the posteriors, the 95% CIs represent the range from the 2.5% to 97.5% quantiles, while the 50% CIs indicate the range from the first to third quartile.

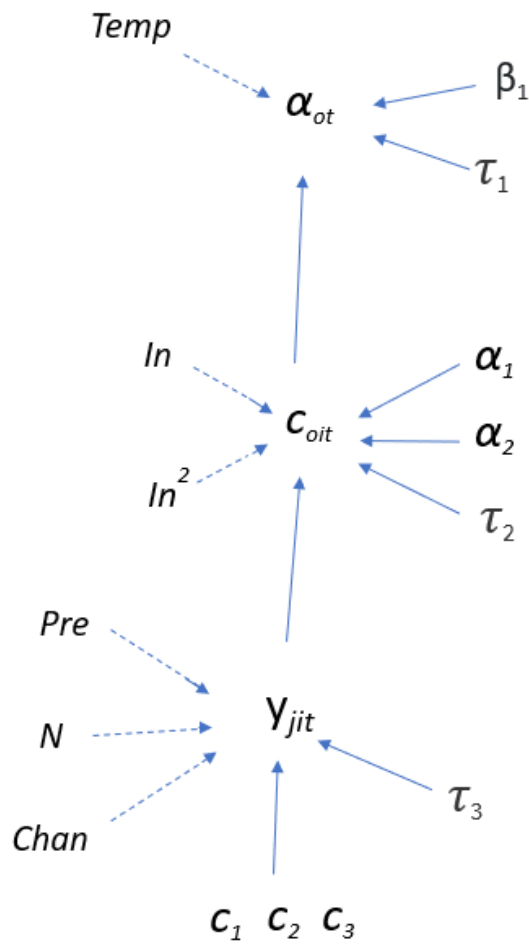


Figure 1.5 Directed Acyclic Graph (DAG) of the multi-level Bayesian Model developed to evaluate impacts of various factors (i.e., inundation, nutrient, etc.) on morphological vegetative productivity (Y).

The subscripts j denotes individual (randomly selected individuals measured in each PVC pot), i is inundation level, t refers to sampling event. The symbols $Temp$ denotes temperature (for year two models, year one models have days since transplant), In is inundation time, In^2 is squared inundation time, N denotes nutrient, Pre stands for pre-condition of the original marsh plants, $Chan$ refers to channel, and α_{ot} , β_1 , c_{oit} , α_1 , α_2 , c_1 , c_2 , c_3 , τ_1 , τ_2 , τ_3 are the parameters in the model (as denoting the coefficients for the covariates, with τ_1 , τ_2 , and τ_3 denoting precision across time/season, inundation level and individual respectively).

$$\begin{aligned}
& [\beta_0, \beta_1, \alpha_1, \alpha_2, c_1 - c_3, \tau_1, \tau_2, \tau_3 | \mathbf{y}_{jit}] \\
& \propto \prod_{t=1}^{12} \prod_{i=1}^6 \prod_{j=1}^8 \text{dnorm}(\mathbf{y}_{jit} | \mathbf{c}_{oit}, c_1, c_2, c_3, \tau_1) \\
& \quad \text{dnorm}(\mathbf{c}_{oit} | \alpha_{ot}, \alpha_1, \alpha_2, \tau_2) \\
& \quad \text{dnorm}(\alpha_{ot} | \beta_0, \beta_1, \tau_1) \\
& \text{dnorm}(\beta_0 | 0, 0.000000001) \quad \text{dnorm}(\beta_1 | 0, 0.000000001) \\
& \text{dnorm}(\alpha_1 | 0, 0.000000001) \quad \text{dnorm}(\alpha_2 | 0, 0.000000001) \\
& \text{dnorm}(c_1 | 0, 0.000000001) \quad \text{dnorm}(c_2 | 0, 0.000000001) \\
& \text{dnorm}(c_3 | 0, 0.000000001) \quad \text{dgamma}(\tau_1 | 0.1, 0.1) \\
& \text{dgamma}(\tau_2 | 0.01, 0.01) \quad \text{dgamma}(\tau_3 | 0.001, 0.001)
\end{aligned}$$

Equation 1.1 Bayesian posterior for the multi-level models to predict vegetation morphology in Year 2 (2022).

$$\begin{aligned}
& [\beta_0, \beta_1, \beta_2, \beta_3, \beta_4, \tau_1 | \alpha_{oi}] \\
& \propto \prod_{i=1}^{24} \text{dnorm}(\alpha_{oi} | \beta_0, \beta_1, \beta_2, \beta_3, \beta_4, \tau_1) \\
& \text{dnorm}(\beta_0 | 0, 0.000000001) \quad \text{dnorm}(\beta_1 | 0, 0.000000001) \\
& \text{dnorm}(\beta_2 | 0, 0.000000001) \quad \text{dnorm}(\beta_3 | 0, 0.000000001) \\
& \text{dnorm}(\beta_4 | 0, 0.000000001) \quad \text{dgamma}(\tau_1 | 0.001, 0.001)
\end{aligned}$$

Equation 1.2 Bayesian posterior for the biomass models.

1.3 Results

1.3.1 Inundation duration

In Year 1 (2021), inundation durations at different rows of the *Spartina alterniflora* marsh organ were similar to what we designed and our original intentions (Figure 1.6). However, due to extreme droughts in 2022, the inundation durations decreased in Year 2, with the maximum duration reaching only 60% to 70% of time (Figure 1.7). Inundation durations of the *Spartina patens* marsh organ were lower than those of the *Spartina alterniflora* marsh organ as they were situated at a higher platform (Fig. 1.8-9). Just like the *Spartina alterniflora* marsh organ, the inundation durations were lower in Year 2 than in Year 1.

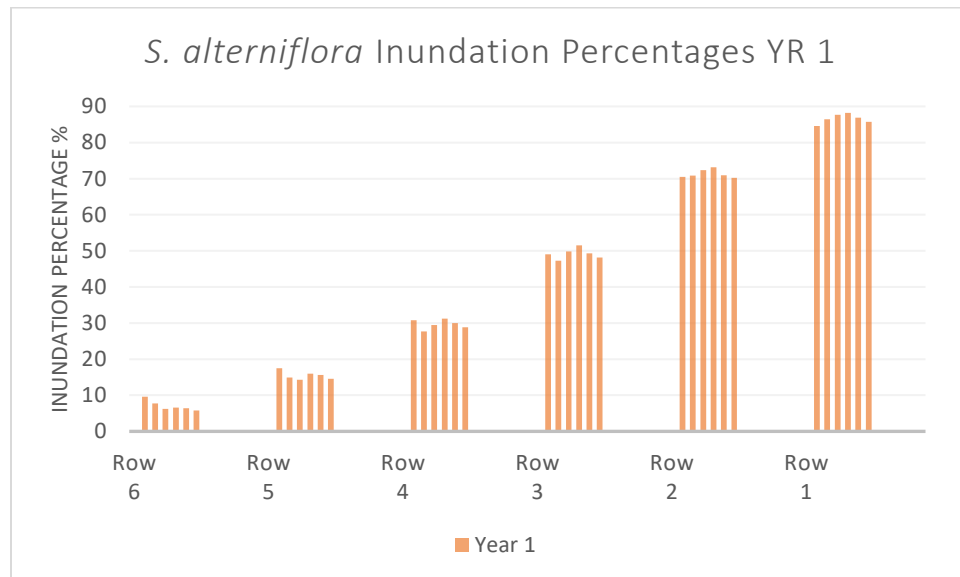


Figure 1.6 Percentage of inundation time of each row in the *S. alterniflora* marsh organ For Year 1.

The row numbers of 1 to 6 represent the lowest to the highest row. In each row, there are six bars representing the sequential sampling events between September 3rd, 2021, and November 18th, 2021.

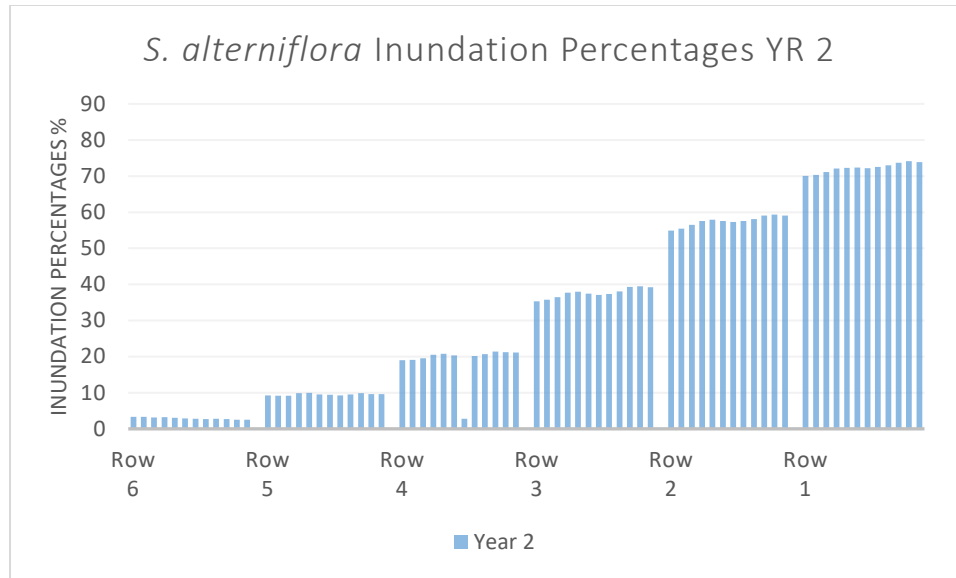


Figure 1.7 Percentage of inundation time of each row in the *S. alterniflora* marsh organ for Year 2.

The row numbers of 1 to 6 represent the lowest to the highest row. In each row, there are twelve bars representing the sequential sampling events between April 30th, 2022, and November 2nd, 2022.

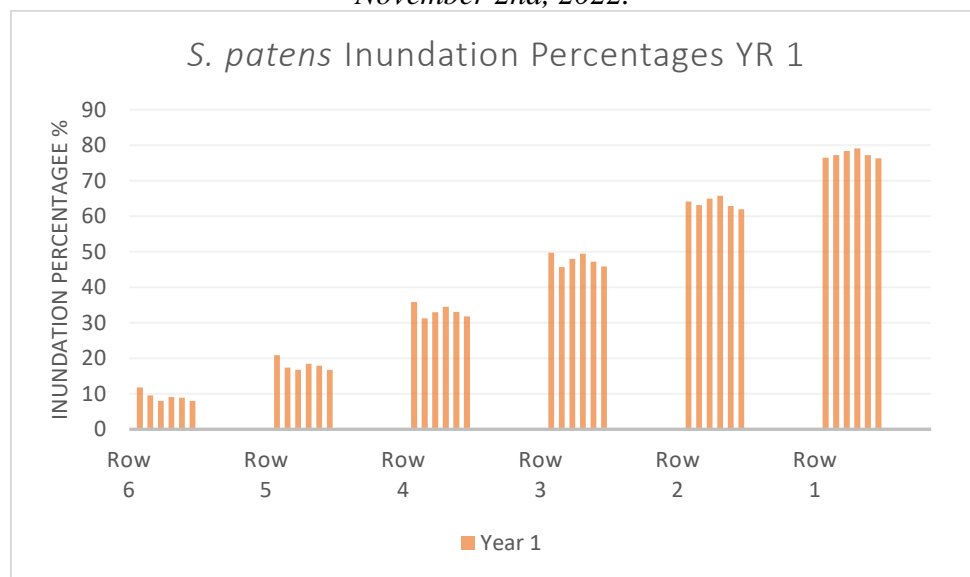


Figure 1.8 Percentage of inundation time of each row in the *S. patens* marsh organ for Year 1.

The row numbers of 1 to 6 represent the lowest to the highest row. In each row, there are six bars representing the sequential sampling events between September 3rd, 2021, and November 18th, 2021.

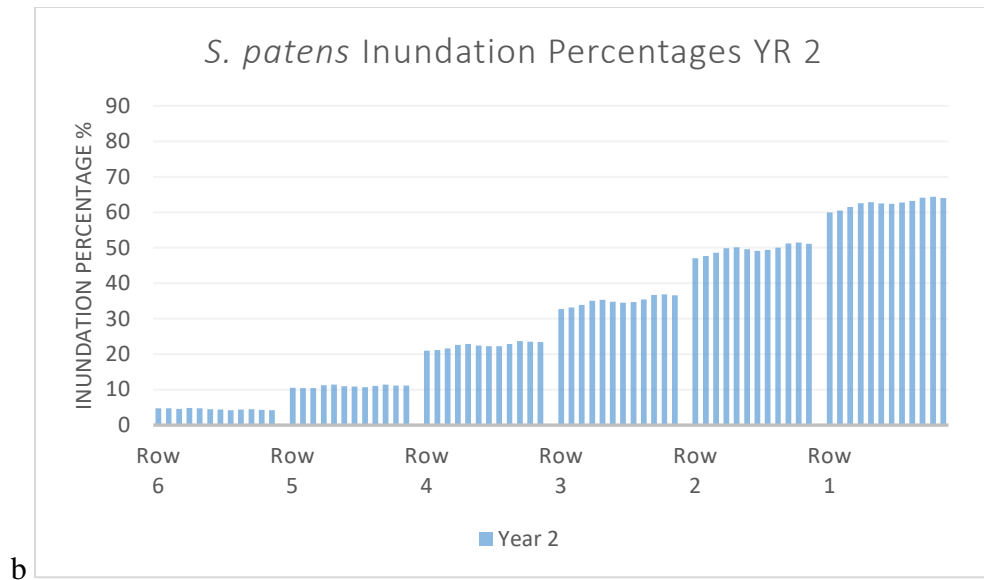


Figure 1.9 Percentage of inundation time of each row in the *S. patens* marsh organ for Year 2.

The row numbers of 1 to 6 represent the lowest to the highest row. In each row, there are twelve bars representing the sequential sampling events between April 30th, 2022, and November 2nd, 2022.

1.3.2 Response of biomass and morphology to inundation, nutrient, pre-condition, and channel

Summary

The effect of nutrient on vegetation traits including biomass and morphological characteristics were consistently positive. Although belowground biomass and some morphological traits, including plant height for both species and stem count for *Spartina patens* in Year 1, did not respond to nutrients, all the vegetation traits in Year 2 showed positive response to addition of nutrients. On the other hand, inundation’s effect varied depending on vegetation traits, species, and temporal scales. The effect can be parabolic with an optimal or least optimal inundation level or it can be linear. Pre-condition of the vegetation generally exhibited either positive or no effect on morphological traits for

either year except for the negative impact on leaf width and stem count in Year 2. Aboveground biomass of *Spartina patens* negatively responded to pre-condition (stem count) in Year 1, while belowground biomass of *Spartina alterniflora* positively responded to pre-condition (leaf count) in Year 1. Pre-condition did not have any impact on above or belowground biomass in Year 2. *Spartina alterniflora* from the east channel generally grew better or similarly when compared to the west channel plants, reflected in the biomass and morphological traits. One exception is that the west channel vegetation exhibited a higher leaf count than the plants from the east channel in Year 1. The interactive effect between inundation and nutrient only showed varying effect on leaf count in Year 1.

1.3.2.1 Above- and below-ground biomass

1.3.2.1.1 Aboveground biomass

In Year 1, aboveground biomass of *Spartina alterniflora* (Sa. thereafter) and *Spartina patens* (Sp. thereafter) exhibited moderate and strong parabolic relationships with inundation time respectively (“moderate” defined as the 50% CIs do not overlap 0, while “strong” defined as overlap 0) (Table 1.2). The biomass reached minimum productivity at 41.3% (median with a large uncertainty indicated by the 95% CI of 0 – 100%) and 51.6% (median with the 95% CI of 44.2 – 74.4%) inundation time for Sa. and Sp. respectively (Table 1.2 and 1.3). By Year 2, inundation time showed a moderate negative effect on aboveground biomass of Sp., while aboveground biomass of Sa. reached maximum productivity at 50.0% of inundation (median with a large uncertainty indicated by 95% CI of 0-100%) (Table 1.2 and 1.3). Nutrient addition had a strong positive impact on aboveground biomass for both species in the short- and long-term

(Table 1.2). Pre-condition (stem count) only had a strong negative impact on Sp. in the short-term, with no impact observed by year two for both species. For *Spartina alterniflora*, channel had a strong negative impact in Year 1, and moderate negative impact in Year 2, indicating that the east channel plants strongly and then moderately outperformed the west channel plants as time progressed.

1.3.2.1.2 Belowground biomass

Belowground biomass of Sa. and Sp. responded to inundation very differently in the short- and long-term (Table 1.2). However, the relationships were consistent for individual species in both years and demonstrated increased impact by Year 2. In both years, belowground biomass of Sa. indicated a parabolic relationship with an inundation maximum at 42.6% (median) and 44.3% (median) of inundation time respectively (Table 1.3). Belowground biomass of Sa. responded negatively to inundation. While nutrient addition had little to no impact on belowground biomass in Year 1, it showed strong positive impact for both species in year two. Pre-condition had only a moderate positive impact on Sa. in the short-term, with little to no impact observed by Year 2 for either species (Table 1.2). Like aboveground biomass, the vegetation from the east channel outperformed the vegetation from the west channel, with the stronger difference in Year 1 than in Year 2.

Table 1.2 Summary of signs of 50% and 95% credible intervals (CIs) based on the posteriors of Bayesian models for biomass of *Spartina alterniflora* and *Spartina patens*.

Also see 50% and 95% CIs in Figures A.1-4 in the appendix (*Sa.* denotes *Spartina alterniflora*, *Sp.* denotes *Spartina patens*) (If no signs were provided for a particular CI, it means the CI intercepted 0).

Metrics	Species	Inundation Time		Inundation Time Squared		Nutrient		Pre-Condition		Channel	
		95% CI	50% CI	95% CI	50% CI	95% CI	50% CI	95% CI	50% CI	95% CI	50% CI
Aboveground Biomass YR 1	<i>Sa.</i>		-		+	+	+			-	-
	<i>Sp.</i>	-	-	+	+	+	+	-	-		
Aboveground Biomass YR 2	<i>Sa.</i>	+	+		-	+	+				-
	<i>Sp.</i>		-			+	+				
Belowground Biomass YR 1	<i>Sa.</i>		+		-				+	-	-
	<i>Sp.</i>		-								
Belowground Biomass YR 2	<i>Sa.</i>	+	+		-	+	+				-
	<i>Sp.</i>	-	-			+	+				

Table 1.3 Summary of the quantiles of the derived inundation percentages when biomass reached the minimum (Min) or maximum (Max) in Year 1 and 2 (Sa. denotes *Spartina alterniflora*, Sp. denotes *Spartina patens*).

Metrics		Quantiles of the derived percent of inundation when biomass reached the minimum or maximum			Max or Min
		2.5% CI	50%	97.50%	
Aboveground Biomass YR 1	Sa.	0.0	41.3	100.0	Min
	Sp.	44.2	51.6	74.4	Min
Belowground Biomass YR 1	Sa.	0.0	42.6	100.0	Max
Aboveground Biomass YR 2	Sa.	0.0	50.0	100.0	Max
Belowground Biomass YR2	Sa.	0.0	44.3	100.0	Max

1.3.2.2 The impact of inundation on morphological traits

In Year 1, inundation time had mixed impact on both species. Inundation had a moderate negative linear impact on Sp. leaf count and height, and strong negative linear impact on and Sp. leaf count, a moderate positive linear impact on Sa. and Sp. stem width, Sa. leaf width, and Sp. leaf length, as well as a strong positive impact on Sp. stem count (Table 1.4). Sa. plant height had a moderate parabolic relation with inundation and it reached the maximum at 56% of inundation time (median). Meanwhile, Sa. leaf length had moderate parabolic relations with inundation, and they reached the minimum at 36% of inundation time (median) (Tables 1.4 and 1.5).

By Year 2, inundation time had more consistent impact across individual species. For *Spartina patens*, inundation exhibited a strong negative impact on plant height, leaf count, and stem width. Leaf length and stem count, on the other hand, showed parabolic

relations with inundation and they reached the minimum at the inundation time of 52% and 84% (medians) respectively (Tables 1.4 and 1.5). For *Spartina alterniflora*, most of the morphological traits, including plant height, leaf count, leaf length and leaf width, showed strong or moderate parabolic relations with inundation with the maximums reached at 89%, 35%, 39%, and 56% (medians) of inundation time respectively (Tables 1.4 and 1.5). Inundation had a strong positive linear impact on Sa. stem width (Tables 1.4).

Table 1.4 Summary of signs of 50% and 95% credible intervals (CIs) of linear and quadratic inundation impact based on the posteriors of multi-level Bayesian models for metrics of *Spartina alterniflora* and *Spartina patens*. Also see 50% and 95% CIs in Figures A.5-14 in the appendix (Sa. denotes *Spartina alterniflora*, Sp. denotes *Spartina patens*) (If no signs were provided for a particular CI, it means the CI intercepted 0).

		Year 1 (5 months)				Year 2 (1.5 years)			
Metrics	Species	Inundation Time		Inundation Time Squared		Inundation Time		Inundation Time Squared	
		95% CI	50 % CI	95% CI	50% CI	95% CI	50 % CI	95% CI	50% CI
Plant Height	Sa.	+	+		-	+	+	-	-
	Sp.		-			-	-		
Leaf Count	Sa.	-	-				+		-
	Sp.		-			-	-		
Leaf Length	Sa.		-		+		+		-
	Sp.				+	-	-	+	+
Stem Width	Sa.		+			+	+		
	Sp.		+			-	-		
Leaf Width	Sa.		+			+	+		-
Stem Count	Sp.	+	+			-	-		+

Table 1.5 Summary of the quantiles of the derived inundation percentages when the metrics reached the minimum (Min) or maximum (Max) in Year 1 and 2 (Sa. denotes *Spartina alterniflora*, Sp. denotes *Spartina patens*).

Metrics		Quantiles of the derived percent of inundation when a metric reached the minimum or maximum			Max or Min
		2.5% CI	50%	97.50%	
Year 1					
Plant Height	Sa.	0.0	55.9	100.0	Max
Leaf Length	Sa.	0.0	36.6	100.0	Min
	Sp.	0.0	0.0	100.0	Min
Year 2					
Plant Height	Sa.	0.0	88.9	100.0	Max
Leaf Count	Sa.	0.0	34.6	100.0	Max
Leaf Length	Sa.	0.0	39.9	100.0	Max
	Sp.	0.0	51.8	100.0	Min
Leaf Width	Sa.	0.0	56.7	100.0	Max
Stem Count	Sp.	0.0	84.1	100.0	Min

1.3.2.3 The impact of channel on morphological traits

In Year 1, nutrient addition had a strong positive impact on Sp. leaf count, Sa. leaf length, and Sa. leaf width, and Sa. stem width, and a moderate positive impact on Sp. leaf length and Sp. stem width (Table 1.6). Nitrogen had varying effect on Sa. leaf count at different inundation levels in the short-term, lending insight to the interactive effect between nitrogen and inundation. Nutrient increased leaf count in the more inundated vegetation, helping alleviate the stress of inundation to some degree. Starting after the

first sampling period when the nutrient addition began, the strong positive effect of nutrient addition on leaf count started to show up in the fourth sampling event in Rows 1, 2 and 4, while it did not show up until the fifth sampling event in Row 3 and 5, and indicated little to no negative/positive effect on Row 6, the least inundated row (Table 1.6 and Figure 1.10). By Year 2, nutrient addition had a strong positive impact on every metric for both species (Table. 1.6).

Table 1.6 Summary of signs of 50% and 95% credible intervals (Cis) of nitrogen impact based on the posteriors of multi-level Bayesian models for metrics of *Spartina alterniflora* and *Spartina patens*.

Also see 50% and 95% Cis in Figures A.5-14 in the appendix (Sa. denotes *Spartina alterniflora*, Sp. denotes *Spartina patens*) (If no signs were provided for a particular CI, it means the CI intercepted 0).

		Year 1 (5 months)		Year 2 (1.5 years)	
Metrics	Species	Nutrient		Nutrient	
		95% CI	50% CI	95% CI	50% CI
Plant Height	Sa.			+	+
	Sp.			+	+
Leaf Count	Sa.	*	*	+	+
	Sp.	+	+	+	+
Leaf Length	Sa.	+	+	+	+
	Sp.		+	+	+
Stem Width	Sa.	+	+	+	+
	Sp.		+	+	+
Leaf Width	Sa.	+	+	+	+
Stem Count	Sp.			+	+

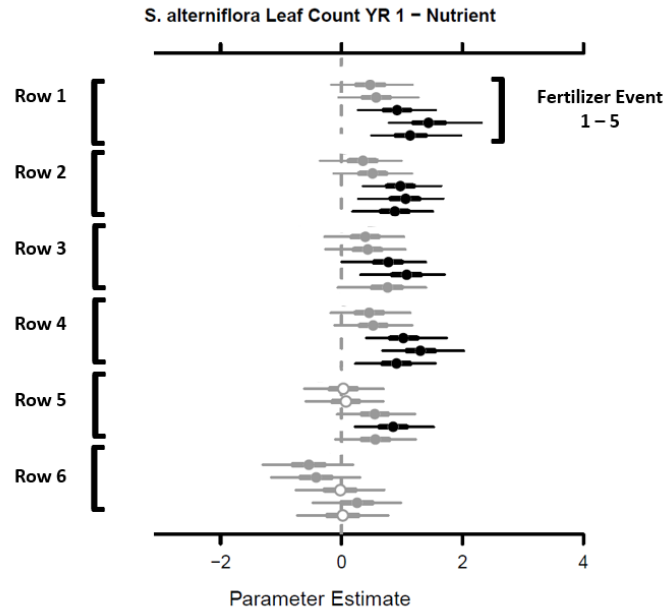


Figure 1.10 Posteriors of nutrient impact on Year 1 *S. alterniflora* leaf count over five nitrogen additions, grouped by rows (Row 1 is the most inundated, Row 6 is the least inundated).

Credible intervals of nutrient impact (nitrogen addition) on leaf count were shown here with the thin lines denoting 95% credible intervals, and the thick lines representing 50% credible intervals. The dots indicate medians of the posteriors. The black color indicates strong impact (95% Cis not overlapping 0), the grey color indicates moderate impact (50% Cis not overlapping 0), and open white circles mean little to no impact (both 95% and 50% Cis overlapping 0). Output was generated in R using the MCMCvis package (Youngflesh 2018).

1.3.2.4 The impact of pre-condition on morphological traits

Pre-condition largely had a positive impact on most of the morphological traits in Year 1, with strong positive impact on Sa. and Sp. plant height, Sa. stem width, and Sp. stem count, as well as a moderate positive impact on Sa. leaf width and Sp. stem width (Table 1.7). Year 2 exhibited more mixed impact, with strong positive impact on Sa. and Sp. plant height (consistent with Year 1), Sp. leaf count, Sa. leaf length, a moderate positive impact on Sp. leaf length, a now strong negative impact on Sp. stem count, and a

moderate negative impact on Sa. leaf count and leaf width (Table 1.7). The mixed effects can mean the tradeoffs of different morphological traits in response to the vegetative initial condition.

Table 1.7 Summary of signs of 50% and 95% credible intervals (CIs) of pre-condition impact based on the posteriors of multi-level Bayesian models for metrics of *Spartina alterniflora* and *Spartina patens*.

Also see 50% and 95% CIs in Figures A.5-14 in the appendix (Sa. denotes *Spartina alterniflora*, Sp. denotes *Spartina patens*) (If no signs were provided for a particular CI, it means the CI intercepted 0).

		Year 1 (5 months)		Year 2 (1.5 years)	
Metrics	Species	Pre-Condition		Pre-Condition	
		95% CI	50% CI	95% CI	50% CI
Plant Height	Sa.	+	+	+	+
	Sp.	+	+	+	+
Leaf Count	Sa.				-
	Sp.			+	+
Leaf Length	Sa.			+	+
	Sp.				+
Stem Width	Sa.	+	+		
	Sp.		+		
Leaf Width	Sa.		+		-
Stem Count	Sp.	+	+	-	-

1.3.2.5 The impact of senescence or seasonality on morphological traits

In Year 1, I focused on the impact of time since the vegetation was planted in the marsh organ. I expected some impact attributable to adaption and senescence. It appears that senescence limited Sa. and Sp. plant heights and some negative impact in Sa. stem width, while it allowed individuals of both species to continue producing new leaves as time progressed (Table 1.8). By Year 2, when the vegetation should be acclimated to the

new environment as recovery generally takes only a few weeks (Brown et al., 2006), we focused on the impact of seasonality because the 2022 measurements spanned the spring, summer, and fall seasons. Temperature showed a largely positive impact. The one exception is the little to no impact of temperature on plant height, and negative impact on *Sa.* leaf length. Again, the mixed impact of temperature can suggest tradeoffs of varying morphological traits.

Table 1.8 *Summary of signs of 50% and 95% credible intervals (CIs) of senescence/seasonality impact based on the posteriors of multi-level Bayesian models for metrics of *Spartina alterniflora* and *Spartina patens*.*

*Also see 50% and 95% CIs in Figures A.5-14 in the appendix (*Sa.* denotes *Spartina alterniflora*, *Sp.* denotes *Spartina patens*) (If no signs were provided for a particular CI, it means the CI intercepted 0).*

		Year 1 (5 months)		Year 2 (1.5 years)	
Metrics	Species	Days		Month Temp	
		95% CI	50% CI	95% CI	50% CI
Plant Height	<i>Sa.</i>	-	-		
	<i>Sp.</i>	-	-		
Leaf Count	<i>Sa.</i>		+	+	+
	<i>Sp.</i>		+		+
Leaf Length	<i>Sa.</i>			-	-
	<i>Sp.</i>				+
Stem Width	<i>Sa.</i>		-		
	<i>Sp.</i>				+
Leaf Width	<i>Sa.</i>				+
Stem Count	<i>Sp.</i>				+

1.3.2.6 The impact of channel on morphological traits

Three traits of *Sa.* plants from the eastern channel outperformed individuals transplanted from the western channel in both years (Table 1.9). Better productivity was consistent in leaf length for the entire duration of the study. The one exception is that vegetation from the west channel exhibited moderately higher leaf counts in Year 1. However, the advantage of the west channel in leaf count disappeared in Year 2 with larger leaf counts from east channel transplants witnessed in Year 2 (Table 1.9).

Table 1.9 Summary of signs of 50% and 95% credible intervals (CIs) of channel impact based on the posteriors of multi-level Bayesian models for metrics of *Spartina alterniflora*.

Also see 50% and 95% CIs in Figures A.5-14 in the appendix (*Sa.* denotes *Spartina alterniflora*) (If no signs were provided for a particular CI, it means the CI intercepted 0).

		Year 1 (5 months)		Year 2 (1.5 years)	
Metrics	Species	Channel		Channel	
		95% CI	50% CI	95% CI	50% CI
Plant Height	<i>Sa.</i>			-	-
Leaf Count	<i>Sa.</i>		+	-	-
Leaf Length	<i>Sa.</i>	-	-	-	-
Stem Width	<i>Sa.</i>	-	-		
Leaf Width	<i>Sa.</i>		-		

1.4 Discussion

We studied the impact of diverse environmental factors and initial condition of individuals on biomass along with a wide variety of key morphological traits of two

common salt marsh vegetation at two different temporal scales. While three-dimensional biomass showed the accumulated result for vegetation growth, studying one-dimensional morphological traits can provide a more in-depth explanation for what was observed in the biomass, and lend more information to the tradeoffs of vegetation growth in order to understand potential strategies plant individuals or species undertook to maximize productivity in a stressful environment. While our measures of time are relative to this study, the different results at different temporal scales emphasize the importance of long-term study to gain better understanding and construct more accurate predictions on vegetation's response to environmental stressors.

The impact of inundation on biomass largely matched their corresponding morphological traits in Year 2, especially for *Spartina alterniflora*. Optimum inundation levels exist for all the *Spartina alterniflora* Year 2 traits except stem width, however, different traits reached the maximum at different inundation levels. Focusing on the medians of the predictions, plant height continued to increase until 89% of inundation time, while leaf count and leaf length increased only until 35% and 40% of inundation time respectively. Leaf width lay in middle, reaching the maximum when inundation was 57% of time. Stem width, as an exception, increased linearly with inundation. These combined responses result in above- and belowground biomass reaching the maximum at 50% and 44% of inundation time. This suggests that *Spartina alterniflora* increased plant height and stem width at the expense of leaf count, leaf length, and then leaf width. This strategy allowed individuals to remain stable and keep leaves above water for photosynthesis under increased inundation.

Spartina patens, on the other hand, negatively responded to inundation in biomass, plant height, leaf count, and stem width. When inundation surpassed 52% of time, leaf length began to increase but was not able to offset the reduction of other traits, and therefore biomass continued to decrease. The better adaption of *Spartina alterniflora* to inundation than *Spartina patens* is consistent, as *Spartina patens* occupies marsh habitat at higher elevation and less inundation than compared to *Spartina alterniflora* (Snedden 2015; Stalter and Baston; 1969). Our findings also align with previous marsh organ experiments (Snedden 2015; Kirwan and Guntenspergen, 2015; Kirwan et al., 2012; Morris, 2007).

Nutrient addition had a strong positive impact on aboveground biomass for both species in the short- and long-term. However, nutrient addition had little to no impact on Sa. and Sp. belowground biomass in Year 1. It was only in Year 2 that we observed the strong positive impact, suggesting that belowground biomass had a lagged response to the nitrogen addition, indicating that the effect of nitrogen on above- and belowground biomass became more pronounced over time. This lagged response of belowground biomass to the nitrogen addition in Year 1 may be due to the resource allocation of the plants, that the extra nitrogen uptake may be used in the aboveground biomass first. Another potential reason for this lagged response may be that the stress the plants experienced from transplantation into the marsh organ could have prevented impact in the belowground biomass, and by Year 2 this stress was reduced and we observed strong impact. Previous papers support these findings that N fertilization increases *Spartina* productivity (Langley et al., 2013; Mendelsohn, 1979). We did not find the interaction between nutrient and inundation important in the majority of the traits except for Sa. leaf

count in Year 1. This interaction shows that nutrient increased leaf count, especially in the higher inundation levels, helping alleviate the stress of inundation.

There exist contrasting results describing elevated nutrient impacts on belowground biomass and the further effects on root strength (Wu et al. in press). Hollis and Turner (2019) and Turner (2011) showed significant decline in root strength after small increases in nutrient availability. Other studies, however, did not show decreased belowground production when introduced to high nutrient addition (Anisfeld and Hill, 2012; Day et al., 2013; Fox et al., 2012). Particularly, greenhouse studies demonstrated that biomass production of *Spartina patens* increased with nitrogen addition, with a more pronounced increase in lower salinity than in higher salinity (DeLaune et al., 2005). Eelsey-Quirk et al. (2019) pointed out that larger sediment availability is necessary to offset the negative impact from the larger variability of environmental factors or excessive nutrients driven by freshwater diversions. However, it is not clear how much is assimilated versus lost through the denitrification process. Whether our findings on the increased above- and belowground biomass from nutrient additions based on the marsh organ experiments can be transferred to field observations requires further investigation.

The pre-condition of plants when they were first planted exhibited some impact on biomass in short-term, but not in long-term, indicating that the environmental factors played a more important role in productivity than the initial condition of the plants. The negative effect of pre-condition on aboveground biomass of Sp. might be due to the artifact of the selected pre-condition metric (stem count). When we studied the individual morphological traits, we found positive to no impact of pre-condition in Year 1, but mixed results in Year 2. The mixed impact might offset each other somehow, partially

explaining why there is no impact in biomass results, in addition to the diminishing impact of initial condition compared to environmental conditions.

For *S. alterniflora* biomass, the eastern channel plants strongly outperformed the western channel plants in the short-term. However, this effect lessened to moderate outperformance in the long-term, suggesting that environmental conditions played a more important role than the source of vegetation as the time went through the adaptation mechanism. The better productivity in the vegetation from the eastern channel was also reflected in the majority of the morphological traits. The eastern channel is much more anthropogenically influenced from urban development, industrial factories on the shorelines, and dredged channels when compared to western channel. The vegetation transplanted from the disturbed sites may have been able to outperform the local individuals given that their environmental constraints were removed. In the field observation, the western channel of the Pascagoula River contained significantly higher belowground biomass than the eastern channel, while vertical distribution of belowground biomass did not strongly vary between channels (Grimes, 2021). While more work could further evaluate the differences between the East and West channel plants, I do not believe that incorporating plants from the two channels strongly impacted my modeling results, especially as the outperformance decreases over time and origin of an individual matters less. Collecting plants from both channels may actually help to better link a biomass function from this study to saltmarsh wetlands under a range of anthropogenic stressors.

Looking at the impact from seasonality, measured either in days since transplant in Year 1 or monthly temperature in Year 2, the mixed responses witnessed in Year one

may be due to the plants adapting and/or senescence resulting in mostly positive impact with temperature. For *S. alterniflora*, the results suggest existence of a tradeoff, where leaf count and leaf width favorably responded to higher temperature at the cost of leaf length.

It should be noted that the overall inundation percentages for Year 1 reflects the original marsh organ design fairly well. However, Year 2 percentages failed to meet the designed inundation percentages. This could be attributed to many reasons, such as storms, precipitation, and seasonal and tidal water changes, as mentioned earlier in this paper. Precipitation for 2022 (Year 2) was almost 20% lower than the precipitation for 2021 (Year 1), and in some months, exhibited up to 70% less precipitation (precipitation data gathered from <https://www.wunderground.com/history/daily/us/ms/gautier/KPQL>). This was particularly noticeable over the winter seasons – which may have resulted in even lower inundation levels due to low, seasonal tides.

1.5 Conclusion

There are a few general trends noticeable from the results of this study. Increased inundation negatively impacted Sp., however there existed an optimal inundation level for Sa. This suggests that the low marsh plant *S. alterniflora* will, to some degree, adapt better to increasing inundation while high marsh plant *S. patens* will struggle to adapt. Nutrient addition stimulated both below- and aboveground biomass for both species, where this effect was more pronounced in the long-term. The incorporation of temporal scales explicitly highlighted the importance of how a longer-term study to lends insight on the adaptation of transplanted individuals to their new environment conditions, which played a more important role than the initial vegetations' status as time progressed. Some

impacts increased over time, such as nitrogen addition, while others decreased, such as source of vegetation. In this study we observed some tradeoffs between different morphological traits in response to environmental stressors, indicating various growth strategies to maximize productivity.

This study benefits our understanding of the factors relevant to sea level rise, freshwater diversions, and climate change in addition to their impact on common, coastal wetland vegetation in the short and longer-term. These findings will therefore potentially facilitate further evaluation of conservation and restoration practices on coastal wetlands.

CHAPTER II - ASSESSING RESILIENCE OF A COASTAL WETLAND TO SEA-
LEVEL RISE CLOSE TO A LOUISIANA NATIVE TRIBE – INTEGRATING
BIOPHYSICAL PREDICTION AND TRADITIONAL ECOLOGICAL KNOWLEDGE

2.1 Introduction

Climate and environmental change have been impacting various cultures and peoples disproportionately. Indigenous peoples in coastal systems are particularly sensitive to climate change, directly influencing their resource-based livelihoods and homes (Wildcat, 2013; Bethel et al., 2022). Because of the vulnerability tribe members face, they have adapted over the generations to account for environmental conditions such as accelerated sea-level rise, extreme weather events, and erosion (Bethel et al., 2022). This generational knowledge passed down among indigenous peoples is described as traditional ecological knowledge (TEK), acquired through observing the natural environment over hundreds of years through direct human contact (Berkes, 1993), and delivered through oral history to better understand the connection between humans and nature (Bethel et al., 2022; Usher, 2000; Nadasdy, 1999). TEK distinguishes itself from typical scientific ecology by centering on a large social context, which, while different than western science, is just as good in many ways (Gadgil et al., 1993; Berkes, 1993).

This type of data is place based and generational; because of that, TEK is linked to culture, livelihood, and resiliency, making it inherently diverse in its content and how it can inform (Thompson et al., 2020). TEK will likely provide more insights if incorporated into quantitative, biophysical models, or science knowledge (SK) models, that focus on integration and prediction (Bethel et al., 2022; Moller et al., 2004). A variety of models have been developed to predict the impact of sea-level rise on coastal

wetlands and to assess saltmarshes' ability to keep pace with rising waters (Wu et al., 2017a, 2020, Morris et al. 2003, Kirwan and Murray, 2007, etc.). These models only incorporate ecological or biophysical data and fail to include broader perspectives (Hatfield et al., 2018), which are often limited by the spatial resolution inputs of LiDAR elevation data. Alternatively, when integrating these ecological approaches with traditional ecological knowledge, this combination produces complementary and overlapping views of the causes and potential consequences for change (Hatfield et al., 2018) because TEK is not a replacement for SK but a counterpart to it (Berkes, 1993; Suzuki and Knudtson, 1992). This combination of TEK and SK models may help to obtain insights that couldn't be captured by GIS data. In terms of people, the combined TEK and SK also strengthens community ties, highlights generational knowledge, reduces barriers to local science, and paves the way for future partnerships while making local science more accessible (Moller et al., 2004).

The combined predictions will enhance the Pointe-au-Chien Indian Tribe members' understanding of their changing coastal system, support more-informed adaptation plans that increase the local resilience to climate change and sea-level rise and give a sense of data ownership while furthering science empowerment (McAllister et al., 2019; Moller et al., 2004). The combination of biophysical models and TEK will better inform the management and environmental monitoring in ways that complement the differences between the two knowledge systems - enriching and adding to the collective ecological knowledge while producing creative strategies and giving the local citizens power to understanding the ecological situation on their own terms (Bethel et al., 2022; Thompson et al., 2020).

2.1.2 Objectives and Hypotheses

This study aims to:

- 1) Predict the impact of sea-level rise on landscapes of *Spartina alterniflora*-dominated coastal wetlands in the Terrebonne Bay close to a local indigenous tribe by Year 2100 using a biophysical, mechanistic model (SK).
- 2) Create a tool that evaluates the coastal vulnerability of the landscape to sea-level rise by combining biophysical modeling and traditional ecological knowledge (TEK).

My hypotheses tested include:

- 1) The Terrebonne Bay area surrounding the Pointe-au-Chien Indian Tribe (PACIT), a State recognized Native American tribe, will show accelerated wetland loss under sea-level rise.
- 2) The incorporation of the TEK assessments with the SK predicted wetland loss will produce a vulnerability that is more extensive compared to the SK or TEK alone.

2.2 Methods

In order to test these hypotheses, I calibrated a mechanistic, biophysical model that spatially predicted coastal wetland change impacted by sea-level rise (Wu et al, 2020). With the model predictions by 2050 and 2100 at different SLR rates, I further derived SLR thresholds beyond which coastal wetlands will be lost dramatically. This SK model simulates elevation change-driven habitat change, informed by its simulated sediment accretion and erosion. The key inputs include elevation, initial coastal wetland distribution, the relation between vegetation productivity and elevation (and soil

porewater salinity), and total suspended sediments. Based on the predicted wetland loss, I classified the landscape into three levels of vulnerability, and then combined it with the vulnerability map that represents the PACIT's TEK in the Terrebonne Bay of southern Louisiana. In combining a SK sea-level model output with the local TEK assessment map, we engaged with multiple knowledge systems (Lake et al., 2018) to create new opportunities of examining coastal land loss through diverse perspectives. The creative strategy recognizes the benefit of local knowledge in applied research and participatory mapping approaches and ultimately helps to break down the barrier between social and scientific knowledge (Bethel et al., 2022; Laituri, 2011).

2.2.2 Study Area

Coastal Louisiana is a dynamic landscape that is home to many indigenous tribes, such as the PACIT (Fig. A.15-16). This state recognized tribe inhabits Louisiana's Terrebonne and Lafourche Parishes along Bayou Pointe-au-Chien, roughly 75 miles southwest of New Orleans (Bethel et al., 2022; Rivard, 2015) (Fig. A.16). The PACIT descends from the regional Chitimacha, Biloxi, and Acolapissa tribes and has roughly 800 members who center around a key subsistence and commercial livelihood base of fishing, shrimping, oyster farming, hunting, and crabbing. Tribe members speak Indian French and continue to live and work with the land despite issues arising from climate change, such as land loss resulting in village migration further north and increased salinity driving away species traditionally used for fishing and trapping (Bethel et al., 2022; Ferguson-Bohnee, 2015; Rivard, 2015).

The PACIT and other tribes in this area face the combined effects of subsidence, continuous erosion, and sea-level rise, resulting in one of the areas with the highest rates

of relative sea-level rise (RSLR) in the world (NOAA, 2012; Bethel et al., 2022; Karimpour et al., 2013) (Fig. A15). The PACIT's ecosystem-dependent livelihood base is a reason for their adaptability and understanding of the land. This way of life, however, contributes to the community vulnerabilities they face living in an area frequently impacted by tropical storms, hurricanes, and issues brought about from climate change such as salinity inundation and land loss. It is important to study the wetlands around the PACIT. Coastal wetlands play an important role in enhancing livelihoods in the area. They have been shown to be effective to mitigate storm surge flood risks (Fairchild et al. 2021, Costanza et al. 2008). In addition, "more than 75% of the commercial and 90% of the recreational harvest of fish and shellfish in the U.S. depend on coastal wetlands for food or habitat during some part of their life cycle" (<https://coastalresilience.tamu.edu/home/wetland-protection/value-of-coastal-fisheries-and-wetlands/>). Understanding this area of incredibly high RSLR will not only help predict ecosystem change but also aid the tribe's knowledge of their landscape; through risk identification and preventative management they can better maintain their way of life, protect sites of cultural importance, and inform potential structures for adaptation (Maldonado, 2014; Bethel, et al., 2022).

The Terrebonne Bay, located in Terrebonne Basin between the Mississippi River bird foot delta and the Atchafalaya delta, was part of a deltaic plain of the Mississippi River several thousand years ago and served as a main distributary within the last 1000 years (Coleman, 1981; Karimpour et al., 2013; Penland et al., 1987; Wang et al., 1993). The bay surrounded by wetlands including a large proportion of saltmarsh habitat, which is a highly productive system of primary production and carbon storage (Chmura et al.,

2003; Hill and Roberts, 2017; Karimpour et al., 2013). The saltmarshes of Terrebonne Bay are dominated by *Spartina alterniflora*, with smaller patches of *Avicennia germinans*, *Spartina patens*, *Distichlis spicata*, and *Juncus roemarianus* also observable (Hill and Roberts, 2017).

The Terrebonne Bay rarely sees clear water and receives little to no fluvial inflow or external sediment deposition – as such the sediment and turbidity changes seen here are attributed to the processes that occur within the wetlands and the bay, such as bay bed erosion, wave activities, cold fronts, and storm influences (Karimpour et al., 2013). The coastal marshes of this region experience low amplitude tides (~0.3 m; Hill and Roberts, 2017) that are diurnal with microtidal fluctuations, as well as irregular floodings, with inundation more influenced by wind and larger-scale meteorological activities than by tides (Childers and Day, 1998; Turner, 2001; Schutte et al., 2020; Wang et al., 1993). Using the Coastwide Reference Monitoring System (CRMS), the average 2022 salinity measured around this study’s field sites were reported as 21.04 (ppt), with an average water temperature of 22.96 (°C). https://www.lacoast.gov/crms_viewer2/Default.aspx).

2.2.3 Field Work

To collect the biophysical data needed for the mechanistic SLR model, including vegetation productivity indicated by peak-season live biomass, soil pore-water salinity, and total suspended system (TSS), we conducted field work in the coastal wetlands of the Terrebonne Bay close to the PACIT’s territory, taking place at the end of the growing season in December 2022 and again in September 2023. The sample sites were determined by accessibility and proximity to the Coastwide Reference Monitoring System locations (Fig. 2.2). We collected above- and belowground biomass at five sites.

At each site, we set up two parallel 3-m transects perpendicular to the coastline. At each transect, we selected three subsites that were about 1 m apart and took duplicate samples at each subsite (Fig. 2.2). Spatial coordinates were measured at each subsite along the transects. To collect aboveground biomass, we placed 25 x 25cm quadrats at each subsite along the transects, cutting the entirety of alive and dead surface biomass within each quadrat, placed in bags, and stored in coolers to stave off decomposition. After removing the aboveground biomass, we collected belowground biomass at the same location using 30 cm long 4-inch (10.16 cm) diameter soil cores, which were then separated into 0 – 5, 6 – 10, 11 – 15, 16 – 20, 21 – 25, and 26 – 30 cm depths using a handsaw and then stored in a cooler (Fig. 2.1). Bags were placed in a cooler until returned to the lab and then stored in 4 °C refrigerators for later processing. We took three water samples using one liter bottle grabs as we approached each site with coordinates recorded in order to derive the total suspended solids (TSS) (Fig. 2.2).



Figure 2.1 *Field work showing below-ground biomass extraction with the PVC soil corer and handsaw to cut below-ground biomass samples into 5 cm sections (left) and soil cores ready for sectioning (right).*

2.2.4 Laboratory Processing

The processing of above- and belowground biomass is the same as in chapter 1. To calculate porewater salinity, I placed 10 grams of wet soil from each depth of each subsite in oven-safe trays and dried it in an oven at 75°C until a constant weight is reached, roughly 3-4 days. After the soil dried, I calculated the difference between the wet and dry weight as the soil moisture content. I added 20 milliliters of distilled water to each sample of dry soil and mixed them thoroughly to allow salts adsorbed onto the soil to be dissolved in water. I then let the solids to settle for at least an hour, after which I then used a refractometer to measure soil salinity in units of parts per thousand (ppt). Using this data, I calculated porewater salinity with a mass balance equation:

$$\text{Porewater salinity (ppt)} = \text{measured salinity (ppt)} * \left(\frac{20}{\text{wet sample weight} - \text{dry sample weight}} \right)$$

To calculate TSS from the water samples, I placed pre-weighed glass fiber filters in a furnace at 400°C for four hours to remove organic content. Once ashed, I weighed the filters again with an analytical balance and used a vacuum pump to filter water samples with duplicates from each bottle to the prepared filter papers, recording the volume used. The wet filter papers were then dried in an oven at 75°C overnight to completely dry out and remove the remaining water. Once dry, the filters with the solids were weighed to collect filter paper and total solids weights. I then put the dried filter papers back in the furnace for four hours and weighed them again to get just the inorganic sediment weights. With this data, I calculated TSS using the equation

$\frac{\text{Inorganic weight (mg)} - \text{Filter weight (mg)}}{\text{Sample volume (L)}}$. The in-situ 2022 biophysical data are listed in

Tables A.10-11.

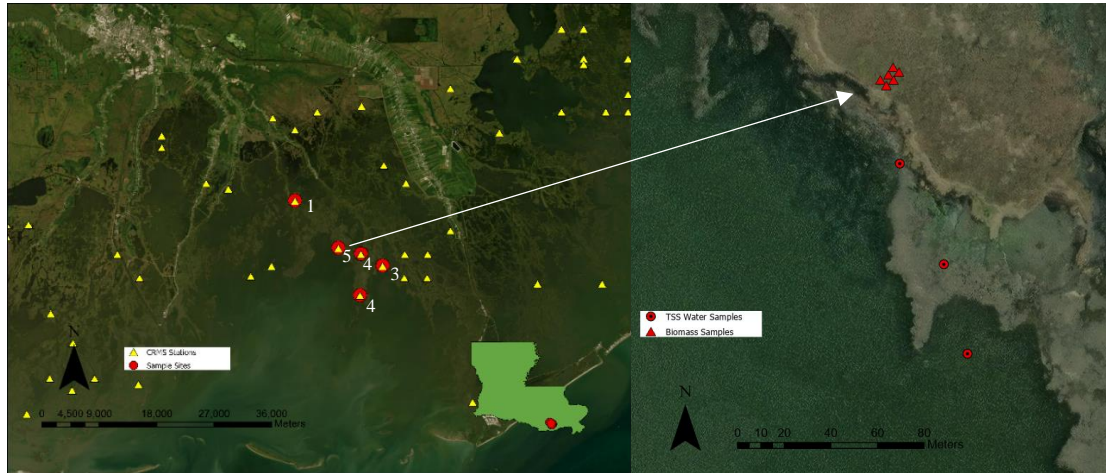


Figure 2.2 Map of southern Louisiana's Terrebonne Bay with five sample sites (red circles) in proximity to the CRMS sites (yellow triangles) (left), and sample site location #5 with the locations for TSS water samples (red circles with black dot) and the biomass samples (red triangles) (right).

2.2.5 Model

I applied a landscape model (Wu et al., 2017a, 2020) to predict coastal wetland change based on biophysical data collected from field site visits in December 2022. This model accounts for vegetation responses and hydrodynamics in order to construct predictions of salt marsh distributions under future scenarios of SLR (Wu et al., 2017a, 2020). It is a two-dimensional and mechanistic model that uses elevation as the key driver for vegetation productivity and landscape change while also simulating accretion and erosion (Wu et al., 2017a, 2020) (Equation 2.1) (Fig. A.17). The model for this study uses biophysical inputs to predict elevational change and the conversion of saltmarshes to estuarine open water once the elevation is below the mean low water level on 2×2 m blocks (Wu et al., 2020).

$$Elev_t = Elev_{t-1} - RSLR_t + A_t - Ero_t$$

Equation 2.1 where Elev denotes elevation, RSLR denotes relative sea-level rise rate, A denotes accretion rate, and Ero denotes erosion rate. The subscript t denotes time (adapted from Wu et al., 2017a).

The model inputs include 2011 LiDAR-derived elevation data from the U.S. Army Corps of Engineers, with a spatial resolution of 2 meters and in the vertical datum of NAVD88. The current relative sea-level rise (RSLR) rate is 9.1 mm/year (Herbert et al., 2021). Sediment bulk density was acquired through the Coastwide Reference Monitoring System (CRMS), averaged from the field locations as 0.289 g/cm³ for the Terrebonne Bay, Louisiana. Saltmarsh spatial distribution maps from 1989 and 2023 were available from the National Wetland Inventory datasets. Both organic and inorganic total suspended solids (TSS), and above- and belowground biomass were collected in-situ, with mineral sediments and belowground biomass contributing to inorganic and organic accretion (Wu et al., 2017a, 2020). For more details on the model, see Wu et al, 2017a.

The output of this spatial model produces maps of predicted coastal wetland distribution. Based on the levels of wetland loss, I classified the maps into different levels of vulnerability. I then combined vulnerability maps derived from the biophysical modeling with previously collected TEK spatial data using an overlay to understand more comprehensively the vulnerability of coastal wetlands to sea-level rise and priority areas that need urgent protection from the PACIT's perspective. The TEK assessment output is based on sustainability goals (listed by low to high priority goal) and vulnerability risk factors (listed by least to most at risk) identified by PACIT members through various

field-based interviews and focus group meetings (Bethel et al., 2022) (Fig. 2.3) (Tables 2.1 and A.12). An area with a high sustainability rating (3) means it contributes greatly to the PACIT's sustainability goals while a high vulnerability rating (3) denotes an area highly vulnerable to sea-level rise and subsidence (Bethel et al., 2022). In order to integrate the SK and TEK predictions, I focused on vulnerability from TEK and combined it with the vulnerability derived from the biophysical model. Then I overlaid sustainability with the combined vulnerability. By combining the TEK and SK maps, the predicted saltmarsh loss will be more informed and lend additional confidence to decision-making for the tribe's members and land-managers in the Terrebonne Bay.

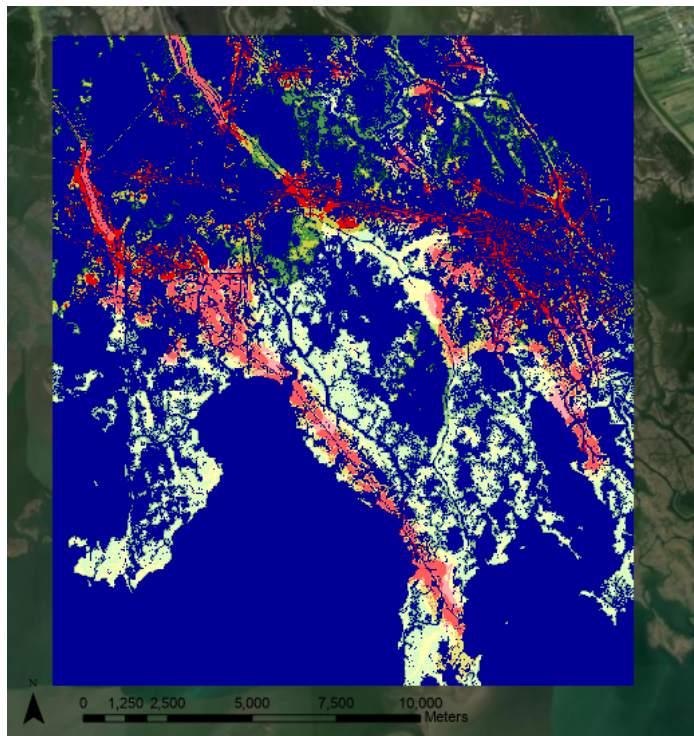


Figure 2.3 *Classification of PACIT's priority areas based on a combination of sustainability and vulnerability assessments from the tribe's citizens, related to differences in perceived risk to coastal hazards (from Bethel et al, 2022).*

Highly fragmented land in dark red (upper right corner of the map) receives more sustainability and vulnerability importance than the lower-level priority areas in light green (for example, in the lower left and middle sections of the map) (Table A.12).

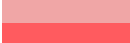
	Combined	Sustainability		Vulnerability	
	SV Code	Class	Level	Class	Level
	10	1	Low	0	Null
	11	1	Low	1	Low
	12	1	Low	2	Medium
	13	1	Low	3	High
	20	2	Medium	0	Null
	21	2	Medium	1	Low
	22	2	Medium	2	Medium
	23	2	Medium	3	High
	30	3	High	0	Null
	31	3	High	1	Low
	32	3	High	2	Medium
	33	3	High	3	High

Table 2.1 *Color codes for the sustainability and vulnerability combinations in Fig. 2.3 (from Bethel et al., 2022).*

2.2.6 Model Calibration and Assessment

I derived linear mixed effects models to simulate above- and belowground biomass as a function of elevation and soil porewater salinity with sample site as a random factor using the “lmerTest” package in R (<https://cran.r-project.org/web/packages/lmerTest/index.html>). We compared the models with different combinations of the covariates based on Akaike Information Criterion (AIC), and the model with the lowest AIC was selected as the best predictive model (Wu et al., 2020, 2017b). I found the best model was the one with only elevation as the covariate. We derived deposition rate by combining contribution from water column borne inorganic matter settled or intercepted by aboveground biomass and organic contribution from belowground biomass. To derive the spatial distribution of inorganic total suspended solids, I developed a mixed effects model relating the inorganic TSS with spatial

Northings in UTM projection with the site as the random factor. Like the other mixed effects models, this model was selected because it had the lowest AIC value.

As we designed our sampling sites to be close to CRMS sites, we could take advantage of existing data at the CRMS sites. We developed a regression to link the measured accretion rates at the CRMS sites with average biomass at our sampling sites. The coefficients derived were directly used in the landscape model to simulate accretion rates as a function of biomass. The five CRMS stations near the study sites report up to an average accretion of 2.54 cm/year with my model's simulated accretion rates ranging from 0 cm/year to 1.87 cm/year (https://www.lacoast.gov/crms_viewer2/Default.aspx). I further calibrated the model by comparing simulated 2023 erosion rates and water velocity to the measured data in literature. One study found that velocity rates for the Terrebonne Bay ranged from -0.5m/s to 0.5m/s (Wang et al., 1993), with my simulated velocity ranging from 0 m/s to 0.094 m/s.

Additionally, I evaluated the accuracy of the simulated saltmarsh distributions in 2023 to the NWI data in 2023 (considered as ground truth). I used a modified kappa that accounts for persistent land cover (van Vliet et al. 2011) and four metrics to evaluate the simulation accuracy on two land cover types (wetland vs. estuarine water): (1) hits (reference land change corrected simulated as change), (2) correct rejections (reference land persistence correctly simulated as persistence), (3) misses (reference change incorrectly simulated as persistence), and (4) false alarms (reference persistence incorrectly simulated as change (Pontius et al. 2011, Wu et al., 2015, 2020).

2.2.7 Model Scenarios and TEK Combination

With the calibrated SLR model, I ran the model under a variety of SLR rate scenarios, from SLR rates of 9 mm/year to 20 mm/year trying to identify the threshold of SLR. Even with the current SLR rate of 9.1 mm/yr, the wetland loss was already dramatic, so I decided to use the SLR rate that predicts wetland areas in 2100 as the half of the predicted wetland areas in 2100 when using the current SLR rate as the SLR threshold. It was determined to be 10 mm/yr. Then I ran the model under this SLR threshold and identified the wetland areas that would be lost by 2050 as the most vulnerable areas, the wetland areas that would be lost by 2100 as the medium vulnerable areas, while the wetlands that would be persistent by 2100 as the least vulnerable area.

To isolate predicted saltmarsh loss, I used the Extract by Mask, ReClassify, and Mosaic Raster tools in ArcPro on the two saltmarsh prediction maps (2050 and 2100 under SLR rate of 10 mm/yr) and the 2023 NWI map. I reclassified the TEK map from two digits to one digit (i.e the previous class 11 is now 1) where the reclassified maps' vulnerability assessments ranges from low (1) to high (3).

I multiplied SLR predictions by 10 and added it to the TEK reclassified vulnerability map using the Raster Calculator tool to derive a combined vulnerability map, with classes ranging from low (11) to high vulnerability (33). If the digits at tens and ones positions differed, the vulnerability classification from TEK and biophysical models did not match. This was expected as they are based on different evaluation methods. Once combined, I further reclassified the vulnerability map to scale from low (1) to high (3) vulnerability classes. Any numbers with the digit of 3 was classified as 3, any numbers with the digit of 2 was classified as 2, and 11 was classified as 1. An area

should be given high or medium vulnerability if either source of data identified it as high or medium vulnerability.

2.3 Results

2.3.1 Calibration

By comparing my predicted wetland map in 2023 and NWI 2023 data, the modified Kappa (van Vliet et al. 2011) that accounts for land persistence is 0.63, indicating a good agreement between the simulated map and reference map. This kappa is the product of $K_{transition}$ and $K_{translocation}$. $K_{transition}$ represents matches of quantities of transitions between reference and simulated maps and $k_{translocation}$ assesses matches of locations (van Vliet et al., 2011). Considering the kappa values, it seems easier to get the quantity correct ($K_{transition} = 0.93$) than to get location correct ($K_{translocation} = 0.68$). This assessment gives confidence that the model can adequately predict coastal wetland change.

2.3.2 Predictions under varying SLR scenarios and 10 mm/yr

Table 2.2 *Proportions of predicted wetland loss by year under various sea-level rise scenarios.*

Scenarios (Sea-Level Rise mm/yr)	Predicted Wetland Loss					
	2050		2075		2100	
	Area(ha)	Proportion	Area(ha)	Proportion	Area(ha)	Proportion
9	151.6648	0.059	214.4276	0.084	288.124	0.112
9.5	321.902	0.126	563.9256	0.22	669.6096	0.261
10	699.3304	0.273	1129.3972	0.44	1193.219	0.465
10.5	1096.3028	0.427	1502.406	0.586	1534.426	0.598
11	1548.9188	0.604	1888.2332	0.736	2553.743	0.74
11.5	1882.8184	0.734	2118.1944	0.826	2122.86	0.828
12	2131.808	0.831	2271.658	0.886	2273.099	0.886
12.5	2304.0744	0.898	2387.4828	0.931	2389.133	0.9315
13	2430.272	0.948	2476.9428	0.966	2478.298	0.966
13.5	2524.312	0.984	2549.2436	0.994	2550.482	0.994
14	2550.8056	0.995	2563.842	0.999	2564.642	0.999
14.5	2556.4664	0.997	2564.0952	0.999	2564.685	0.999
15	2559.456	0.998	2564.2704	0.999	2564.71	0.999
15.5	2560.9188	0.999	2564.3884	0.999	2564.722	0.999
16	2561.7996	0.999	2564.478	0.999	2564.73	0.999
16.5	2562.366	0.999	2564.5492	0.999	2564.734	0.999
17	2562.8028	0.999	2564.5976	0.999	2564.737	0.999
18	2563.4212	0.999	2564.67	0.999	2564.74	0.999
18.5	2563.6768	0.999	2564.6932	0.999	2564.741	0.999
19	2563.866	0.999	2564.7084	0.999	2564.742	0.999
19.5	2564.0216	0.999	2564.7176	0.999	2564.742	0.999
20	2564.742	0.999	2564.7236	0.999	2564.742	0.999

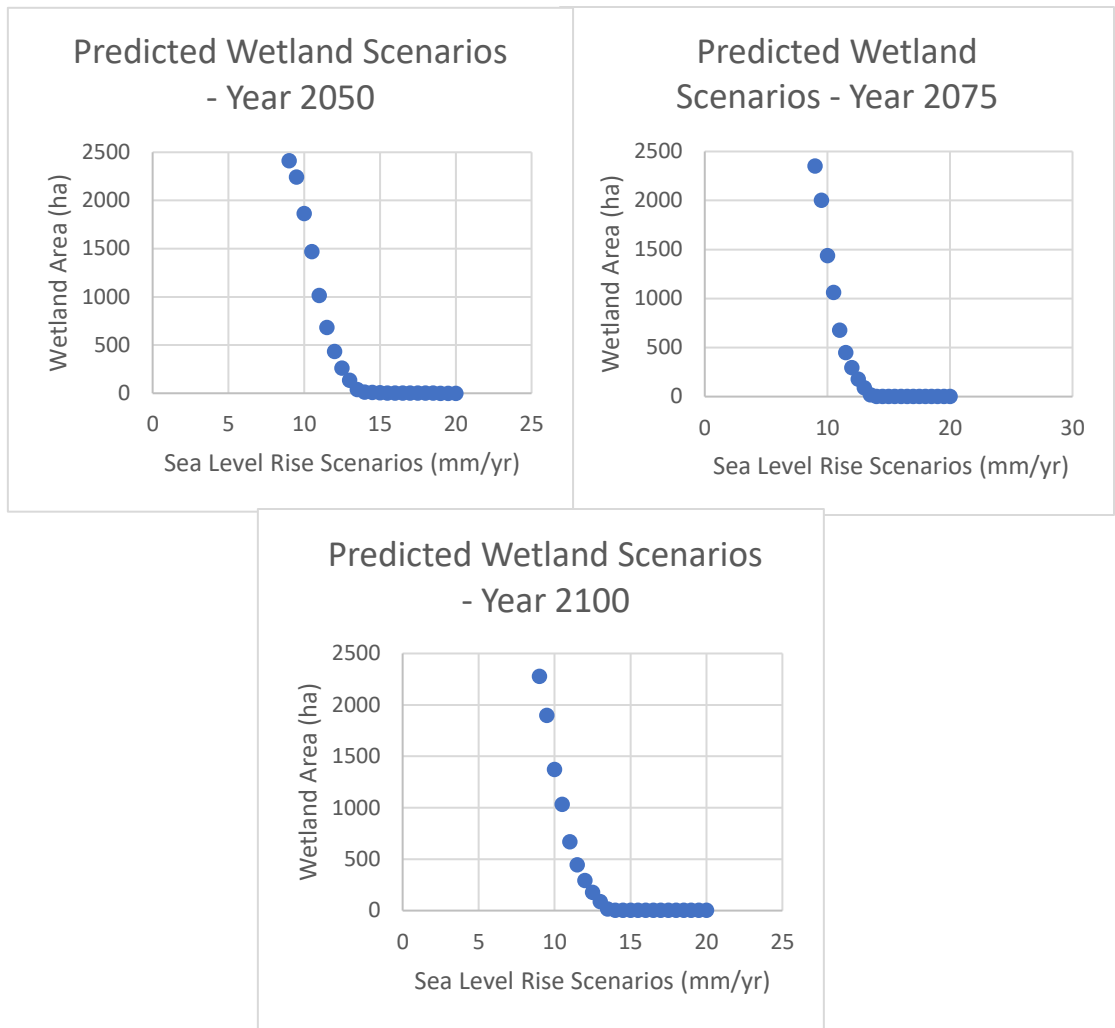
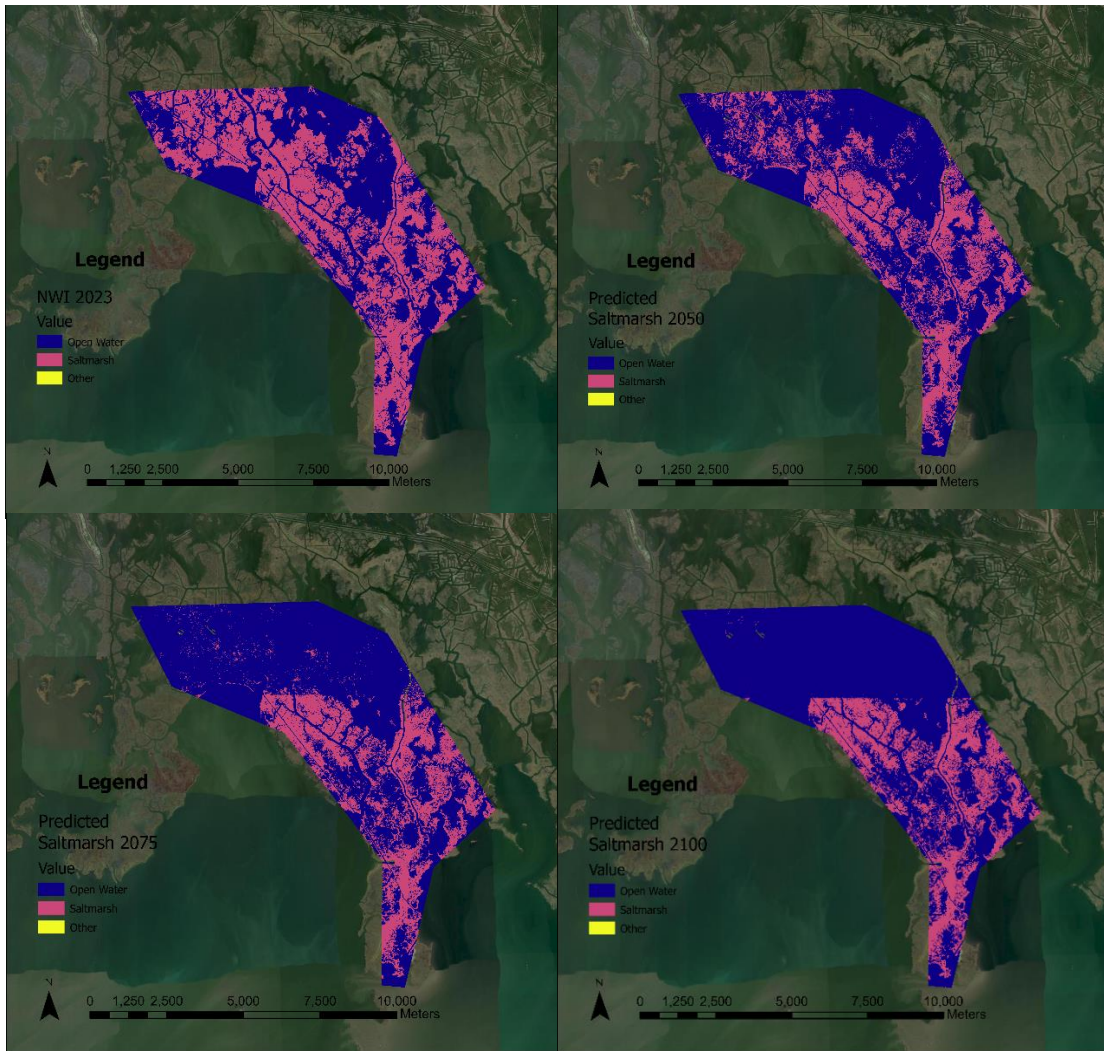


Figure 2.4 *Predicted wetland area (ha) under various sea-level rise scenarios (mm/yr), at years 2050, 2075, and 2100.*



Figures 2.5-8 NWI wetland map (top left) and wetland predictions by the year 2050 (top right), 2075 (bottom left) and 2100 (bottom right), produced from the SLR mechanistic model using 10mm/year SLR.

Wetland Predictions		
Year	Area (ha)	Proportion of Loss
2023	2564.743	0
2050	1865.412	0.273
2075	1435.346	0.44
2100	1371.524	0.465

Table 2.3 Current and predicted wetland loss area (ha) and proportion of loss by the year 2100, based on 10 mm/yr SLR (Figs. 2.5-8).

The proportion of predicted wetland loss under various sea-level rise scenarios for 2050, 2075, and 2100 indicate that wetland loss will accelerate after only a slight increase to the current RSLR of 9 mm/year (Table 2.2). Much of this predicted acceleration begins around 10.5 - 11 mm/year, after which the predicted wetland loss levels out at a proportion of 0.99. This is confirmed when observing the inflection points from the sea-level rise threshold graphs, where after 10 mm/year, the decrease in wetland area (ha) is much steeper (Fig. 2.4). From the biophysical model predictions (Figs. 2.6 – 2.8), much of the predicted wetland loss is located in the northern section of the PACIT study area, as well as around some of the fragmented habitat in the central area. The SLR model's predictions suggest that almost half of the wetland habitat in this study area will be lost by 2100 under the SLR threshold of 10 mm/year (Table 2.3).

2.3.3 Vulnerability from SK/SLR model

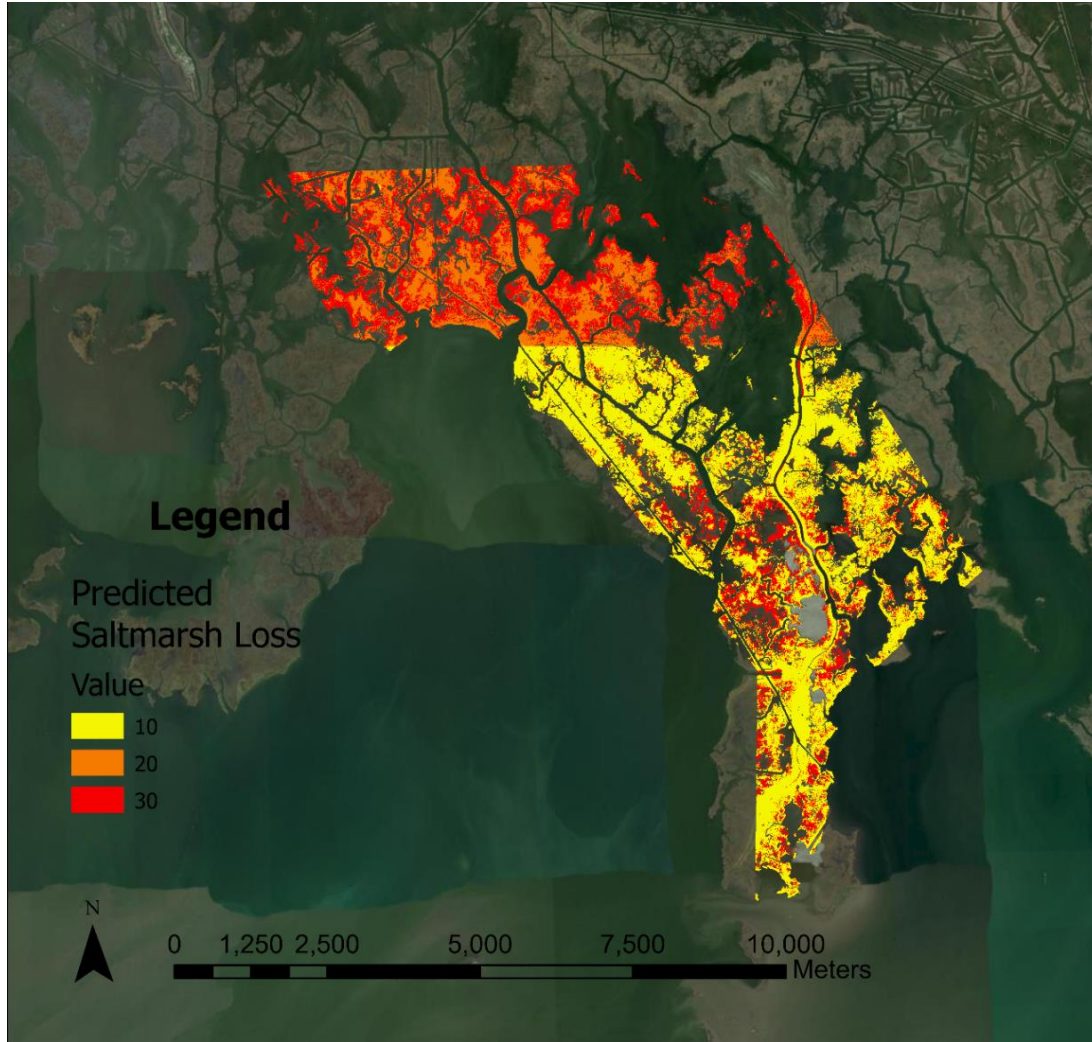


Figure 2.9 Coastal wetland vulnerability classified as high (red, loss by 2050), medium (orange, loss by 2100), and low (yellow, little to no predicted loss).

The predicted saltmarsh loss map from the SLR model classifies vulnerability based on persistence by 2100 (yellow), loss by 2100 (orange), and loss by 2050 (red).

The highest wetland vulnerability is centered in the northern part the study area as well as some of the edges of fragmented areas in the center (Fig 2.9). These will be the areas that require special attention by the resource managers. Orange or medium vulnerability areas, also largely in the northern section, require less attention as they reflect

vulnerability by the end of the century. The yellow areas take up most of the southern portion of the map and require the least attention from the PACIT or land managers (Fig. 2.9).

2.3.4 Combining TEK and SK vulnerability predictions

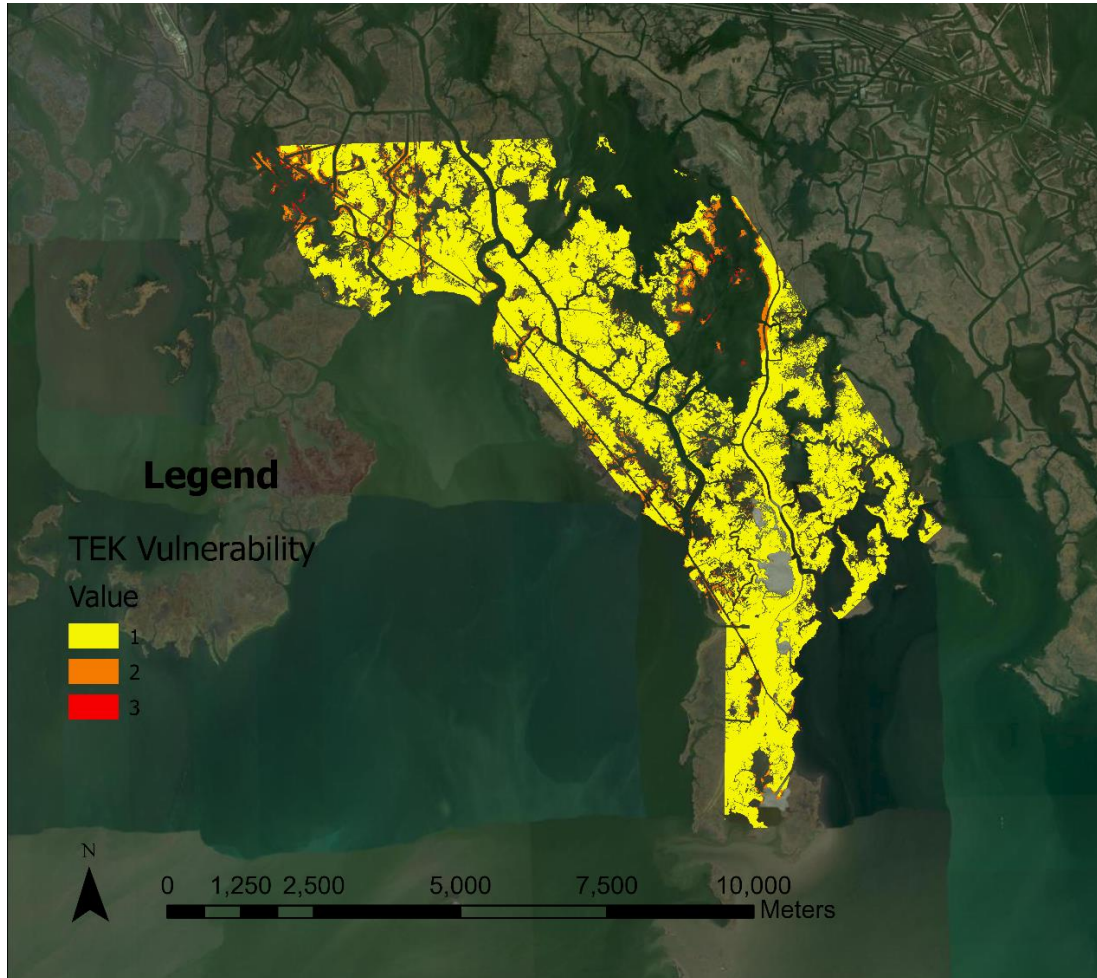


Figure 2.10 *Reclassified TEK vulnerability assessment, based on high (3) to low (1) vulnerability.*

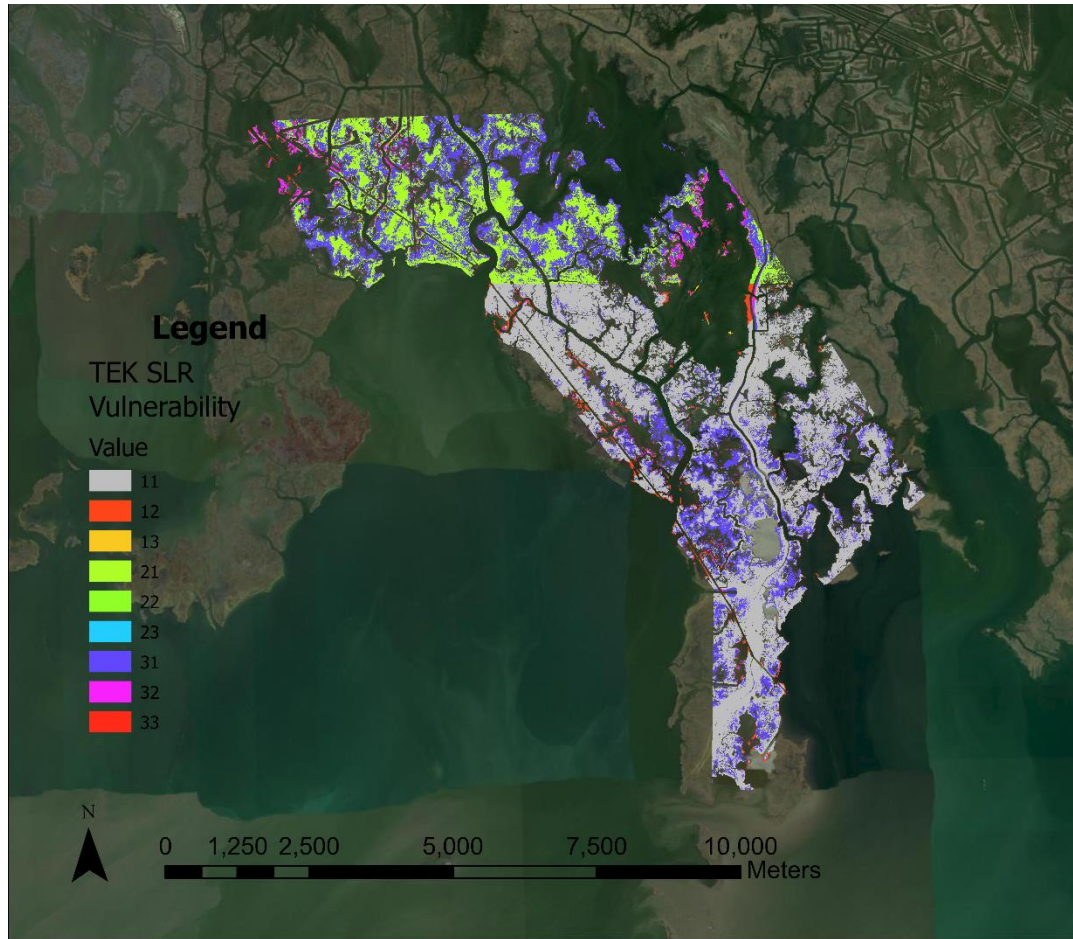


Figure 2.11 Saltmarsh vulnerability map based on TEK and SK data, constructed by combining the TEK vulnerability map (Fig 2.10) and the SLR saltmarsh loss prediction map (Fig 2.9).

Table 2.4 Classes, corresponding area, and proportion of area from Fig. 2.11.

TEK SLR Vulnerability Assessment		
Class	Area(ha)	Proportion
11	1159.3488	0.473
12	34.6404	0.014
13	0.7588	0.0003
21	438.9372	0.179
22	25.0664	0.01
23	0.6344	0.0003
31	721.7456	0.294
32	67.1412	0.027
33	5.5284	0.002

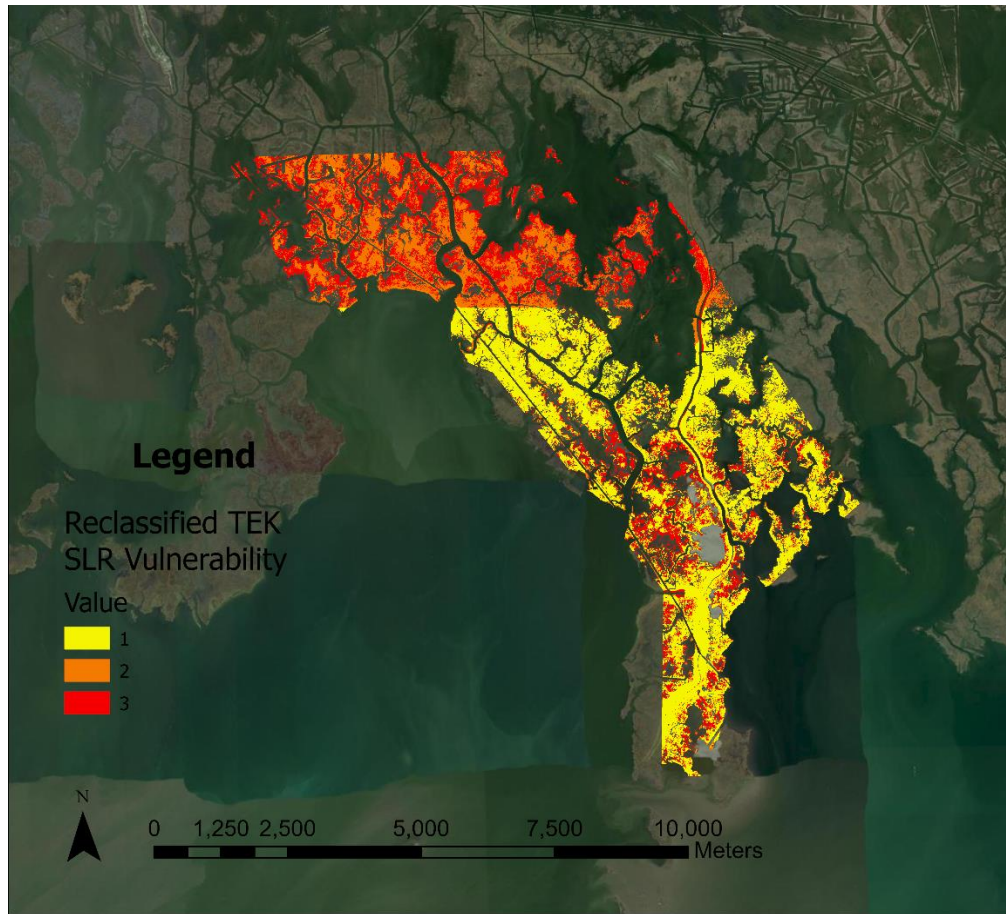


Figure 2.12 *Reclassified TEK SLR map from Fig. 2.11. High vulnerability areas are red (3), medium vulnerability is orange (2), and low vulnerability is yellow (1).*

Table 2.5 *Classes, corresponding area, and proportion of area from Fig. 2.12.*

Reclassified TEK SLR Vulnerability Assessment		
Class	Area(ha)	Proportion
1	1159.349	0.472
2	498.644	0.203
3	795.8084	0.324

Table 2.6 *Proportion of vulnerable areas (ha) by class for the TEK assessment, SLR predictions, and combined TEK + SLR assessment.*

Proportion of Vulnerable Areas			
Class	TEK	SLR	TEK + SLR
1	0.942	0.478	0.472
2	0.055	0.183	0.203
3	0.003	0.339	0.324

The separated TEK vulnerability assessments indicates that most of the PACIT study area is classified as low or nonvulnerable with a proportion of 0.94 (Fig. 2.10) (Table 2.6). The combination of TEK and SK produced a single map that identified vulnerable areas (Figs. 2.11). In this map, the class scale ranged from the lowest (11) to the highest (33) (Fig. 2.11). The first digit refers to information from the biophysical predictions and the second is from the TEK map (i.e., class 23, where 2 is from the biophysical model predicted map and 3 is from the TEK assessment).

The vulnerable areas that show agreement between the TEK and SLR maps are those that correspond with the classes 11, 22, and 33 (Fig. 2.11). We found the largest agreement is from class 11 with a proportion of 0.47, indicating that the two vulnerability assessments agree most on low or non-vulnerable saltmarsh habitat (Fig 2.11) (Table 2.4). The other classes show moderate to severe disagreement based on class arrangement (i.e., 21 is moderate disagreement while 13 is severe disagreement). Class 31 indicates there is large disagreement (0.29 proportion) between the TEK and biophysical vulnerability predictions (Fig. 2.11) (Table 2.4). This is because high vulnerability in the TEK assessment is very small (proportion 0.003), while the most vulnerable saltmarsh habitat,

most of which is predicted in the northern third of the SLR map, is much larger (proportion 0.339) (Table 2.6).

The combined TEK SK vulnerability map further reclassified to represent vulnerability from low (1) to high (3) shows the majority of coastal wetlands can persist under SLR (Fig. 2.12). High (red) and medium (orange) vulnerability areas are more highly concentrated in the northern third of the study area and around certain wetland edges in the southern section of the study area, while low (yellow) wetland vulnerability areas lie in the southern section of the study area (Fig. 2.12). This combined map shows much more high vulnerability (proportion 0.324) than the TEK vulnerability assessment (0.003), similar to high vulnerability shown in the SLR model predictions (proportion 0.339) (Fig. 2.12) (Table 2.5-6).

2.3.5 Sustainability and vulnerability

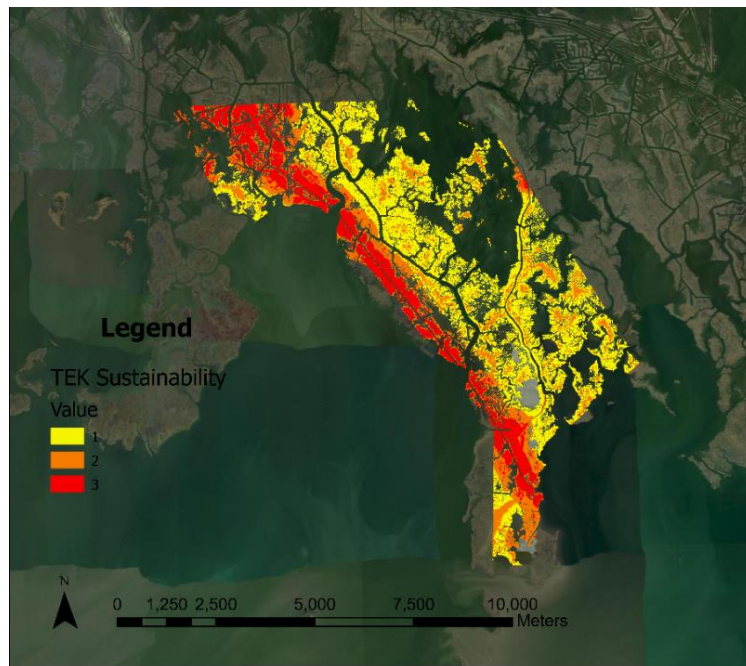


Figure 2.13 *Reclassified TEK sustainability assessment, based on high (3) to low (1) sustainability priority.*

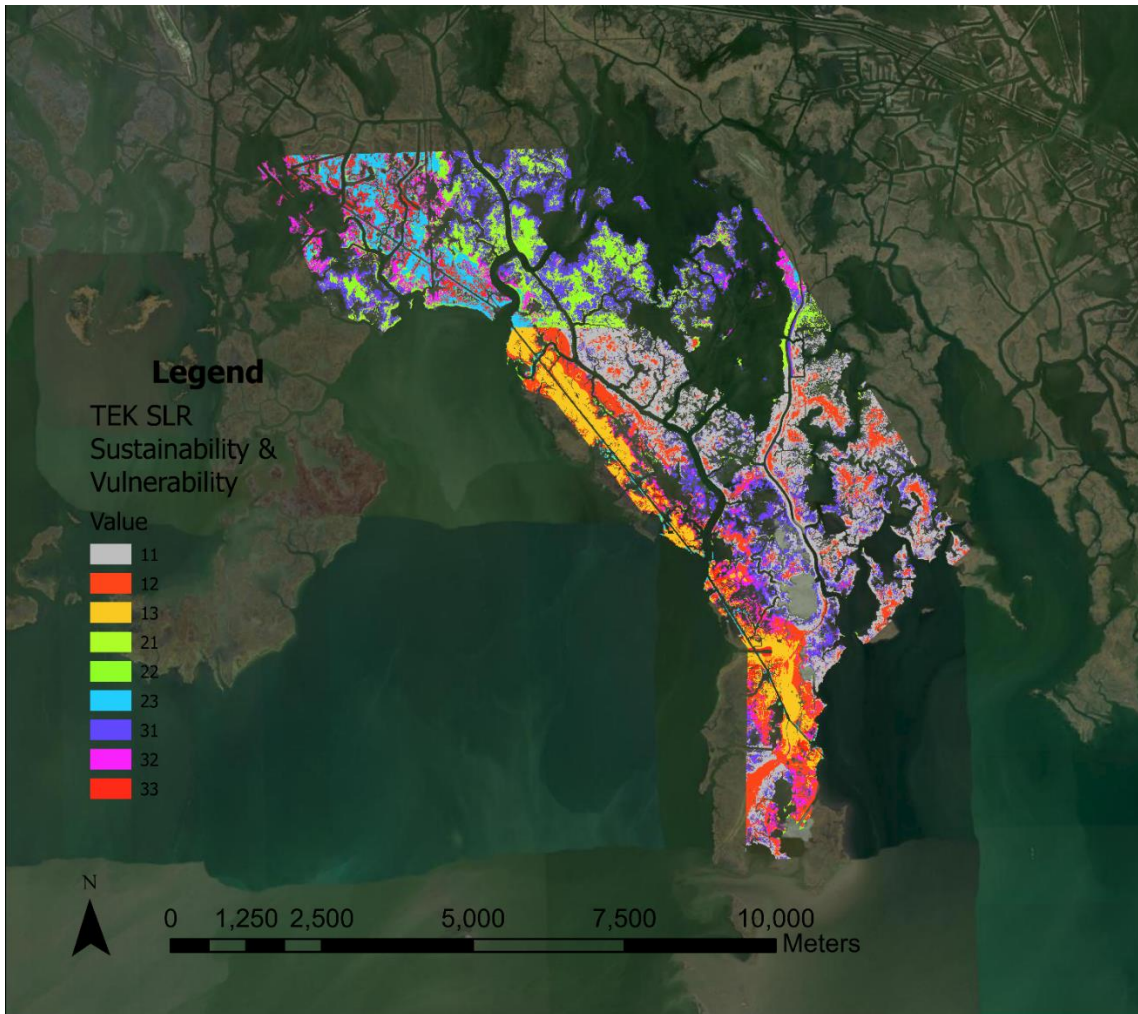


Figure 2.14 *Final sustainability and vulnerability map created using the TEK SLR vulnerability map from Fig. 2.12 combined with the TEK sustainability assessment from 2.13.*

The first digit refers to vulnerability and the second digit denotes sustainability goals, based on low (1) priority to high (3) priority.

Table 2.7 *Classes, corresponding area, and proportion of area from Fig. 2.14.*

Final Sustainability and Vulnerability Map		
Class	Area(ha)	Proportion
11	616.916	0.251
12	327.1416	0.133
13	215.2912	0.088
21	194.9332	0.079
22	143.108	0.058
23	160.6028	0.065
31	491.6596	0.203
32	187.6296	0.076
33	116.5192	0.047

The TEK sustainability assessment shows that most of the PACIT’s high priority sustainability goals lie along the major bayou (Bayou Pointe au Chien) that runs from the northwest to southeast of the map (Fig 2.13). The medium priority sustainability goals are located largely in the centers of the study area (Fig. 2.13). The output from integrating the TEK SK vulnerability map with the TEK sustainability assessment indicates how vulnerability from risk factors (the first digit) aligns or mismatches with the tribe’s sustainability goals (the second digit, where 1 is a low sustainability goal and 3 is a high sustainability goal) (Fig 2.14). An area with low vulnerability and low sustainability goal area is listed as class 11 (proportion 0.25) while a high vulnerability and high sustainability goal area is denoted by class 33 (proportion 0.047) (Table 2.7). (Fig. 2.14).

2.4 Discussion

The effort to combine the PACIT’s TEK assessments and the biophysical, mechanistic predictions of the SLR impact produced a vulnerability map built from various forms of knowledge and local concerns. Evaluating the TEK and SLR

vulnerability map reveals areas where the two assessments agree and disagree. There is large disagreement with class 31 of the TEK SLR vulnerability map. The SLR model likely denoted this section of the map as more vulnerable because of low accretion rates. The CRMS accretion rate for the most vulnerable section (2.54 cm/year, CRMS station 3296) is lower than the average accretion rate for the rest of the map (3.18 cm/year). This area of lower accretion may be because it's less frequently inundated due to lack of riverine inputs, as being far away from the tidal inlets means lower sediment in the water columns which leads to lower sedimentation. Like accretion, aboveground biomass for the highly vulnerable section of the SLR map is also lower (294.38 g/m²) than the average aboveground biomass for the rest of the map (381.92 g/m²). Saltmarsh habitat are key systems for organic and inorganic accretion, as this accumulation combats sea-level rise; thus, if the accretion rate is lower than the degree of sea-level rise, vulnerability of saltmarsh loss from subsidence increases (Stevenson et al, 1986).

Additionally, the sample sites are distributed more towards the southern half of the study area, due to our attempt to align our sampling sites to the CRMS station locations to take advantage of CRMS' long-term data. Increasing sample sites in the northern half of the study area may improve landscape predictions. Moreso, the SLR model was calibrated using the 2022 biomass data, which may underestimate vegetation productivity as the samples were collected in middle of December due to logistic and weather reasons. As mentioned in Chapter 1, this region experienced a drier-than normal year in 2022, and as such the biomass we collected may have caused our SLR model's predictions to overestimate wetland loss. Including 2023 data collected in September once processed may strengthen the model's landscape predictions. The TEK vulnerability

assessment considered risk factors such as proximity to spoil banks, canals, and highly fragmented areas, which were not considered in the SLR model. Moreso, while the original TEK vulnerability assessment takes into account historical land loss, predicted land change, and uses a projected SLR increase of 0.7m by 2060 (Sweet et al., 2017), it fails to account for land loss at a site-specific sea-level rise threshold (10 mm/year, 0.37m by 2060) through the end of the century in the SLR model. The TEK assessment also lacks spatial variability captured from site-specific inputs, like the biophysical inputs in by the SLR model.

Working within the PACIT community during my field visits was eye-opening, detailing a completely new piece to the climate change puzzle that western science traditionally ignores (Gadgil et al., 1993; Berkes, 1993). This incorporation of traditional and social data is essential. As impacts from climate change worsen, the knowledge systems from TEK provide generational familiarity of previous ecological changes, which can lend insight for successful adaptation plans (Maldonado et al., 2014). One of the initial goals of this collaboration initiated by M/ Bethel was not only to aid the PACIT's planning for hazard mitigation, but to serve as a means of communicating their needs to external partners and government agencies for consideration in protective and restorative projects (Bethel et al., 2022).

In creating this decision support tool, the tribe's members have a means for assessing climate change impacts of territory they've lived and worked in for generations. It helps them prepare for further adaptation to a changing landscape while protecting their sites of cultural significance (Maldonado, 2014; Bethel, et al., 2022). I believe this TEK SK tool presents hope for the resilience of these coastal wetlands and the PACIT's way

of life. The combined vulnerability map shows moderate to low vulnerability in many areas, roughly 66%, suggesting that these saltmarsh systems can be resilient to some sea level rise, in this study specifically, up to 10mm/yr SLR. In the sustainability and vulnerability map, we can locate where actions should be taken based on combinations of vulnerability and sustainability goals (ex. class 33 in Fig. 2.14), demonstrating targetable areas addressable through informed, restorative projects. Class 13 indicates the wetland habitat is at low vulnerability but is a high sustainability goal area – this may suggest that there is a high chance of success for protective and restorative actions. On the other hand, areas with high sustainability goals and high vulnerability risk (class 33), may be suitable for more intensive restorative actions such as living shorelines, a restoration we are working with the PACIT on to implement in the near future. By incorporating generational and cultural data into the landscape predictions, we dealt with broader perspectives that are often missing from the limited biophysical, mechanistic models (Hatfield et al., 2018).

I suggest further work with the SLR model. The abrupt boundary between the predicted 2075 and 2100 maps may result from the quality of the LiDAR data or the mean low water level used in the model that triggers the conversion from marshes to water. The boundary begins to appear after the model ran for 100 years, which is reasonable since the model predictions involve more uncertainties as time progresses, as in any other dynamic models. Incorporation of September 2023 biomass data is necessary as it better represents vegetation productivity, a key driver for accretion in the model. The current biomass used was collected at the end of the growing season and it is likely an underestimate though the leaves had not turned yellow at the time of collection. A

sensitivity analysis on the biomass function in the model will shed light on how this can affect model predictions and vulnerability derived. In addition, during the most recent field visit in September 2023, one of the sample sites showed a potential transition from *Spartina alterniflora* dominated coastal wetland habitat to a mix of *S. alterniflora*, *Salicornia bigelovii* Torr. (Dwarf glasswort), and *Avicennia germinans* (Black Mangrove). The current model does not account for species change, which is not an issue with the 2022 biophysical data, collected from *Spartina alterniflora* monocultures. However, with the presence of other species collected in the 2023 site data, I recommend altering the model to factor in this diversity. Further visits to this site will potentially show continued presence of these new species or others, which can provide more insight for the model's landscape predictions.

Likewise, the presence of the glasswort and mangrove species may be indicative of ecological succession – as climate change continues, these new species may continue to expand poleward into territory previously dominated by *Spartina alterniflora*. This expansion of black mangroves into the Terrebonne Bay could affect landscapes of this region dramatically and further challenges spatial predictions. Mangroves can be more tolerant to increased inundation than *S. alterniflora* as they can build elevation more rapidly. However, these plants can collapse abruptly due to quick decomposition of necromass after mortality (Morris et al. 2023). In addition, mangroves are more susceptible to freeze events (McKee et al., 2004; Alleman and Hester; 2011). The biophysical model can be further developed by collecting data near dredged channels to factor in the impact of channels on vegetation and sediment dynamics. The literature suggests more research is needed to understand what ecological consequences may arise

from this shift in Louisiana's coastal wetland habitats (Perry and Mendelsohn, 2009; Guo et al., 2013).

2.5 Conclusion

Spatial analysis of the PACIT study area from the combined TEK SK model predictions allowed a comprehensive understanding of the vulnerability of coastal wetlands from historical, current, and future perspectives. The mechanistic assessment gave information to vulnerable areas using biophysical data and can make predictions in the future while the TEK assessments were based on sustainability goals and vulnerability risk factors identified by the PACIT members. The combined TEK SK vulnerability map showed areas of similarity and dissimilarly, as the two assessments were constructed by varying means. The TEK vulnerability assessment was comprised mostly of medium to low/no priority areas, while the SK vulnerability map demonstrated a large section of high to medium priority, likely influenced by its biophysical inputs and sample sites.

Working with the PACIT and their TEK provided critical information that bolstered the SK predictions and will continue to lend insight as climate change exacerbates changes in this landscape. The vulnerability and sustainability assessment developed from this chapter can act as a tool for the PACIT and local land managers for understanding how this region of the Terrebonne Bay may change and identifying what areas should be protected based on prioritization and sustainability goals. Additionally, I encourage continued field site visits to observe potential ecological succession and areas close to dredged channels to account for this anthropogenic influence, which can provide

more awareness to landscape predictions, and to strengthen the bond forged with the PACIT community.

CHAPTER III - LINKING THE IMPACTS OF SEA-LEVEL RISE TO *SPARTINA*'S
MECHANISMS OF ADAPTION AND TO THE COASTAL RESILIENCY OF
SPARTINA ALTERNIFLORA-DOMINATED WETLANDS

The combined effects of climate change and sea-level rise are intensifying pressures on coastal wetlands and their nearby communities, as increased inundation and ensuing saltwater intrusion can lead to lowered saltmarsh productivity, decreased plant biomass, and finally plant death - ultimately resulting in land subsidence. Chapter 1 of this thesis examines the interactive effects of inundation and nitrogen on two commonly found saltmarsh species, *Spartina alterniflora* and *Spartina patens*. To do so I observed the responses of their one- and three-dimensional characteristics (productivity and morphological traits respectively) to these two environmental stressors using a marsh organ experiment, a controlled in-situ mesocosm that was situated in the western channel of the Pascagoula River, Mississippi. Our results describe varying productivity responses between species that also differed as the experiment continued, with impact varying from the short- and long-term. The low marsh plant *Spartina alterniflora* generally had quadratic relations with increased inundation while the high marsh plant *Spartina patens* had mostly negative impact. Both *Spartina* species responded positively to increased nitrogen via ammonium nitrate additions in the above- and belowground biomass, however responses to the nitrogen addition in the belowground biomass only appeared in the long-term, suggesting a lagged response.

By chapter 2, I expanded my focus from the mechanisms of adaptation to evaluate the impact of sea-level rise on a saltmarsh wetland home to an underrepresented

community in coastal Louisiana's Terrebonne Bay. I partnered with the state recognized Pointe-au-Chien Indian Tribe (PACIT) and Louisiana Sea Grant to more comprehensively predict local saltmarsh resiliency to future sea-level rise. To do so I calibrated a mechanistic landscape model that spatially predicts saltmarsh platform change when impacted by increasing inundation. With this mechanistic, science-knowledge (SK) model, I compared the model's saltmarsh vulnerability predictions to the vulnerability assessments derived from the PACIT's traditional ecological knowledge (TEK), a highly cultural, social-based knowledge system passed down by indigenous peoples. The integration of this biophysical model's predictions with the land-based, generational assessments highlighted the susceptibility of a local saltmarsh system to sea-level rise. By including the tribe's sustainability goals with the new vulnerability predictions, I created a more extensive decision support tool for the PACIT and local land managers in order to prioritize coastal wetland restoration in the Terrebonne Bay.

The two chapters of this thesis are linked in many ways, from the foundation of my knowledge with *Spartina* biology to future implications regarding the resiliency of real-world coastal ecosystems. The in-situ mesocosm experiment in chapter 1 served as a clear foundation for my experience with saltmarsh ecology in the Gulf of Mexico. This experiment prepared my understanding of how these commonly found saltmarsh plants' (*Spartina alterniflora* and *Spartina patens*) will react to future environmental scenarios and their mechanisms for adaptation. This ecological background in saltmarsh biology and behavior served as a necessary springboard for my comprehension of the conditions and threats coastal wetlands face in the Gulf of Mexico. Ultimately, the experience

acquired from chapter 1 was an indispensable source I continuously referred back to when approaching the field work and vulnerability assessments of *Spartina alterniflora*-dominated wetlands in chapter 2. As the first chapter was an exploration of the mechanisms behind saltmarsh adaptation to major environmental drivers like increased inundation, the second chapter scales up from a species perspective to an overall landscape assessment. The broader impacts of chapter 2 evaluate the coastal resiliency of local saltmarshes under increasing sea-level rise predictions and suggests implications for the future of a local indigenous tribe.

While chapter 1 shaped my understanding for the saltmarshes in chapter 2, it also served as preparation for what field work in Louisiana's marshes would look like. The field collection skills that I previously acquired from harvesting my marsh organ biomass helped streamline the biomass collection process in Louisiana, as above- and belowground biomass harvest was largely similar. Like with field work, the laboratory processing was fairly identical for the biomass inputs in both chapters. The familiarity gained from working with *Spartina alterniflora* throughout my thesis built upon itself, which better informed my expectations and made my interpretations of the second chapter's SK model grounded in personal understanding, gained from first-hand experience and prior information. Additionally, by incorporating a variety of anthropogenically impacted vegetation in the first chapter's mesocosm experiment, we can more comprehensively relate a potential biomass function to a range of disturbed saltmarsh wetlands in the Terrebonne Bay and possibly the Gulf of Mexico.

Regarding modeling and a potential biomass function, the data from chapter 1 can inform the biomass function in chapter 2. Currently, we applied biomass data collected from the field in order to make empirical predictions and to better match real-world landscapes. However, the mechanistic predictions of chapter 2 can benefit from the biomass function derived from chapter 1, especially considering that geographic source of vegetation has less impact on vegetation productivity as time progresses. Due to the late season collection of *Spartina* biomass used in chapter 2, we are considering a sensitivity analysis of biomass functions to account for the samples of peak-biomass season in 2023 as well as a biomass function derived from the controlled experiment in chapter 1.

Through witnessing the impact of sea-level rise on the *Spartina* species via a mechanistic experiment, I better understood the gravity of climate change for landscape predictions. This knowledge also inspired hope for resiliency, that the local saltmarshes have the ability to mitigate some stress induced from future sea-level rise. Overall, the findings from this thesis build upon our understanding of *Spartina*'s mechanisms for adaptation, saltmarsh resiliency, and ecosystem health under future stressor events, thus improving our predictions of future sea-level rise and climate change.

APPENDIX A – Supplemental Data for the Thesis

Table A.1 *S. alterniflora* Year 1 metrics model comparisons using DIC and PPL.

Sa. YR1								
Height								
		inundation	inundation2	nutrient	channel	days	DIC	PPL
	model 1 - all covariates	x	x	x	x	x	2529	69758.94
	model 2 - no precondition	x	x	x	x		2569	78653.28
	model 3 - no inundation 2	x		x	x	x	2531	70247.28
	model 4 - no channel	x	x	x		x	2527	69623.93
	model 5 - no pre-condition or inundation2	x		x	x		2569	78831.81
	model 6 - no inundation2 or channel	x		x		x	2530	70234.34
	model 7 - no precondition or channel	x	x	x			2573	79776.06
	model 8 - no channel, precondition, or inundation2	x		x			2573	79986.47
Stem Width								
		inundation	inundation2	nutrient	channel	days	DIC	PPL
	model 1 - all covariates	x	x	x	x	x	-1083	1.394522
	model 2 - no precondition	x	x	x	x		-1012	1.730293
	model 3 - no inundation 2	x		x	x	x	-1084	1.392667
	model 4 - no channel	x	x	x		x	-1079	1.41618
	model 5 - no pre-condition or inundation2	x		x	x		-1012	1.731094
	model 6 - no inundation2 or channel	x		x		x	-1080	1.414547
	model 7 - no precondition or channel	x	x	x			-995.3	1.825915
	model 8 - no channel, precondition, or inundation2	x		x			-995.7	1.825756
Leaf Width								
		inundation	inundation2	nutrient	channel	days	DIC	PPL
	model 1 - all covariates	x	x	x	x	x	-725.5	4.094624
	model 2 - no precondition	x	x	x	x		-720.2	4.172509
	model 3 - no inundation 2	x		x	x	x	-726.2	4.095406
	model 4 - no channel	x	x	x		x	-725.8	4.104466
	model 5 - no pre-condition or inundation2	x		x	x		-721.1	4.169028
	model 6 - no inundation2 or channel	x		x		x	-726.7	4.099945
	model 7 - no precondition or channel	x	x	x			-722.1	4.179904
	model 8 - no channel, precondition, or inundation2	x		x			-722.9	4.153656
Leaf Length								
		inundation	inundation2	nutrient	channel	days	DIC	PPL
	model 1 - all covariates	x	x	x	x	x	631.2	1251.458
	model 2 - no precondition	x	x	x	x		629.5	1246.254
	model 3 - no inundation 2	x		x	x	x	631.4	1256.889
	model 4 - no channel	x	x	x		x	645.8	1395.545
	model 5 - no pre-condition or inundation2	x		x	x		630.7	1259.427
	model 6 - no inundation2 or channel	x		x		x	645.6	1399.961
	model 7 - no precondition or channel	x	x	x			644.6	1395.651
	model 8 - no channel, precondition, or inundation2	x		x			645.2	1406.687
Leaf Count								
		inundation	inundation2	nutrient	channel	pre-condition	DIC	PPL
	model 1 - all covariates	x	x	x	x	x	1050	842.8402
	model 2 - no precondition	x	x	x	x		1048	838.9651
	model 3 - no inundation 2	x		x	x	x	1049	840.6168
	model 4 - no channel	x	x	x		x	1049	841.9762
	model 5 - no pre-condition or inundation2	x		x	x		1047	838.2969
	model 6 - no inundation2 or channel	x		x		x	1048	841.2955
	model 7 - no precondition or channel	x	x	x			1047	839.6768
	model 8 - no channel, precondition, or inundation2	x		x			1046	838.7791

Table A.2 *S. alterniflora* Year 2 metrics model comparisons using DIC and PPL.

Sa, YR2									
Height									
		inundation	inundation2	nutrient	channel	pre-condition	temperature	DIC	PPL
	model 1 - all covariates	x	x	x	x	x	x	4510	155888.8
	model 2 - no precondition	x	x	x	x		x	4549	167723.7
	model 3 - no inundation 2	x		x	x	x	x	4511	155933.1
	model 4 - no channel	x	x	x			x	4525	161176.5
	model 5 - no pre-condition or inundation2	x		x	x		x	4548	167597.4
	model 6 - no inundation2 or channel	x		x		x	x	4524	160811.1
	model 7 - no precondition or channel	x	x	x			x	4548	167789.2
	model 8 - no channel, precondition, or inundation2	x		x			x	4546	167578
Leaf Length									
		inundation	inundation2	nutrient	channel	pre-condition	temperature	DIC	PPL
	model 1 - all covariates	x	x	x	x	x	x	3946	61520.76
	model 2 - no precondition	x	x	x	x		x	3983	65412.64
	model 3 - no inundation 2	x		x	x	x	x	3947	61779.53
	model 4 - no channel	x	x	x		x	x	3952	62435.64
	model 5 - no pre-condition or inundation2	x		x	x		x	3983	65399.21
	model 6 - no inundation2 or channel	x		x		x	x	3954	62629.36
	model 7 - no precondition or channel	x	x	x			x	3993	66459.65
	model 8 - no channel, precondition, or inundation2	x		x			x	3993	66525.49
Leaf Width									
		inundation	inundation2	nutrient	channel	pre-condition	temperature	DIC	PPL
	model 1 - all covariates	x	x	x	x	x	x	1785	1368.21
	model 2 - no precondition	x	x	x	x		x	1786	1373.388
	model 3 - no inundation 2	x		x	x	x	x	1785	1367.83
	model 4 - no channel	x	x	x		x	x	1784	1366.233
	model 5 - no pre-condition or inundation2	x		x	x		x	1786	1373.191
	model 6 - no inundation2 or channel	x		x		x	x	1784	1366.714
	model 7 - no precondition or channel	x	x	x			x	1785	1373.673
	model 8 - no channel, precondition, or inundation2	x		x			x	1785	1373.843
Stem Width									
		inundation	inundation2	nutrient	channel	pre-condition	temperature	DIC	PPL
	model 1 - all covariates	x	x	x	x	x	x	1271	557.1118
	model 2 - no precondition	x	x	x	x		x	1270	556.4027
	model 3 - no inundation 2	x		x	x	x	x	1271	557.0398
	model 4 - no channel	x	x	x		x	x	1270	556.4828
	model 5 - no pre-condition or inundation2	x		x	x		x	1269	556.6381
	model 6 - no inundation2 or channel	x		x		x	x	1270	556.591
	model 7 - no precondition or channel	x	x	x			x	1269	556.591
	model 8 - no channel, precondition, or inundation2	x		x			x	1268	555.9236
Leaf Count									
		inundation	inundation2	nutrient	channel	pre-condition	temperature	DIC	PPL
	model 1 - all covariates	x	x	x	x	x	x	1728	1268.516
	model 2 - no precondition	x	x	x	x		x	1727	1270.195
	model 3 - no inundation 2	x		x	x	x	x	1727	1269.469
	model 4 - no channel	x	x	x		x	x	1742	1298.45
	model 5 - no pre-condition or inundation2	x		x	x		x	1727	1269.374
	model 6 - no inundation2 or channel	x		x		x	x	1740	1297.248
	model 7 - no precondition or channel	x	x	x			x	1742	1302.53
	model 8 - no channel, precondition, or inundation2	x		x			x	1742	1302.927

Table A.3 *S. patens* Year 1 metrics model comparisons using DIC and PPL.

Sp. YR1								
Height								
		inundation	inundation2	nutrient	pre-condition	days	DIC	PPL
	model 1 - all covariates	x	x	x	x	x	2298	33424.88
	model 2 - no precondition	x	x	x		x	2349	39159.7
	model 3 - no inundation 2			x	x	x	2298	33434.35
model 4 - no pre-condition or inundation2	x		x		x	2349	39152.5	
Stem Width								
		inundation	inundation2	nutrient	pre-condition	days	DIC	PPL
	model 1 - all covariates	x	x	x	x	x	-746.7	3.803158
	model 2 - no precondition	x	x	x		x	-743.9	3.856962
	model 3 - no inundation 2			x	x	x	-747.3	3.802887
model 4 - no pre-condition or inundation2	x		x		x	-744.4	3.851417	
Leaf Length								
		inundation	inundation2	nutrient	pre-condition	days	DIC	PPL
	model 1 - all covariates	x	x	x	x	x	543.3	677.5054
	model 2 - no precondition	x	x	x		x	541.5	674.2134
	model 3 - no inundation 2			x	x	x	544.2	682.8845
model 4 - no pre-condition or inundation2	x		x		x	542.8	679.6922	
Leaf Count								
		inundation	inundation2	nutrient	pre-condition	days	DIC	PPL
	model 1 - all covariates	x	x	x	x	x	913.7	570.15
	model 2 - no precondition	x	x	x		x	912.9	568.59
	model 3 - no inundation 2			x	x	x	912.5	568.2027
model 4 - no pre-condition or inundation2	x		x		x	911.4	567.4571	
Stem Count								
		inundation	inundation2	nutrient	pre-condition	days	DIC	PPL
	model 1 - all covariates	x	x	x	x	x	2343	42516.73
	model 2 - no precondition	x	x	x		x	2392	44668.68
	model 3 - no inundation 2			x	x	x	2343	42494.87
model 4 - no pre-condition or inundation2	x		x		x	2392	44683.6	

Table A.4 *S. patens* Year 2 metrics model comparisons using DIC and PPL.

Sp. YR2								
Height								
		inundation	inundation2	nutrient	pre-condition	temperature	DIC	PPL
	model 1 - all covariates	x	x	x	x	x	4891	306918.4
	model 2 - no precondition	x	x	x		x	4893	312238.6
	model 3 - no inundation 2			x	x	x	4890	303242.1
model 5 - no pre-condition or inundation2	x		x		x	4900	309044.4	
Leaf Length								
		inundation	inundation2	nutrient	pre-condition	temperature	DIC	PPL
	model 1 - all covariates	x	x	x	x	x	3916	55696.37
	model 2 - no precondition	x	x	x		x	3915	55743.77
	model 3 - no inundation 2			x	x	x	3917	55710.32
model 4 - no pre-condition or inundation2	x		x		x	3917	55715.95	
Stem Width								
		inundation	inundation2	nutrient	pre-condition	temperature	DIC	PPL
	model 1 - all covariates	x	x	x	x	x	2533	5307.681
	model 2 - no precondition	x	x	x		x	2532	5305.379
	model 3 - no inundation 2			x	x	x	2531	5295.863
model 5 - no pre-condition or inundation2	x		x		x	2531	5305.442	
Leaf Count								
		inundation	inundation2	nutrient	pre-condition	temperature	DIC	PPL
	model 1 - all covariates	x	x	x	x	x	1861	1576.443
	model 2 - no precondition	x	x	x		x	1880	1643.401
	model 3 - no inundation 2			x	x	x	1860	1576.34
model 4 - no pre-condition or inundation2	x		x		x	1879	1642.487	
Stem Count								
		inundation	inundation2	nutrient	pre-condition	temperature	DIC	PPL
	model 1 - all covariates	x	x	x	x	x	5597	704552.6
	model 2 - no precondition	x	x	x		x	5625	627138.6
	model 3 - no inundation 2			x	x	x	5597	706107.5
model 4 - no pre-condition or inundation2	x		x		x	5625	629353.8	

Table A.5 *S. alterniflora* Year 1 biomass model comparisons using DIC and PPL.

Sa. YR1								
Aboveground biomass								
		inundation	inundation2	nutrient	channel	pre-condition	DIC	PPL
	model 1 - all covariates	x	x	x	x	x	332.7	2170954
	model 2 - no channel	x	x	x		x	335.5	2547012
	model 3 - no pre-condition	x	x	x	x		330.3	2052023
	model 4 - no inundation2	x		x	x	x	332.2	2226037
	model 5 - no inundation2 or pre-condition	x		x	x		329.7	2093053
	model 6 - no inundation2 or channel	x		x		x	334.2	2522352
	model 8 - no channel or pre-condition	x	x	x			332.2	2427149
	model 7 - no inundation2, channel, or pre-condition	x		x			332.8	2397909
Belowground biomass		inundation	inundation2	nutrient	channel	pre-condition	DIC	PPL
	model 1 - all covariates	x	x	x	x	x	418	77107338
	model 2 - no channel	x	x	x		x	432.6	148830950
	model 3 - no pre-condition	x	x	x	x		417.9	79976585
	model 4 - no inundation2	x		x	x	x	417.6	78266484
	model 5 - no inundation2 or pre-condition	x		x	x		417	78894136
	model 6 - no inundation2 or channel	x		x		x	432.2	150522210
	model 7 - no inundation2, channel, or pre-condition	x		x			432.2	156613782
	model 8 - no channel or pre-condition	x	x	x			433.1	157816385

Table A.6 *S. alterniflora* Year 2 biomass model comparisons using DIC and PPL.

Sa. YR2								
Aboveground biomass								
		inundation	inundation2	nutrient	channel	pre-condition	DIC	PPL
	model 1 - all covariates	x	x	x	x	x	364.9	8279323
	model 2 - no channel	x	x	x		x	365.4	8831476
	model 3 - no pre-condition	x	x	x	x		362.9	7984784
	model 4 - no inundation2	x		x	x	x	365.9	9077140
	model 5 - no inundation2 or pre-condition	x		x	x		365.2	9157315
	model 6 - no inundation2 or channel	x		x		x	365.7	9331221
	model 7 - no inundation2, channel, or pre-condition	x		x			365.3	9646830
	model 8 - no channel or pre-condition	x	x	x			363.8	8613986
Belowground biomass		inundation	inundation2	nutrient	channel	pre-condition	DIC	PPL
	model 1 - all covariates	x	x	x	x	x	424.4	100709591
	model 2 - no channel	x	x	x		x	425.7	111873907
	model 3 - no pre-condition	x	x	x	x		422.1	94775422
	model 4 - no inundation2	x		x	x	x	428.3	121871572
	model 5 - no inundation2 or pre-condition	x		x	x		426.3	117342121
	model 6 - no inundation2 or channel	x		x		x	428.5	127515956
	model 7 - no inundation2, channel, or pre-condition	x		x			426.9	125827766
	model 8 - no channel or pre-condition	x	x	x			423.8	106979578

Table A.7 *S. patens* Year 2 biomass model comparisons using DIC and PPL.

Sp. YR1							
Aboveground biomass							
		inundation	inundation2	nutrient	pre-condition	DIC	PPL
	model 1 - all covariates	x	x	x	x	356.1	5993842
	model 2 - no pre-condition	x	x	x		366.9	9911575
	model 3 - no inundation2	x		x	x	365.3	9252657
	model 4 - no inundation2 or pre-condition	x		x		370.8	12039268
Belowground biomass							
		inundation	inundation2	nutrient	pre-condition	DIC	PPL
	model 1 - all covariates	x	x	x	x	443.2	231846779
	model 2 - no precondition	x	x	x		441.5	225351145
	model 3 - no inundation2	x		x	x	443.4	237533396
	model 4 - no inundation2 or pre-condition	x		x		441.6	233635561

Table A.8 *S. patens* Year 2 biomass model comparisons using DIC and PPL.

Sp. YR1							
Aboveground biomass							
		inundation	inundation2	nutrient	pre-condition	DIC	PPL
	model 1 - all covariates	x	x	x	x	356.1	5993842
	model 2 - no pre-condition	x	x	x		366.9	9911575
	model 3 - no inundation2	x		x	x	365.3	9252657
	model 4 - no inundation2 or pre-condition	x		x		370.8	12039268
Belowground biomass							
		inundation	inundation2	nutrient	pre-condition	DIC	PPL
	model 1 - all covariates	x	x	x	x	443.2	231846779
	model 2 - no precondition	x	x	x		441.5	225351145
	model 3 - no inundation2	x		x	x	443.4	237533396
	model 4 - no inundation2 or pre-condition	x		x		441.6	233635561

Table A.9 *Scaler vs. nutrient array metrics model comparisons using DIC.*

Model	Scaler DIC	Nutrient Array DIC
YR 1 Sa. leaf count	1047	1037
YR 1 Sp. leaf count	911.4	913.5
YR 1 Sa. height	2527	3023
YR 1 Sp. height	2298	2878
YR 1 Sa. leaf length	629.5	631.8
YR 1 Sp. leaf length	541.4	584.1
YR 1 Sa. stem width	-1084	-629.2
YR 1 Sp. stem width	-747.3	101.3
YR 1 Sa. leaf width	-726.2	-463
YR 1 Sp. stem count	2343	2482
YR 2 Sa. leaf count	1785	1888
YR 2 Sp. leaf count	1860	1938
YR 2 Sa. height	4510	4882
YR 2 Sp. height	4890	5034
YR 2 Sa. leaf length	3946	3972
YR 2 Sp. leaf length	3916	4018
YR 2 Sa. stem width	1268	1418
YR 2 Sp. stem width	2531	2572
YR 2 Sa. leaf width	1784	1979
YR 2 Sp. stem count	5597	5881

Figure A.1 Posteriors for *Spartina alterniflora* aboveground biomass Year 1 (left) and Year 2 (right).

Credible intervals of the parameters of inundation, inundation squared for quadratic impact, nutrient (nitrogen addition), pre-condition, and channel in the model to evaluate the impact of environmental factors. The thin line denotes a 95% credible interval, and the thick line indicates a 50% credible interval. The black color indicates strong impact, the grey color indicates moderate impact, and open white circles mean little to no impact, as the credible interval overlaps 0. Outputs were generated in R using the MCMCvis package (Youngflesh 2018).

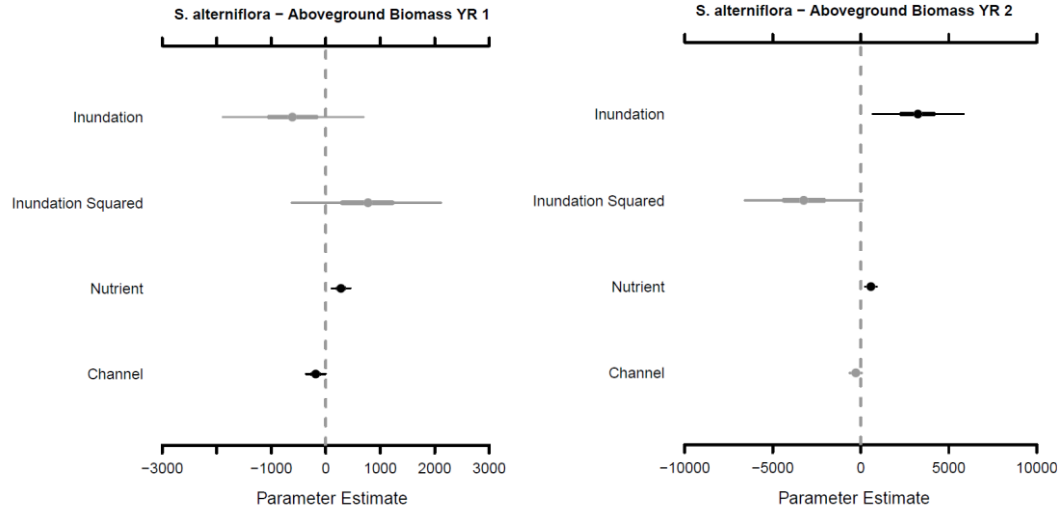


Figure A.2 Posteriors for *Spartina patens* aboveground biomass Year 1 (left) and Year 2 (right).

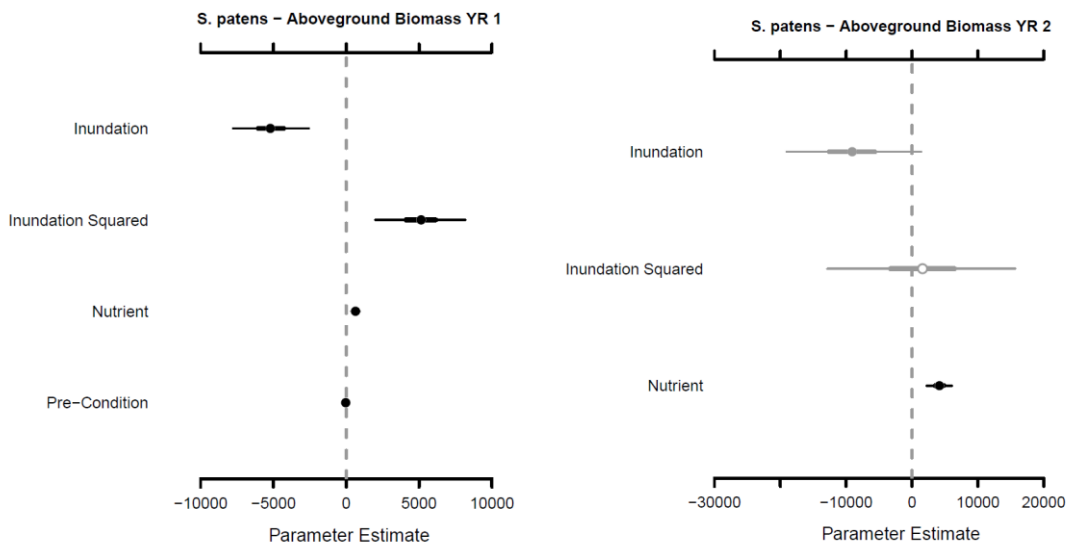


Figure A.3 Posteriors for *Spartina alterniflora* belowground biomass Year 1 (left) and Year 2 (right).

Credible intervals of the parameters of inundation, inundation squared for quadratic impact, nutrient (nitrogen addition), pre-condition, and channel in the model to evaluate the impact of environmental factors. The thin line denotes a 95% credible interval, and the thick line indicates a 50% credible interval. The black color indicates strong impact, the grey color indicates moderate impact, and open white circles mean little to no impact, as the credible interval overlaps 0. Outputs were generated in R using the MCMCvis package.

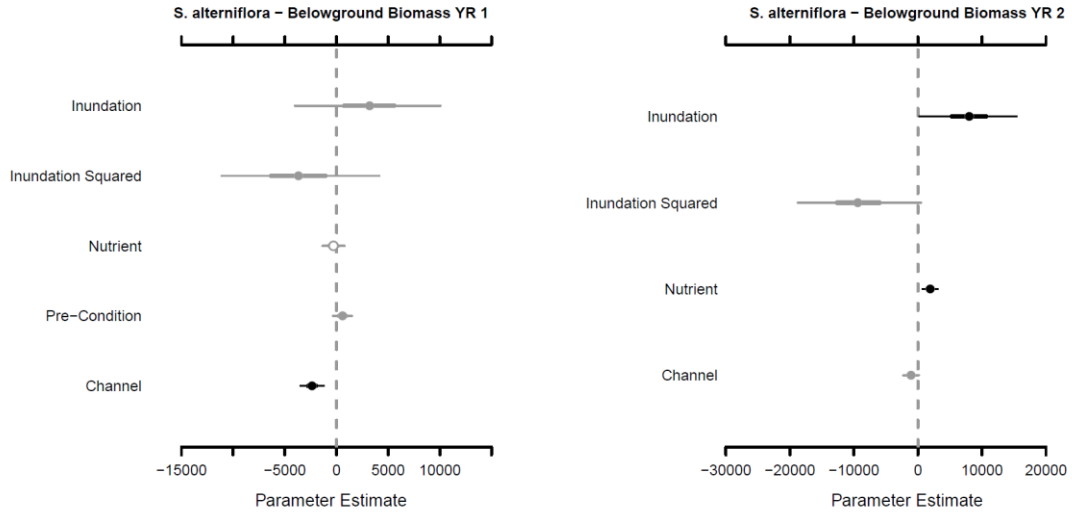


Figure A.4 Posteriors for *Spartina patens* belowground biomass Year 1 (left) and Year 2 (right).

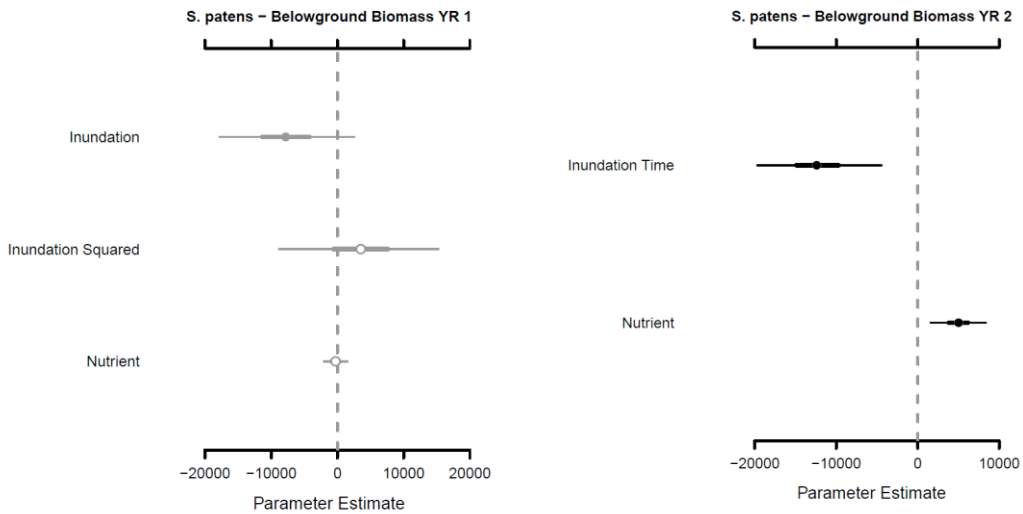


Figure A.5 Posteriors for *Spartina alterniflora* leaf count Year 1 (left) and Year 2 (right). Credible intervals of the parameters of inundation, inundation squared for quadratic impact, nutrient (nitrogen addition), pre-condition, days/temperature, and channel in the model to evaluate the impact of environmental factors. The thin line denotes a 95% credible interval, and the thick line indicates a 50% credible interval. The black color indicates strong impact, the grey color indicates moderate impact, and open white circles mean little to no impact, as the credible interval overlaps 0. Outputs were generated in R using the MCMCvis package.

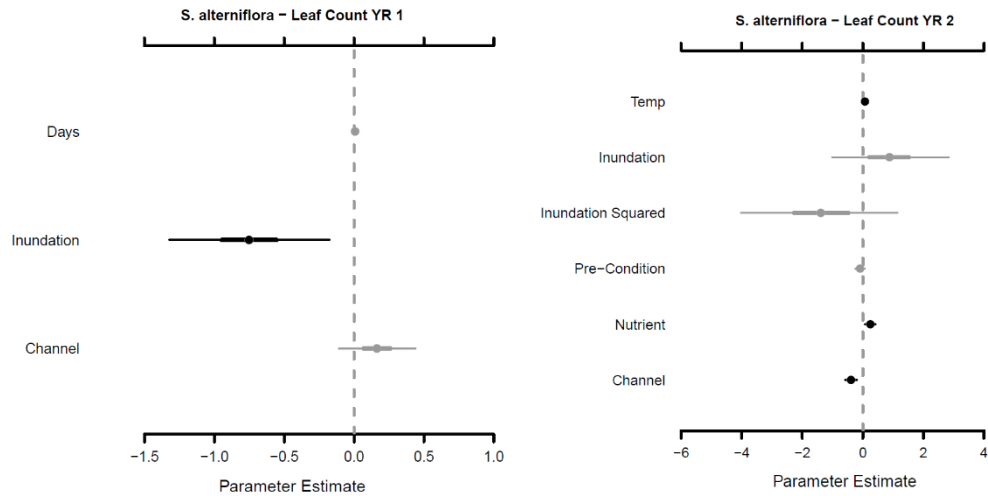


Figure A.6 Posteriors for *Spartina patens* leaf count Year 1 (left) and Year 2 (right).

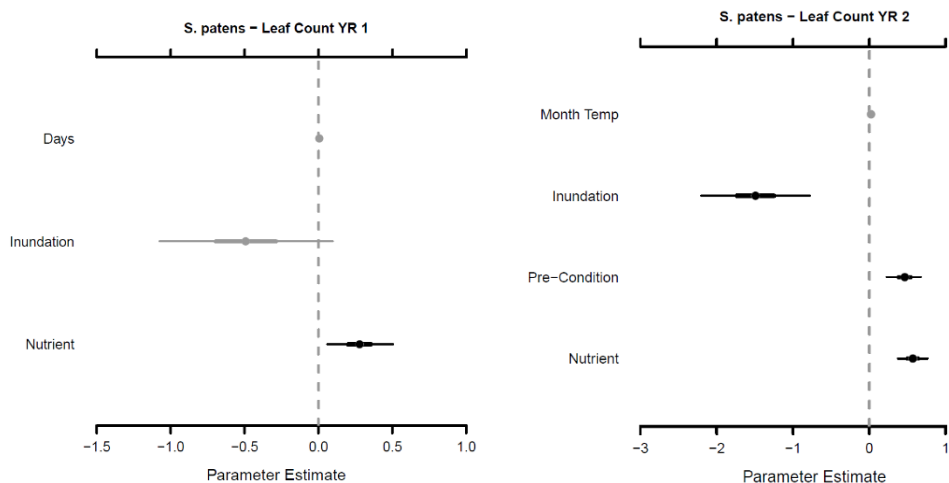


Figure A.7 Posteriors for *Spartina alterniflora* height Year 1 (left) and Year 2 (right). Credible intervals of the parameters of inundation, inundation squared for quadratic impact, nutrient (nitrogen addition), pre-condition, days/temperature, and channel in the model to evaluate the impact of environmental factors. The thin line denotes a 95% credible interval, and the thick line indicates a 50% credible interval. The black color indicates strong impact, the grey color indicates moderate impact, and open white circles mean little to no impact, as the credible interval overlaps 0. Outputs were generated in R using the MCMCvis package.

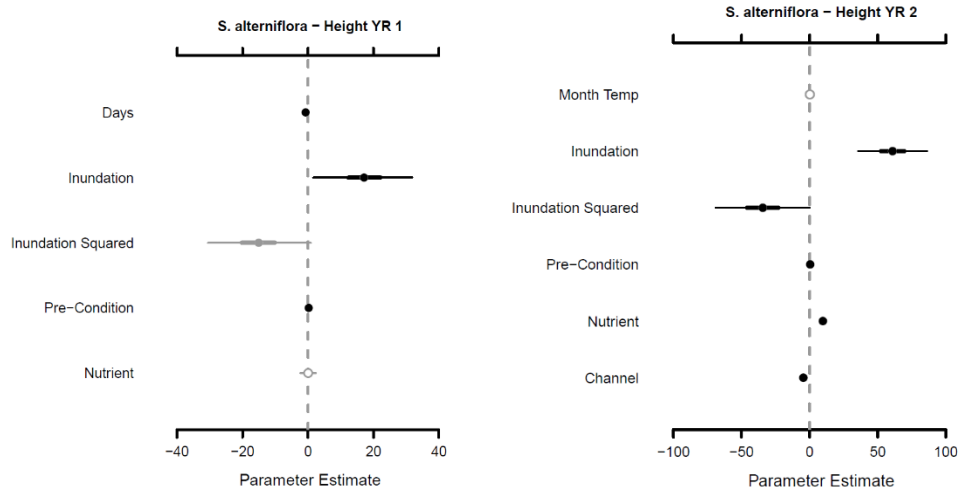


Figure A.8 Posteriors for *Spartina patens* height Year 1 (left) and Year 2 (right).

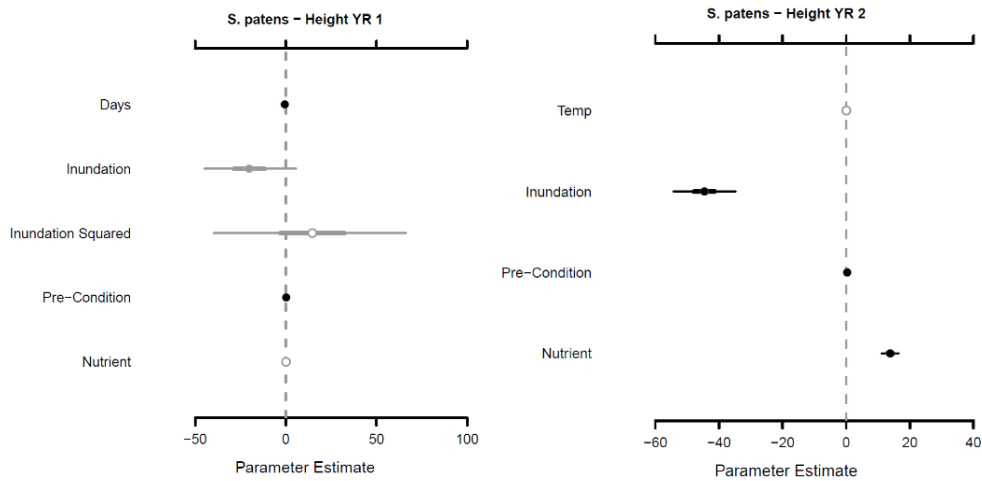


Figure A.9 Posteriors for *Spartina alterniflora* leaf length Year 1 (left) and Year 2 (right).

Credible intervals of the parameters of inundation, inundation squared for quadratic impact, nutrient (nitrogen addition), pre-condition, days/temperature, and channel in the model to evaluate the impact of environmental factors. The thin line denotes a 95% credible interval, and the thick line indicates a 50% credible interval. The black color indicates strong impact, the grey color indicates moderate impact, and open white circles mean little to no impact, as the credible interval overlaps 0. Outputs were generated in R using the MCMCvis package.

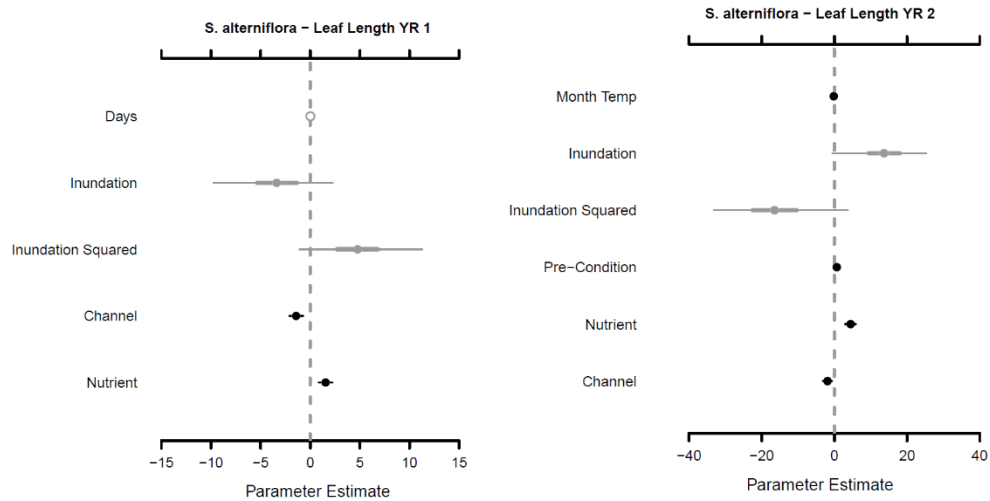


Figure A.10 Posteriors for *Spartina patens* leaf length Year 1 (left) and Year 2 (right).

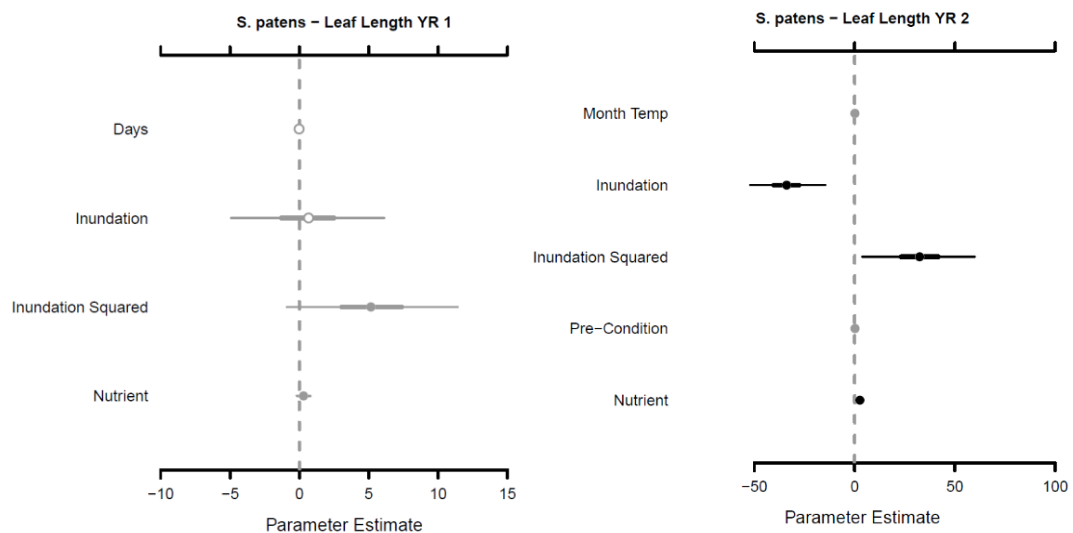


Figure A.11 Posteriors for *Spartina alterniflora* stem width Year 1 (left) and Year 2 (right).

Credible intervals of the parameters of inundation, inundation squared for quadratic impact, nutrient (nitrogen addition), pre-condition, days/temperature, and channel in the model to evaluate the impact of environmental factors. The thin line denotes a 95% credible interval, and the thick line indicates a 50% credible interval. The black color indicates strong impact, the grey color indicates moderate impact, and open white circles mean little to no impact, as the credible interval overlaps 0. Outputs were generated in R using the MCMCvis package.

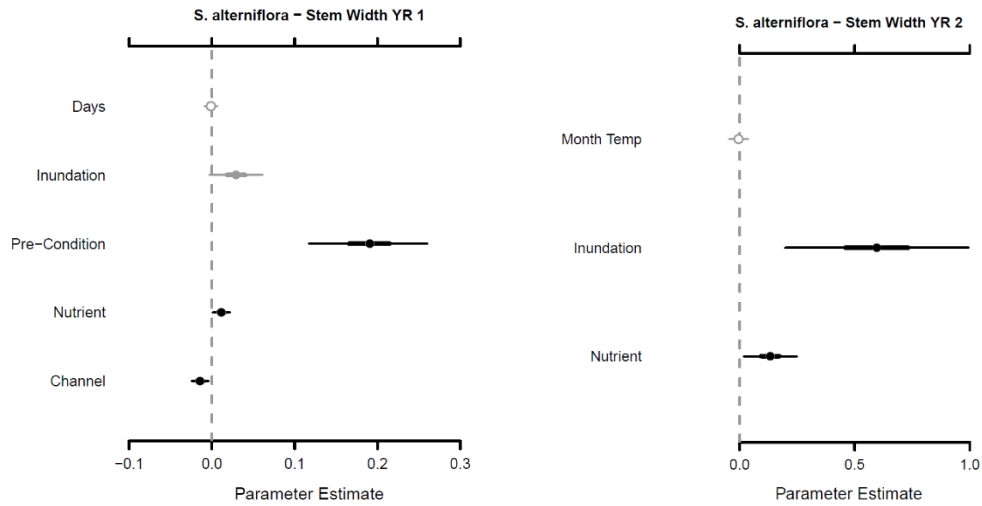


Figure A.12 Posteriors for *Spartina patens* stem width Year 1 (left) and Year 2 (right).

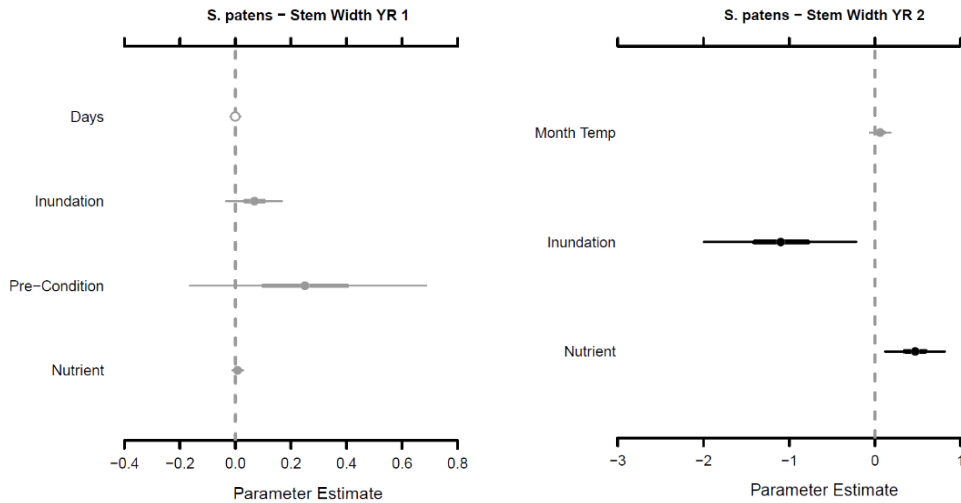


Figure A.13 *Posteriors for Spartina alterniflora leaf width Year 1 (left) and Year 2 (right).*

Credible intervals of the parameters of inundation, inundation squared for quadratic impact, nutrient (nitrogen addition), pre-condition, days/temperature, and channel in the model to evaluate the impact of environmental factors. The thin line denotes a 95% credible interval, and the thick line indicates a 50% credible interval. The black color indicates strong impact, the grey color indicates moderate impact, and open white circles mean little to no impact, as the credible interval overlaps 0. Outputs were generated in R using the MCMCvis package.

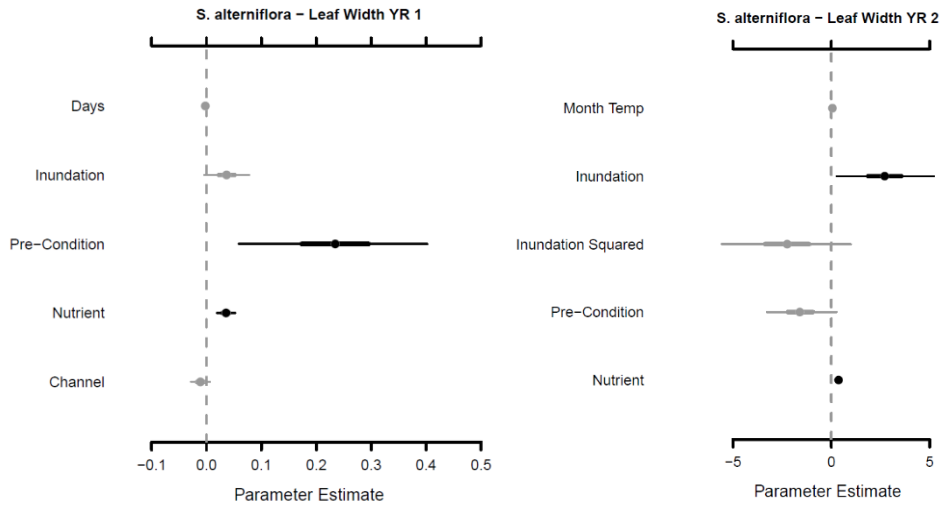
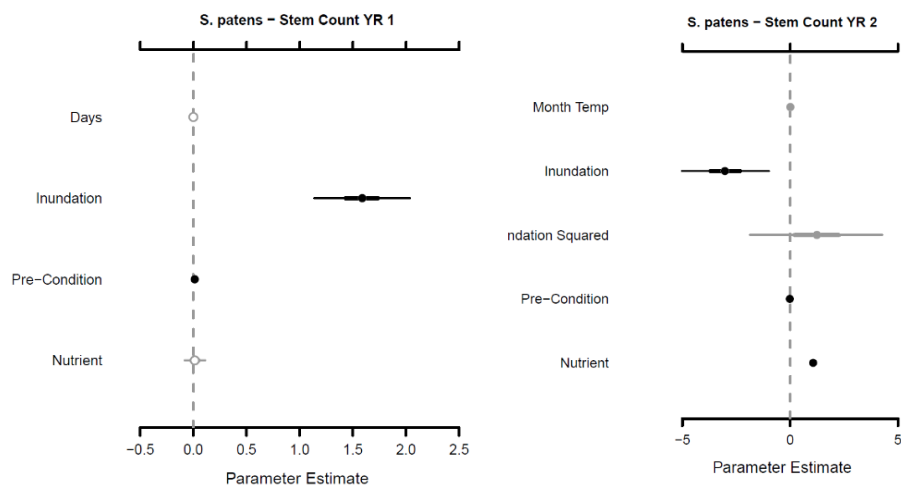


Figure A.14 *Posteriors for Spartina patens stem count Year 1 (left) and Year 2 (right).*





100+ Years of Land Change for Coastal Louisiana

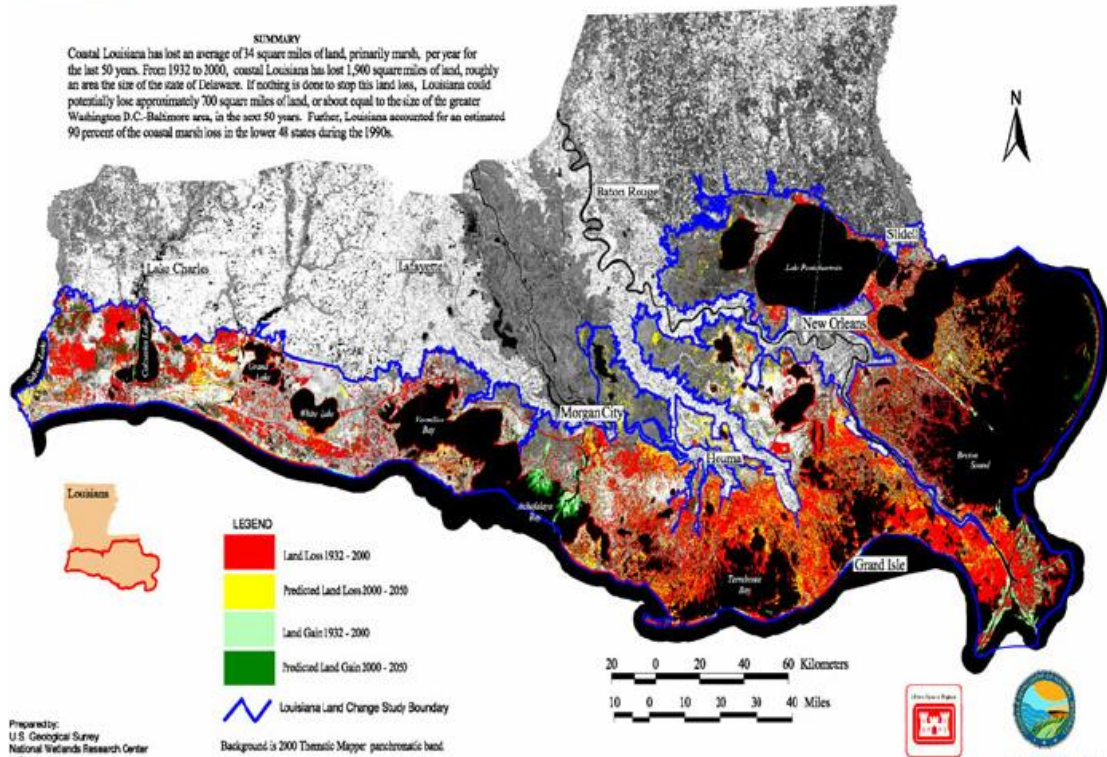


Figure A.15 This map represents southern Louisiana's land loss and land gain from 1932 to 2000, marked by red and light green, and predicted land loss and land gain from 2000 to 2050, as marked by yellow and darker green (Source: USGS, https://www.researchgate.net/figure/Historical-and-projected-land-loss-from-coastal-Louisiana-Map-reproduced-from-Barras-et_fig1_226220800)



Figure A.16 This map shows the indigenous tribes in Southern Louisiana currently losing land due to sea-level rise (Source: Yeoman <https://www.sapiens.org/culture/louisiana-native-americans-climate-change/>).

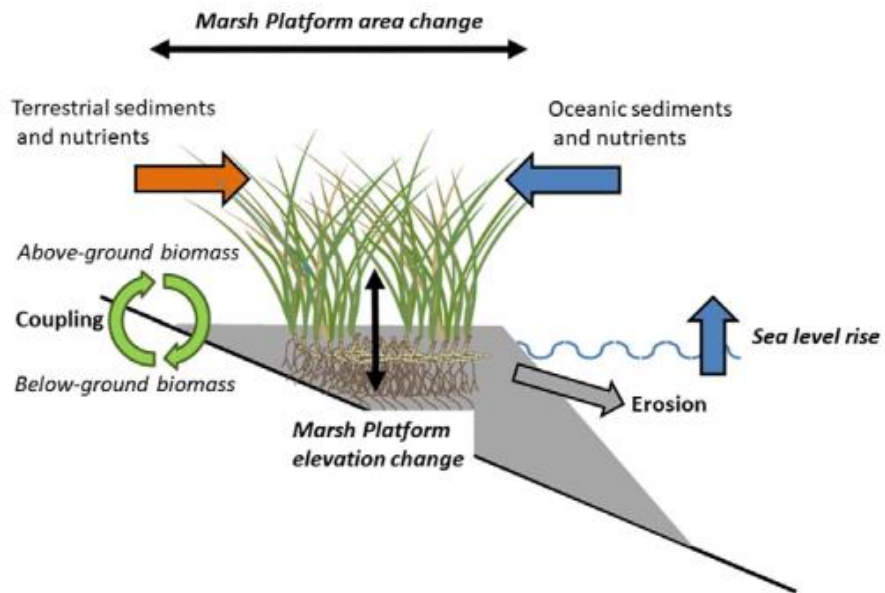


Figure A.17 The conceptual diagram illustrating the processes and drivers in the model to predict salt marsh platform change in this study (Wu et al. 2017a, 2022).

Table A.10 Site data at the Terrebonne Bay, Louisiana collected in December of 2022 unless otherwise specified (The site numbers correspond to Fig. 2.3).

Site	Transect	Sample	Live Above-ground Biomass (g/m ²)	Live Below-ground Biomass (g/m ²)	Soil porewater Salinity (PPT)	UTM Easting	UTM Northing	Elevation (2011, m)
1	1	1	143.76	1632.48	30.53	744636.78	3253826.17	0.32
1	1	2	135.2	2099.95	31.81	744634.39	3253829.22	0.38
1	1	3	500.24	3363.01	31.064	744633.45	3253832.09	0.38
1	2	4	200.64	5	28.50	744632.87	3253823.09	0.30
1	2	5	282.4	3340.19	31.14	744631.72	3253826.61	0.39
1	2	6	504.08	2007.45	32.69	744628.95	3253829.1	0.43
2	1	1	136.48	4748.18	33.27	754132.48	3246279.68	0.43
2	1	2	252.96	4749.41	31.20	754128.69	3246279.26	0.43
2	1	3	69.6	4602.01	35.73	754126.02	3246277.21	0.47
2	2	4	224	4899.89	28.56	754133.91	3246276.39	0.38
2	2	5	300.32	5292.75	32.52	754131.02	3246275.32	0.49
2	2	6	589.68	6840.73	35.32	754129.24	3246272.29	0.42
3	1	1	542	4238.15	33.03	756902.84	3245320.27	0.20
3	1	2	268.16	1980.93	34.11	756899.56	3245319.31	0.18
3	1	3	605.12	4900.51	34.54	756896.74	3245319.25	0.28
3	2	4	630.48	6475.01	32.49	756903.96	3245318.08	0.25
3	2	5	257.36	2286.82	34.54	756900.96	3245317.57	0.23
3	2	6	493.76	4557.61	28.94	756897.78	3245316.5	0.27
4	1	1	208	1642.96	31.68	753851.11	3240492.54	0.46
4	1	2	270.8	2643.91	32.65	753851.44	3240495.32	0.48

Table A10 (continued).

4	1	3	152.48	2441.00	33.059	753853.53	3240497.36	0.35
4	2	4	163.04	3234.73	33.75	753848.34	3240494.47	0.47
4	2	5	239.28	1381.47	31.60	753849.17	3240496.38	0.43
4	2	6	287.68	1831.06	33.17	753851.06	3240499.08	0.38
5	1	1	531.36	1063.85	38.22	750133.64	3247545.65	0.35
5	1	2	475.52	556.90	36.79	750136.61	3247547.6	0.37
5	1	3	656.4	389.77	31.18	750138.3	3247550.41	0.29
5	2	4	573.52	2305.32	36.87	750135.92	3247543.59	0.33
5	2	5	581.92	1027.47	34.99	750138.6	3247545.65	0.30
5	2	6	656.16	1533.18	30.31	750140.57	3247548.68	0.31

Table A.11 *Water quality data at each study site at the Terrebonne Bay, Louisiana collected in December of 2022 (The site numbers correspond to Fig 2.3 and the bottle numbers represent the locations when approaching the site with 1 closest to the site and 3 furthest away from the site).*

Site	Bottle	UTM Easting	UTM Northing	Salinity (PPT)	Inorganic TSS (mg/L)	Organic TSS (mg/L)
1	1	744704.49	3253749.22	21	13.09	11.22
1	2	744681.31	3253774.67	23	18.72	12.20
1	3	744651.37	3253816.61	23	22.19	9.22
2	1	754152.09	3246289.11	21	16.63	9.52
2	2	754140.03	3246285.4	20	14.16	10.23
2	3	754135.49	3246279.86	23	28.13	14.07
3	1	756878.17	3245392.47	23	14.39	8.17
3	2	756899.31	3245368.88	23	14.14	6.86
3	3	756911.19	3245333.66	22	31.30	12.79
4	1	753791.59	3240379.19	25	21.05	7.80
4	2	753820.21	3240443.27	26	19.37	7.78
4	3	753853.63	3240488.38	26	50.00	20.36
5	1	750168.53	3247444.27	25	21.43	13.33
5	2	750158.96	3247477.33	23	16.32	10.44
5	3	750141.62	3247514.44	25	21.05	12.96

Table A.12 Refers to the list of sustainability goals and vulnerability risk factors for coastal Louisiana (Bethel et al., 2022; Lambeth, 2016).

Code Table from Lambeth (2016, p. 136–137).

Levee Alignment – Sustainability Resident Solution: Levees Resident Solution: Marsh Creation	Levee Alignment - Vulnerability Levees
Shoreline Protection – Sustainability Resident Solution: Shoreline Protection Resident Solution: Shoreline Restoration Resident Solution: Rock Off Canals	Land Loss - Vulnerability Land Loss Erosion/Subsidence Saltwater Intrusion Lost Barrier Islands
Speed Bump – Sustainability Resident Solution: Spoil Banks	Oil Canal Erosion - Vulnerability Widening Canals Spoil Banks
Adaptability - Sustainability Resident Solution: Buy New Land Culturally Relevant Sites Resident Solution: House Elevation Cultural Subsistence Areas Attachment to Place	Loss of Utility - Vulnerability Sea Level Rise Accelerated Sea Level Rise Relocation Increased Storm Surge Loss of Trapping Industry Less Fishing/Shrimping Moving up the Bayou Younger Generations Moving Away Lost Communities Increased Current BP Oil Spill

REFERENCES

- Alleman, L. K., & Hester, A. (2011). Refinement of the fundamental niche of black mangrove (*Avicennia germinans*) seedlings in Louisiana: applications for restoration. *Wetlands Ecology and Management*, *19*, 47-60.
<https://link.springer.com/article/10.1007/s11273-010-9199-6>
- Anisfeld, S. C., & Hill, T. D. (2012). Fertilization effects on elevation change and belowground carbon balance in a Long Island Sound tidal marsh. *Estuaries and Coasts*, *35*, 201-211.
- Berkes, F. (1993). Traditional ecological knowledge in perspective. *Traditional ecological knowledge: Concepts and cases*, *1*, 1-9.
https://books.google.ie/books?hl=en&lr=&id=J2CNS64AFvsC&oi=fnd&pg=PA1&dq=berkes+1993+traditional+ecological+knowledge&ots=KCmoBdymHr&sig=9g6ZsiGJPYBuhChwg0MYHal1zFk&redir_esc=y#v=onepage&q=berkes%201993%20traditional%20ecological%20knowledge&f=false
- Bertness, M. D. (1991). Zonation of *Spartina patens* and *Spartina alterniflora* in New England salt marsh. *Ecology*, *72*(1), 138-148. <https://doi.org/10.2307/1938909>
- Bethel, M. B., Braud, D. H., Lambeth, T., Dardar, D. S., & Ferguson-Bohnee, P. (2022). Mapping risk factors to climate change impacts using traditional ecological knowledge to support adaptation planning with a Native American Tribe in Louisiana. *Journal of Environmental Management*, *301*.
<https://doi.org/10.1016/j.jenvman.2021.113801>
- Brown, C. E., Pezeshki, S. R., & DeLaune, R. D. (2006). The effects of salinity and soil

drying on nutrient uptake and growth of *Spartina alterniflora* in a simulated tidal system. *Environmental and Experimental Botany*, 58(1-3), 140-148.

<https://doi.org/10.1016/j.envexpbot.2005.07.006>

Bulsecu, A. N., Giblin, A. E., Tucker, J., Murphy, A. E., Sanderman, J., Hiller-Bittrolff, K., & Bowen, J. L. (2019). Nitrate addition stimulates microbial decomposition of organic matter in salt marsh sediments. *Global Change Biology*, 25(10), 3224-3241. <https://doi.org/10.1111/gcb.14726>

Childers, D. L., & Day Jr, J. W. (1988). A flow-through flume technique for quantifying nutrient and materials fluxes in microtidal estuaries. *Estuarine, Coastal and Shelf Science*, 27(5), 483-494. [https://doi.org/10.1016/0272-7714\(88\)90079-0](https://doi.org/10.1016/0272-7714(88)90079-0)

Chmura, G. L., Anisfeld, S. C., Cahoon, D. R., & Lynch, J. C. (2003). Global carbon sequestration in tidal, saline wetland soils. *Global biogeochemical cycles*, 17(4). <https://doi.org/10.1029/2002GB001917>

Clark, J. S. (2005). Why environmental scientists are becoming Bayesians. *Ecology letters*, 8(1), 2-14. <https://doi.org/10.1111/j.1461-0248.2004.00702.x>

Coleman, J. M. (1981). *Deltas: Processes of Deposition and Models for Exploration* (2nd ed.). Minneapolis: Burgess.

Costanza, R., d'Arge, R., De Groot, R., Farber, S., Grasso, M., Hannon, B., ... & Van Den Belt, M. (1997). The value of the world's ecosystem services and natural capital. *nature*, 387(6630), 253-260. <https://www.nature.com/articles/387253a0>

Costanza, R., Pérez-Maqueo, O., Martinez, M. L., Sutton, P., Anderson, S. J., & Mulder, K. (2008). The value of coastal wetlands for hurricane protection. *Ambio*, 241-

248. <https://www.jstor.org/stable/25547893>.

Currin, C. A. (2019). Living shorelines for coastal resilience. In *Coastal wetlands* (pp.

1023-1053). Elsevier. <https://doi.org/10.1016/B978-0-444-63893-9.00030-7>

Darby, F. A., & Turner, R. E. (2008). Effects of eutrophication on salt marsh root and rhizome biomass accumulation. *Marine Ecology Progress Series*, 363, 63-70.

<https://doi.org/10.3354/meps07423>

Day, J., Lane, R., Moerschbaecher, M., DeLaune, R., Mendelsohn, I., Baustian, J., & Twilley, R. (2013). Vegetation and soil dynamics of a Louisiana estuary receiving pulsed Mississippi River water following Hurricane Katrina. *Estuaries and Coasts*, 36, 665-682.

DeLaune, R. D., Feijtel, T. C., & Patrick, W. H. (1989). Nitrogen flows in Louisiana Gulf Coast salt marsh: spatial considerations. *Biogeochemistry*, 8, 25-37.

<https://link.springer.com/article/10.1007/BF02180165>

DeLaune, R. D., Pezeshki, S. R., & Jugsujinda, A. (2005). Impact of Mississippi River freshwater reintroduction on *Spartina patens* marshes: responses to nutrient input and lowering of salinity. *Wetlands*, 25(1), 155-161.

Dynesius, M., & Nilsson, C. (1994). Fragmentation and flow regulation of river systems in the northern third of the world. *Science*, 266(5186), 753-762.

<https://doi.org/10.1126/science.266.5186.753>

Else-Quirk, T., Graham, S. A., Mendelsohn, I. A., Snedden, G., Day, J. W., Twilley, R. R., ... & Lane, R. R. (2019). Mississippi river sediment diversions and coastal wetland sustainability: Synthesis of responses to freshwater, sediment, and

nutrient inputs. *Estuarine, Coastal and Shelf Science*, 221, 170-183.

<https://doi.org/10.1016/j.ecss.2019.03.002>

Engle, V. D. (2011). Estimating the provision of ecosystem services by Gulf of Mexico coastal wetlands. *Wetlands*, 31(1), 179-193.

<https://link.springer.com/article/10.1007/s13157-010-0132-9>

Fairchild, T. P., Bennett, W. G., Smith, G., Day, B., Skov, M. W., Möller, I., ... & Griffin, J. N. (2021). Coastal wetlands mitigate storm flooding and associated costs in estuaries. *Environmental Research Letters*, 16(7), 074034.

<https://doi.org/10.1088/1748-9326/ac0c45>.

Ferguson-Bohnee, P. (2015). The impacts of coastal erosion on tribal cultural heritage. *Forum Journal*, 29(4), 58-66. National Trust for Historic Preservation.

<https://muse.jhu.edu/article/587542>

Fox, L., Valiela, I., & Kinney, E. L. (2012). Vegetation cover and elevation in long-term experimental nutrient-enrichment plots in Great Sippewissett Salt Marsh, Cape Cod, Massachusetts: implications for eutrophication and sea level rise. *Estuaries and Coasts*, 35, 445-458.

Gadgil, M., Berkes, F., & Folke, C. (1993). Indigenous knowledge for biodiversity conservation. *Ambio*, 22(2/3), 151-156. <https://www.jstor.org/stable/4314060>

Grimes, E. (2021). *Spatial and Seasonal Patterns of Above-and Belowground Spatial and Potential Drivers in the Pascagoula River Delta, MS* (Master's thesis, University of Southern Mississippi). Retrieved from

https://aquila.usm.edu/masters_theses/849/

Guo, H., Zhang, Y., Lan, Z., & Pennings, S. C. (2013). Biotic interactions mediate the expansion of black mangrove (*Avicennia germinans*) into salt marshes under climate change. *Global change biology*, 19(9), 2765-2774.

<https://doi.org/10.1111/gcb.12221>

Hatfield, C. S., Marino, E., Whyte, K. P., Dello, K. D., & Mote, P. W. (2018). Indian time: time, seasonality, and culture in Traditional Ecological Knowledge of climate change. *Ecological Processes*, 7(1), 1-11.

<https://link.springer.com/article/10.1186/s13717-018-0136-6>

Herbert, R. A. (1999). Nitrogen cycling in coastal marine ecosystems. *FEMS microbiology reviews*, 23(5), 563-590.

<https://doi.org/10.1111/j.1574-6976.1999.tb00414.x>

Herbert, E. R., Windham-Myers, L., & Kirwan, M. L. (2021). Sea-level rise enhances carbon accumulation in United States tidal wetlands. *One Earth*, 4(3), 425-433.

[https://www.cell.com/one-earth/pdf/S2590-3322\(21\)00117-2.pdf](https://www.cell.com/one-earth/pdf/S2590-3322(21)00117-2.pdf)

Hill, T. D., & Roberts, B. J. (2017). Effects of seasonality and environmental gradients on *Spartina alterniflora* allometry and primary production. *Ecology and Evolution*, 7(22), 9676-9688. <https://doi.org/10.1002/ece3.3494>

Historical and projected land loss from coastal Louisiana. Map reproduced from Barras et al. (2003). Historical and projected coastal Louisiana land changes: 1978–2050. USGS Open File Report 03–334, 39.

Hollis, L. O., & Turner, R. E. (2019). The tensile root strength of *Spartina patens*: Response to atrazine exposure and nutrient addition. *Wetlands*, 39, 759-775.

- Hooten, M. B., & Hobbs, N. T. (2015). A guide to Bayesian model selection for ecologists. *Ecological monographs*, 85(1), 3-28.
<https://doi.org/10.1890/14-0661.1>
- Karimpour, A., Chen, Q., & Jadhav, R. (2013). Turbidity Dynamics in Upper Terrebonne Bay, Louisiana. *Sediment Transport: Monitoring, Modeling and Management, Nova Sc. Pub*, 339-360. <https://www.researchgate.net/publication/271374878>
- Kirwan, M. L., & Murray, A. B. (2007). A coupled geomorphic and ecological model of tidal marsh evolution. *Proceedings of the National Academy of Sciences*, 104(15), 6118-6122. <https://doi.org/10.1073/pnas.0700958104>
- Kirwan, M. L., Guntenspergen, G. R., d'Alpaos, A., Morris, J. T., Mudd, S. M., & Temmerman, S. (2010). Limits on the adaptability of coastal marshes to rising sea level. *Geophysical research letters*, 37(23).
<https://doi.org/10.1029/2010GL045489>
- Kirwan, M. L., & Guntenspergen, G. R. (2012). Feedbacks between inundation, root production, and shoot growth in a rapidly submerging brackish marsh. *Journal of Ecology*, 100(3), 764-770. <https://doi.org/10.1111/j.1365-2745.2012.01957.x>
- Kirwan, M. L., & Guntenspergen, G. R. (2015). Response of plant productivity to experimental flooding in a stable and a submerging marsh. *Ecosystems*, 18, 903-913. <https://link.springer.com/article/10.1007/s10021-015-9870-0>
- Laituri, M. (2011). Indigenous peoples' issues and indigenous uses of GIS. *The SAGE handbook of GIS and society*, 1996, 202-221.
<http://dx.doi.org/10.4135/9781446201046.n11>

- Lake, F. K., Parrotta, J., Giardina, C. P., Davidson-Hunt, I., & Uprety, Y. (2018). 12 Integration of Traditional and Western knowledge in forest landscape restoration. *Forest landscape restoration: Integrated approaches to support effective implementation*, 198-226.
- https://books.google.ie/books?hl=en&lr=&id=WMSuDwAAQBAJ&oi=fnd&pg=PT330&dq=lake+2018+integration+of+traditional&ots=BJZewh6yG3&sig=cIgKsKAMs95R4szllid7kfpeHXA&redir_esc=y#v=onepage&q=lake%202018%20integration%20of%20traditional&f=false
- Lambeth, T. (2016). *Coastal Louisiana: Adaptive Capacity in the Face of Climate Change* (Doctoral Dissertation, University of New Orleans). Retrieved from <https://scholarworks.uno.edu/td/2228/>
- Lamonds, A.G., and Boswell, E.H. (1985) Mississippi Surface Water Resources: National Water Summary 1985. *United States Geological Survey Water Supply Paper 2300*, 295-300.
- Langley, A. J., Mozdzer, T. J., Shepard, K. A., Hagerty, S. B., & Patrick Megonigal, J. (2013). Tidal marsh plant responses to elevated CO₂, nitrogen fertilization, and sea level rise. *Global Change Biology*, 19(5), 1495–1503.
- <https://doi.org/10.1111/gcb.12147>
- Leonard, L. A., & Croft, A. L. (2006). The effect of standing biomass on flow velocity and turbulence in *Spartina alterniflora* canopies. *Estuarine, Coastal and Shelf Science*, 69(3-4), 325-336. <https://doi.org/10.1016/j.ecss.2006.05.004>
- Maldonado, J. K. (2014). A multiple knowledge approach for adaptation to environmental

- change: lessons learned from coastal Louisiana's tribal communities. *Journal of Political Ecology*, 21(1), 61-68. <https://doi.org/10.2458/v21i1.21125>
- McAllister, T., Clavin, C., Ellingwood, B., Van de Lindt, J., Mizzen, D. R., & Lavelle, F. M. (2019). *Data, information, and tools needed for community resilience planning and decision-making*. US Department of Commerce, National Institute of Standards and Technology. <https://nvlpubs.nist.gov/nistpubs/specialpublications/NIST.SP.1240.pdf>
- McHugh, M. L. (2012). Interrater reliability: the kappa statistic. *Biochemia medica*, 22(3), 276-282.
- McKee, K. L., & Patrick, W. H. (1988). The relationship of smooth cordgrass (*Spartina alterniflora*) to tidal datums: a review. *Estuaries*, 11, 143-151. <https://link.springer.com/article/10.2307/1351966>
- McKee, K. L., & Mendelssohn, I. A. (1989). Response of a freshwater marsh plant community to increased salinity and increased water level. *Aquatic Botany*, 34(4), 301-316. [https://doi.org/10.1016/0304-3770\(89\)90074-0](https://doi.org/10.1016/0304-3770(89)90074-0)
- McKee, K. L., Mendelssohn, I. A., & D. Materne, M. (2004). Acute salt marsh dieback in the Mississippi River deltaic plain: A drought-induced phenomenon?. *Global Ecology and Biogeography*, 13(1), 65-73. <https://doi.org/10.1111/j.1466-882X.2004.00075.x>
- Mendelssohn, I. A. (1979). The influence of nitrogen level, form, and application method on the growth response of *Spartina alterniflora* in North Carolina. *Estuaries*, 2, 106-112. <https://doi.org/10.2307/1351634>

- Mendelssohn, I. A., & McKee, K. L. (1988). *Spartina alterniflora* die-back in Louisiana: time-course investigation of soil waterlogging effects. *The Journal of Ecology*, 509-521. <https://doi.org/10.2307/2260609>
- Moller, H., Berkes, F., Lyver, P.O.B., & Kislalioglu, M. (2004). Combining science and traditional ecological knowledge: monitoring populations for co-management. *Ecology and society*, 9(3). <https://www.jstor.org/stable/26267682>
- Mossa, J., & Coley, D. (2004). Planform change rates in rivers with and without instream and floodplain sand and gravel mining: Assessing instability in the Pascagoula River and Tributaries, Mississippi. *Gainesville, FL, University of Florida*.
- Morris, J. T., Sundareshwar, P. V., Nietch, C. T., Kjerfve, B., & Cahoon, A. D. R. (2002). Responses of coastal wetlands to rising sea level. *Ecology*, 83(10), 2869-2877. [https://doi.org/10.1890/0012-9658\(2002\)083\[2869:ROCWTR\]2.0.CO;2](https://doi.org/10.1890/0012-9658(2002)083[2869:ROCWTR]2.0.CO;2)
- Morris, J. T. (2007). Estimating net primary production of salt marsh macrophytes. *Principles and standards for measuring primary production*, 10, 1093.
- Morris, J. T., Langley, J. A., Vervaeke, W. C., Dix, N., Feller, I. C., Marcum, P., & Chapman, S. K. (2023). Mangrove Trees Outperform Saltmarsh Grasses in Building Elevation but Collapse Rapidly Under High Rates of Sea-Level Rise. *Earth's Future*, 11(4), e2022EF003202. <https://doi.org/10.1029/2022EF003202>
- Nadasdy, P. (1999). The politics of TEK: Power and the "integration" of knowledge. *Arctic Anthropology*, 1-18. <https://www.jstor.org/stable/40316502>

- Nyman, J. A., DeLaune, R. D., Roberts, H. H., & Patrick Jr, W. H. (1993). Relationship between vegetation and soil formation in a rapidly submerging coastal marsh. *Marine Ecology Progress Series*, 269-279.
<https://www.jstor.org/stable/24833555>
- Nyman, J. A., Walters, R. J., Delaune, R. D., & Patrick, W. H. (2006). Marsh vertical accretion via vegetative growth. *Estuarine, Coastal and Shelf Science*, 69(3-4), 370-380. <https://doi.org/10.1016/j.ecss.2006.05.041>
- Penland, S., Suter, J. R., & McBride, R. A. (1987). Delta plain development and sea level history in the Terrebonne coastal region, Louisiana. *Coastal Sediments*, 1689-1705.
- Perry, C. L., & Mendelsohn, I. A. (2009). Ecosystem effects of expanding populations of *Avicennia germinans* in a Louisiana salt marsh. *Wetlands*, 29, 396-406.
- Pontius Jr, R. G., Peethambaram, S., & Castella, J. C. (2011). Comparison of three maps at multiple resolutions: a case study of land change simulation in Cho Don District, Vietnam. *Annals of the Association of American Geographers*, 101(1), 45-62. <https://doi.org/10.1080/00045608.2010.517742>
- Rivard, C. (2015). Archival recognition: the Pointe-au-Chien's and Isle de Jean Charles Band of the Biloxi-Chitimacha Confederation of Muskogee's fight for federal recognition. *Settler Colonial Studies* 5(2), 117-127.
<https://doi.org/10.1080/2201473X.2014.957257>
- Robert, C. & Casella, G. (2004). *Monte Carlo statistical methods* (2nd e., Vol. 2). New York: Springer.

- Schutte, C. A., Marton, J. M., Bernhard, A. E., Giblin, A. E., & Roberts, B. J. (2020). No evidence for long-term impacts of oil spill contamination on salt marsh soil nitrogen cycling processes. *Estuaries and coasts*, *43*, 865-879.
<https://link.springer.com/article/10.1007/s12237-020-00699-z>
- Snedden, G. A., Cable, J. E., Swarzenski, C., & Swenson, E. (2007). Sediment discharge into a subsiding Louisiana deltaic estuary through a Mississippi River diversion. *Estuarine, Coastal and Shelf Science*, *71*(1-2), 181-193.
<https://doi.org/10.1016/j.ecss.2006.06.035>
- Snedden, G. A., Cable, J. E., & Wiseman, W. J. (2007). Subtidal sea level variability in a shallow Mississippi River deltaic estuary, Louisiana. *Estuaries and Coasts*, *30*, 802-812. <https://link.springer.com/article/10.1007/bf02841335>
- Snedden, G. A., Cretini, K., & Patton, B. (2015). Inundation and salinity impacts to above- and belowground productivity in *Spartina patens* and *Spartina alterniflora* in the Mississippi River deltaic plain: Implications for using river diversions as restoration tools. *Ecological Engineering*, *81*, 133–139.
<https://doi.org/10.1016/j.ecoleng.2015.04.035>
- Stalter, R., & Batson, W. T. (1969). Transplantation of salt marsh vegetation, Georgetown, South Carolina. *Ecology*, *50*(6), 1087-1089.
<https://doi.org/10.2307/1936901>
- Stevenson, J. C., Ward, L. G., & Kearney, M. S. (1986). Vertical accretion in marshes with varying rates of sea level rise. In *Estuarine variability* (pp. 241-259). Academic Press. <https://doi.org/10.1016/B978-0-12-761890-6.50020-4>

- Suzuki, D., & Knudtson, P. (1992). *Wisdom of the elders: Honoring sacred native visions of nature*. New York: Bantam Books.
- Sweet, W. V., Kopp, R. E., Weaver, C. P., Obeysekera, J., Horton, R. M., Thieler, E. R., & Zervas, C. (2017). *Global and regional sea level rise scenarios for the United States* (No. CO-OPS 083).
- Thompson, K. L., Lantz, T., & Ban, N. (2020). A review of Indigenous knowledge and participation in environmental monitoring. *Ecology and Society*, 25(2). 10.
<https://doi.org/10.5751/ES-11503-250210>
- Turner, R. E. (2001). Of manatees, mangroves, and the Mississippi River: Is there an estuarine signature for the Gulf of Mexico? *Estuaries*, 24, 139-150.
<https://link.springer.com/article/10.2307/1352940>
- Usher, P.J., 2000. Traditional ecological knowledge in environmental assessment and management. *Arctic*, 53(2), 183–193.
<https://www.proquest.com/scholarly-journals/traditional-ecological-knowledge-environmental/docview/197663518/se-2?accountid=14504>
- van Vliet, J., Bregt, A. K., & Hagen-Zanker, A. (2011). Revisiting Kappa to account for change in the accuracy assessment of land-use change models. *Ecological modelling*, 222(8),1367-1375. <https://doi.org/10.1016/j.ecolmodel.2011.01.017>
- Wang, F. C., Lu, T., & Sikora, W. B. (1993). Intertidal marsh suspended sediment transport processes, Terrebonne Bay, Louisiana, USA. *Journal of Coastal Research*, 209-220.<https://www.jstor.org/stable/4298078>
- Wang, H., Gilbert, J. A., Zhu, Y., & Yang, X. (2018). Salinity is a key factor driving the

- nitrogen cycling in the mangrove sediment. *Science of the Total Environment*, 631–632, 1342–1349. <https://doi.org/10.1016/j.scitotenv.2018.03.102>
- Wildcat, D. R. (2013). Introduction: climate change and indigenous peoples of the USA. *Climate change and Indigenous Peoples in the United States: Impacts, experiences and actions*, 1-7.
- Wu, W., Clark, J. S., & Vose, J. M. (2012). Application of a Full Hierarchical Bayesian Model in Assessing Streamflow Response to a Climate Change Scenario at the Coweeta Basin, NC, USA. *Journal of Resources and Ecology*, 3(2), 118–128. <https://doi.org/10.5814/j.issn.1674-764x.2012.02.003>
- Wu, W., Yeager, K. M., Peterson, M. S., & Fulford, R. S. (2015). Neutral models as a way to evaluate the Sea Level Affecting Marshes Model (SLAMM). *Ecological Modelling*, 303, 55-69. <https://doi.org/10.1016/j.ecolmodel.2015.02.008>
- Wu, W., Bethel, M., Mishra, D. R., and Hardy, T. (2018). Model selection in Bayesian framework to identify the best WorldView-2 based vegetation index in predicting green biomass of salt marshes in the northern Gulf of Mexico. *GIScience and Remote Sensing*, 55(6), 880–904. <https://doi.org/10.1080/15481603.2018.1460934>
- Wu, W., Biber, P., & Bethel, M. (2017a). Thresholds of sea-level rise rate and sea-level rise acceleration rate in a vulnerable coastal wetland. *Ecology and Evolution*, 7(24), 10890-10903. <https://doi.org/10.1002/ece3.3550>
- Wu, W., Huang, H., Biber, P., & Bethel, M. (2017b). Litter decomposition of *Spartina alterniflora* and *Juncus roemerianus*: Implications of climate change in salt marshes. *Journal of Coastal Research*, 33(2), 372-384.

<https://doi.org/10.2112/JCOASTRES-D-15-00199.1>

Wu, W., Biber, P., Mishra, D. R., & Ghosh, S. (2020). Sea-level rise thresholds for stability of salt marshes in a riverine versus a marine dominated estuary. *Science of the Total Environment*, 718, 137181.

<https://doi.org/10.1016/j.scitotenv.2020.137181>

Yeoman, B. (2017). *Reclaiming Native Ground* [Infographic]. Sapiens.

<https://www.sapiens.org/culture/louisiana-native-americans-climate-change/>